HIG-73-6

A COMPARISON OF STORM-WAVE AND TRADEWIND-WAVE ENERGIES OFF KANEOHE BAY, OAHU, HAWAII

By

KEITH M. SHIMADA

MAY 1973

Prepared for
NATIONAL SCIENCE FOUNDATION
under Grant GH-93
and
NATIONAL OCEANIC AND ATMOSPHERIC ADMINISTRATION
under National Sea Grant Program Grant 2-35-243

HAWAII INSTITUTE OF GEOPHYSICS
UNIVERSITY OF HAWAII

HIG-73-6

A COMPARISON OF STORM-WAVE AND TRADEWIND-WAVE ENERGIES OFF KANEOHE BAY, OAHU, HAWAII*

By

Keith M. Shimada

May 1973

Prepared for
National Science Foundation
under grant GH-93
and
National Oceanic and Atmospheric Administration
under National Sea Grant Program grant 2-35-243

*A thesis submitted to the Graduate Division of the University of Hawaii in partial fulfillment of the requirements for the degree of Master of Science in Oceanography, May 1973.

Approved by Director

George P. Woollard

Date: 1 May 1973

ACKNOWLEDGMENTS

I am grateful to Professors Robert Tait, Gaylord Miller, Brent Gallagher, and Keith Chave for their guidance and encouragement during the course of this study.

Useful discussions were held with Dr. Klaus Wyrtki. I thank Dr. Harold Loomis who provided the computer subroutine to calculate the spectral values, and Mrs. Shikiko Nakahara who assisted in writing the computer program. The preparation of figures was done by William E. Chase.

I wish to thank the organizations which made weather data available to me: the National Weather Service, Kaneohe Marine Corps Air Station, Fleet Weather Central, and the Meteorology Department of the University of Hawaii.

For providing and repairing the instruments to measure and record sea-surface elevations, I thank Dr. Martin Vitousek and his assistants, Jerry Packard and Jordan Ige.

I am grateful to those who assisted in the installation of the instruments: Gary and Susan Niemeyer, Dr. Edward Stroup, Christine Sakai, Thomas Daniel, Theodore Hirano, and especially Gene Gilley who directed the initial installation.

Special thanks to those who, in rain and sunshine, calm and rough seas, helped replace the car batteries that powered the pressure gauge and the transmitter: Norman H. Yoshida, Sylvia Koo, Daniel Teruya, Ralph Saito, Lydia Oi, Ronald J. Nagata, Margo Otsuka, Frank Gonzalez, Brian Yoshida, William and Dora Emery, Gary Meyers, Paul Jubinski, Jackson Tsujimura, and Joyce Mizukami.

I gratefully acknowledge the assistance of Mrs. Ethel McAfee and Mrs. Rita Pujalet for their many suggestions and improvements in the writing of this manuscript.

For typing the drafts and the final thesis manuscript, I thank Mrs. Carol Koyanagi.

This research was supported by the National Science Foundation under grant GH-93 and the National Oceanic and Atmospheric Administration under National Sea Grant Program grant 2-35-243.

A COMPARISON OF STORM-WAVE AND TRADEWIND-WAVE ENERGIES OFF KANEOHE BAY, OAHU, HAWAII

A THESIS SUBMITTED TO THE GRADUATE DIVISION OF THE
UNIVERSITY OF HAWAII IN PARTIAL FULFILLMENT
OF THE REQUIREMENTS FOR THE DEGREE OF

MASTER OF SCIENCE

IN OCEANOGRAPHY

MAY 1973

By

Keith Masato Shimada

Thesis Committee:

Robert J. Tait, Chairman
Keith E. Chave
Brent S. Gallagher
Gaylord R. Miller

ABSTRACT

Sea-surface elevations were measured outside the reef protecting Kaneohe Bay, Oahu, Hawaii, from 22 January to 8 August, 1971, in a study of the wave energy associated with storm waves and tradewind waves approaching the Bay. When energy spectra of the storm waves were compared with those of the tradewind waves, it was found that: (1) Strong local tradewinds produce more wave energy than do distant storms in the north or south Pacific. (2) Strong local tradewinds produce twice as much wave energy as do weak local tradewinds. (3) The tradewinds produce more wave energy than do local southerly winds. (4) The effect of Hurricane Denise, which passed southeast of Hawaii, was negligible.

TABLE OF CONTENTS

LIST OF TABLES

LIST OF FIGURES

INTRODUCTION

The purpose of this study is to compare the energies of storm waves and tradewind waves off Kaneohe Bay, Oahu, Hawaii, and the distribution of this energy in time. Kaneohe Bay, located on the northeast, windward side of the island, is sheltered by the island land mass from waves approaching from the south and west, but is exposed to waves from the north and northeast. A barrier reef, on which incoming waves initially break, extends almost entirely across the mouth of the Bay. Two passages separate this reef from the fringing reef along the coastline of Oahu. Within the Bay are other fringing reefs and patch reefs (Roy, 1970). Knowledge of the relative energies of storm waves and tradewind waves in the Bay could help to relate their relative importance to the construction or destruction of the reefs. In addition, the relation between the distribution of energies associated with the waves and the distribution of organisms in Kaneohe Bay may be revealed.

As a first step in determining wave energies, sea-surface elevations were measured with a Vibrotron pressure gauge located off Kapapa Island centered at the mouth of Kaneohe Bay. Measurements began on 22 January and ended on 8 August, 1971. Next, surface weather maps, surface wind summaries, and marine forecast records were examined to determine the time and location of storm and tradewind occurrences during this period. The corresponding sea-surface elevation records were then selected, and wave-energy spectra showing wave energy as a function of wave frequency were calculated. Previous studies conducted elsewhere of wave-energy spectra have been primarily concerned with storm waves (see Snodgrass *et al*., 1966; Munk *et al*., 1963; Dinger, 1962), not with local wind waves.

WAVE TYPES

Four major types of waves are present in Hawaiian waters (Moberly and Chamberlain, 1964) (Fig. 1). The most frequent are the Northeast Trade Waves, which may be present all year long and are dominant between April and November. These waves are generated by strong tradewinds which are associated with high-pressure areas located north of the Hawaiian Islands. The winds blow over long distances northeast of the Islands. The North Pacific Swell may also be present all year long, but is generally largest and most prevalent from October through May. The waves, which approach the Islands from the northwest, north, and northeast, are generated by low-pressure areas near the Aleutians and in mid-latitudes. The Southern Swell, generated by strong winds near Australia and in the Southern Ocean, arrives between April and October. Snodgrass _et al_. (1966), and Munk _et al_. (1963) tracked these swells from the south and determined their generating storms. The fourth, Kona Storm Waves, occur infrequently from December to March. Generated by local fronts and low pressure areas, they approach the Islands from the southeast through the southwest.

Of these, the North Pacific Swell, Southern Swell, and Kona Storm Waves may be thought of as storm-generated waves, i.e., generated by winds associated with low-pressure areas, by gales (low-pressure areas with winds greater than 33 knots), or by storms (low-pressure areas with winds greater than 47 knots). The effect of Southern Swell on Kaneohe Bay is negligible since the waves approach from the south (Fig. 1). Ho and Sherretz (1969) found the sea conditions off Makapuu Point, south of Kaneohe Bay (Fig. 1), to be mainly a product of local wind conditions. It would therefore not be unreasonable to expect that Kaneohe Bay would also be affected by local winds. Although Kona Storm Waves approach from the southeast through the southwest, they are accompanied by changes in the local wind direction (from northeasterly to southerly and westerly) and so will be studied. The waves of prime interest are therefore tradewind waves (Northeast Trade Waves) and storm waves (including North Pacific Swell and Kona Storm Waves) generated in the North Pacific.

SITE AND SAMPLING

To measure sea-surface elevations, a Vibrotron pressure gauge was installed seaward of Kapapa Island (Fig. 2). The pressure gauge was anchored on the bottom in 8 meters of water. (See Appendix A for a description of the data acquisition system.)

Recording of sea-surface elevations was begun on 22 January 1971 and was intended to continue for a year. However, instrument failure forced discontinuance on 8 August 1971. Nevertheless, this period was long enough to include the occurrence of the four major types of waves under study.

Sea-surface elevations were sampled once every 2 seconds during a period of 2 hours, 16 minutes, and 32 seconds. With a lapse of 6 hours, 49 minutes, and 36 seconds between periods, there were two, and sometimes three, wave records per day.

SPECTRAL ANALYSIS

Aliasing

If there is appreciable wave energy at frequencies greater than the Nyquist or folding frequency (one-half the sampling frequency), this energy will be falsely reported at frequencies lower than that and consequently the wave energy spectrum will be aliased. To prevent this, the pressure gauge may be installed deep enough so that the water acts as a filter to attenuate the higher frequency energy. According to Airy wave theory, at the instrument depth of 8 meters the energy density at the Nyquist frequency of .25 cycles per second (250 milliHz) has been reduced to 0.0628 of its surface value; i. e., of its value if the pressure gauge had been installed just below the surface. Since attenuation increases with increasing frequency, aliasing of the spectrum has been avoided.

The Spectrum

The power spectrum in this study is labeled an energy or wave-energy spectrum (Kinsman, 1965). It shows the manner in which wave energy varies with wave frequency. With sea-surface elevation given in centimeters and frequency in milliHz (millicycles per second), the dimensions of normalized energy become cm^2/milliHz, and the total normalized energy within a frequency interval becomes cm^2.

Each wave-energy spectrum presented here is the result of calculations using 4096 sea-surface elevation values to obtain 256 wave energy (or spectral density) estimates with a resolution of .98 milliHz. The degrees of freedom equals 32. Thus for each spectral density estimate, confidence is 80 per cent that the true, long-term value lies between 1/1.33 and 1/.70 of the spectral density estimate (Blackman and Tukey, 1958).

The computer program used to calculate the wave-energy spectra first searched the data for errors, then corrected the errors by averaging the two values on either side of an error, and finally calculated and plotted the spectra. This averaging procedure may have smoothed the high-frequency waves, but because of the relatively few errors extant in the selected wave records the smoothing may have been insignificant. (See Appendix A for a detailed explanation of this correction procedure and Table 1 for a copy of the entire computer program.) Figures 3 through 60 present the plots of the calculated spectra.

DATA AND DISCUSSION

Comparing Storm and Tradewind Conditions

Energy spectra for all the available wave records could not be calculated for comparison of the wave energies associated with tradewinds and those associated with storms, because the computer cost would have been too great. The occurrence of the weather conditions pertinent to this study needed to be determined first; and then the desired spectra could be calculated.

To determine the time of occurrence and location of storms and tradewinds, three types of data were examined: (1) the marine forecast records of the National Weather Service, which report smallcraft warnings; (2) the surface-wind summaries of the Marine Corps Air Station at Kaneohe Bay, which furnish hourly wind velocities over Kaneohe Bay; and (3) the North Pacific surface-weather maps of the National Weather Service, First Weather Wing, and Fleet Weather Central, which show high-pressure and low-pressure areas, including gales, storms, tropical depressions, tropical storms, typhoons, and hurricanes, in the North Pacific.

Upon examination of these types of data, it was noticed that tropical depressions, tropical storms, typhoons, and hurricanes usually remained in the western and eastern Pacific, south of the Hawaiian Islands.

Since Kaneohe Bay is sheltered to the southwest and southeast, the effects of waves generated by these tropical low pressure areas were assumed to be negligible and were ignored in this study. However, Hurricane Denise is discussed because she approached closer to the Hawaiian Islands than did any other tropical storm or hurricane during the period of study. It was also noticed that gales were more numerous and were usually of longer duration than storms. As wave height is considered a function of wind duration and fetch (the distance over which the wind blows)--in addition to being a function of the mean wind speed--gales may also generate higher than normal waves and may significantly affect the wave energy in Kaneohe Bay. It was therefore important to compare the wave energies of gales and storms with those of tradewinds.

Gales and storms in various locations were selected to study the effects of waves approaching Kaneohe Bay from various directions. Also, occasions of strong and weak local tradewinds were selected to study the effects of wind speed on the wave energy in Kaneohe Bay. Smallcraft warnings were used as a guide to distinguish between strong and weak local winds. These warnings are issued when high wind speeds (channel winds between the Islands reaching approximately 25 knots) become hazardous to small boats; Table 2 summarizes the occurrence of gales, storms, and smallcraft warnings, and the days for which energy spectra have been calculated.

In the study of the spectra and their associated weather conditions, it was difficult to ascertain the specific low pressure area that was responsible for energy peaks in a spectrum since several low-pressure areas may exist at the same time. One method of locating the source was to construct a frequency-time diagram (Snodgrass *et al.*, 1966; Munk *et al.*, 1963; Dinger, 1962). In such a diagram, the dispersive arrivals from a distant source appear as a ridge in the energy contours since long-period, low-frequency waves travel faster than short-period, high-frequency waves. These dispersive arrivals cause energy peaks whose shifts in frequency can be followed in consecutive spectra over several days. In contrast, dispersive arrivals from nearby sources appear as broad peaks in a spectrum and in the energy contours of a frequency-time diagram, since both the low- and high-frequency waves having less distance to travel arrive at closer intervals. However, construction of a frequency-time diagram requires at least two spectra per day for several days. As an example of this, a frequency-time diagram was constructed for 20-25 March (Fig. 61) and a distant source was located. Such diagrams were not constructed for the other spectra since none of them were consecutive for a long enough period.

Among the weather conditions discussed here are a gale to the northwest, a low to the northwest, a storm to the north, a hurricane to the southeast of the Islands, and strong and weak tradewinds. In the discussion of these events:

(1) All times are given in local time, HST.

(2) Most of the locations of lows, gales, and storms mentioned in the text and in Table 2 were read from the daily 0200 HST surface weather maps of Fleet Weather Central and the First Weather Wing. They were used instead of the 0200 HST National Weather Service maps since lows (L), gales (G), and storms (S) are labelled separately, whereas the National Weather Service maps lump them all together as lows (L). However, the National Weather Service maps were used in constructing Figures 63 through 65.

(3) Each spectrum is referred to by the starting time of the wave record on which the spectrum is based.

(4) Unless the frequency band or energy peak is specified, the total energy is the sum of the energy in the entire spectrum between 0 and 250 milliHz. The average total energy (unless the frequency band is specified) is the average of the total energies for more than one spectrum.

(5) Energies at frequencies greater than 180 milliHz are compared for various weather conditions. These

frequencies were chosen since in most spectra energy levels off at approximately 180 milliHz. Local winds may be primarily responsible for generating waves at frequencies greater than 180 milliHz (5.5 seconds).

(6) Table 3 summarizes the total wave energies for these events.

<u>Gale to the Northwest</u>

Smallcraft and gale warnings for south and west-southwest winds were in effect 26-28 January (wave energy spectra, Figs. 3-5). These high winds were caused by a gale situated northwest of the Hawaiian Islands on 27 January at 27°N, 169°W, approximately 1200 km northwest of Oahu. This gale was moving northeastward. Waves at the peak frequency of 82 milliHz (12 seconds) for the spectrum of 2236 28 January (Fig. 5) would have been travelling at 18 knots and would have been 1500 km distant at 0200 27 January. This calculation suggests a wave-generating area in the western part of the gale (centered at 27°N, 169°W), which is reasonable as the winds there would have been northwesterly and the resulting waves would be travelling toward the Hawaiian Islands. Southerly winds averaged 6, 20, and 12 knots for 26-28 January at Kaneohe Bay. Despite the high winds, the total energies of the spectra for the three days were only 970 cm^2, 687 cm^2, and 717 cm^2. The average total energy in the broad energy peak between 50 and 180 milliHz (20.0 and 5.5 seconds) was 687 cm^2. The energies at frequencies greater than 180 milliHz (periods less than 5.5 seconds), where the energy tended to level off, were less than or equal to 1 cm^2 per milliHz. The average total energy between 180 and 250 milliHz was 62 cm^2. As will be shown later, the wave energies for strong tradewinds at frequencies greater than 180 milliHz were greater than or equal to 5 cm^2 per milliHz, and the average total energy between 180 and 250 milliHz was 512 cm^2.

Low to the Northwest

A frequency-time diagram (Fig. 61) revealed the effects of a low-pressure area northwest of the Hawaiian Islands. In this diagram, a ridge in the energy contours represented the dispersive arrivals (Fig. 62) from a source calculated to be approximately 5000 km distant at 1748 16 March, suggesting that the wave-generating area was in the western part of the low-pressure area centered at 53°N, 175°W on 16 March (Fig. 63). The average total energy in the dispersive peaks in the spectra of 1248 20 March, 2154 20 March, and 0700 21 March (Fig. 6-8), was 23 cm^2, or 5 per cent of the average total energy of the three spectra.

Storm to the North

The frequency-time diagram (Fig. 61) also revealed the effects of a storm centered at 39°N, 162°W, approximately 2000 km north of Oahu, on 21 March (Fig. 64). On 22 March, the National Weather Service reported 8-foot swells from the northwest. On 21 and 22 March, energy increased in the main energy peak between 60 and 110 milliHz. Accompanying this increase was another at lower frequencies, between 0 and 35 milliHz. The average total energy for the spectra of 1606 21 March, 1019 22 March, and 1925 22 March (Figs. 9-11) was 2029 cm^2. The average total energy in the main energy peak between 60 and 110 milliHz for these spectra was 1397 cm^2. The average total energy between 180 and 250 milliHz was 168 cm^2.

Beginning 23 March, as this storm moved farther away, the total energy decreased. The average total energy of the spectra between 0431 23 March and 1655 24 March was 501 cm^2 (Figs. 12-16). Beginning 1337 23 March, the energies at frequencies greater than 180 milliHz were less than or equal to 1 cm^2 per milliHz.

Strong and Weak Tradewinds

From 22 January to 8 August, 1971, there were 13 instances of strong tradewinds, either from the northeast or the east-northeast. There were at least two occasions of strong tradewinds each month except in January and May, when there were none. Spectra were calculated for six instances of strong tradewinds (Figs. 21-25, 28-37). The average total energy was 3013 cm^2, with the two lowest being 1863 cm^2 for the spectrum of 1412 13 July and 1904 cm^2 for 0757 20 February (Figs. 37 and 21). For these two, the energies above 180 milliHz were greater than 1 cm^2 per milliHz. For all the other spectra, the energies at frequencies above 180 milliHz were greater than or equal to 5 cm^2 per milliHz. For all the spectra, the average total energy between 180-250 milliHz was 512 cm^2.

When weak tradewinds occurred, their average total energy was 1262 cm^2 (Figs. 38-60). The energies above 180 milliHz were greater than 1 cm^2 per milliHz. The average total energy between 180 and 250 milliHz was 325 cm^2.

The total energy of each spectrum during tradewind conditions was compared with the wind speed recorded at the Marine Corps Air Station on Kaneohe Bay (Fig. 66). In this comparison, the effects of gales and storms that might have occurred during tradewind conditions were ignored because: (1) the distant low of 16 March had little effect on the total energies of the spectra for 20 and 21 March; and (2) only an approximate comparison was intended.

In general, as the wind speed of strong tradewinds increased, the total wave energy increased. But, for weak tradewinds, there appeared to be no increase with increasing wind speeds; total energies remained less than 2200 cm^2. In the case of the weak tradewinds, although wind speeds over the Bay were 6-15 knots, the channel winds had not reached 25 knots, and winds farther away may have had lower speeds. In the case of the strong tradewinds, although wind speeds over the Bay were only 9-17 knots, the channel winds had reached 25 knots, and winds farther away may also have had higher speeds. Thus, as expected, higher wind speeds over longer distances resulted in greater wave energies.

Strong Southerly Winds

The five instances of smallcraft warnings for southerly winds occurred in January through March. The southerly winds were caused by gales and storms disrupting the usual tradewinds. Spectra for four instances of strong southerly winds were calculated (Figs. 3-7, 10-20), with an average total energy of 703 cm^2. The average total energy between 180 and 250 milliHz was 73 cm^2. The energies at frequencies greater than 180 milliHz were less than 5 cm^2 per milliHz, and for 26-28 January, 20 March, and 23-24 March, they were less than 1 cm^2 per milliHz.

On 19 February and 25 March, as the wind shifted from southerly to northeasterly, the total wave energy increased. This was not unexpected as Kaneohe Bay is exposed to the northeast. On both occasions, smallcraft warnings for southerly winds (strong southerly winds) were changed to smallcraft warnings for northeasterly winds (strong tradewinds).

During 17-19 February, when strong southerly winds existed, the average total wave energy was 582 cm^2 (Figs. 17-20). On the 19th at 1100, the winds began shifting from south to northwest, until at 1900 they became northeasterly. With this shift, the total wave energy increased to 1904 cm^2 for the spectrum of 0757 20 February (Fig. 21). This increase in the total energy may have been partly caused by a storm which was situated 2800 km northwest of the Hawaiian Islands on 20 February. It generated 20-foot surf which pounded the northern coasts of Kauai and Oahu on 20 February. However, the total energy continued to increase (Figs. 22-25) as the effects of this storm decreased. Strong tradewinds on 20-24 February, caused by a high pressure area at 35°N (Fig. 65), generated swells from the east-northeast that were 6 feet high on 22 February. The total energy increased to 5660 cm^2, the largest of all the spectra, for the spectrum of 1753 23 February (Fig. 25).

Strong southerly winds for 22-24 March were followed by strong tradewinds for 25-30 March. On 25 March, as the wind again shifted from southerly to northeasterly, the total wave energy increased from 316 cm^2 at 1655 24 March (Fig. 16) to 1960 cm^2 at 0202 25 March (Fig. 26).

The entire spectrum increased, especially the energy at frequencies greater than 120 milliHz (8.3 seconds). Later, energy increased to 3224 cm^2 for 1313 30 March (Fig. 27). The increase in total energy may have been due to the change in the local wind direction only, as there were no discernible dispersive energy peaks in this or in any of the previous five spectra (Figs. 12-16, and 26) which would indicate the effect of a distant source. Also, there were no nearby storms during this period.

Hurricane Denise

Hurricane Denise approached closer to the Hawaiian Islands than did any other tropical storm or hurricane during the period of study. Denise appeared as a tropical storm southeast of the Islands at 14°N, 108°W, at 0800 4 July. Travelling westward, she covered 5500 km in 9 days. She became a hurricane at 0800 6 July at 13°N, 117°W. As a hurricane, her closest approach to the Islands was to 19°N, 149°W, approximately 900 km southwest of Oahu, at 0200 12 July. Spectra were calculated for 10, 12, and 13 July (Figs. 35-37), during which time strong tradewinds and a gale to the northwest also existed. The spectra were probably not the product of Hurricane Denise nor of the gale, but of the strong tradewinds because: (1) the total energies (2799 cm^2, 2766 cm^2, and 1863 cm^2) are indicative of total energies for strong tradewinds and not of a gale; (2) there were no traceable dispersive energy peaks that would indicate distant storms or other distant sources; and (3) there were no nearby-storms during this period.

RESULTS AND CONCLUSIONS

After the wave-energy spectra comparisons had been made, the following results were apparent:

(1) The average total energy of all the spectra for the strong local tradewinds was found to be greater than the average total energy of all the spectra for identifiable storms.

(2) The average total energy of all the spectra for the strong local tradewinds was twice as great as that for the weak local tradewinds. The average total energy between 180 and 250 milliHz, resulting from the local wind, was also twice as great for strong tradewinds.

(3) The average total energy of all the spectra for strong local tradewinds was four times as great as that for strong local southerly winds. The average total energy between 180 and 250 milliHz was seven times greater for strong tradewinds.

(4) Hurricane Denise and other tropical storms and hurricanes southeast of the Hawaiian Islands had little effect on the energy structure in Kaneohe Bay.

Thus for Kaneohe Bay, the direction of the local wind or the location of the storm is very important. Tradewinds produce higher waves than do southerly winds; storms to the northeast, north, or northwest have greater effect on the Bay than do storms to the southeast, south, southwest, or west. Of all storms, storms to the north or northeast which generate swells that approach directly into Kaneohe Bay could be expected to produce the greatest wave energy. Although no such storm occurred during the period of study, there was such a storm toward the end of January 1972. A gale centered at 36^{o}N, 150^{o}W (approximately 1800 km northeast of Oahu) on 28 January, became a storm and was reported at 31^{o}N, 151^{o}W (approximately 1500 km northeast of Oahu) on 29 January. On 29-30 January, 10-foot swells from the north caused high surf warnings to be in effect for the north shore. During that time, waves seen in Kaneohe Bay were higher than any seen during the study period.

Thus there is the possibility that on any given day a storm may generate more wave energy than strong tradewinds. However, over periods as long as a year, strong tradewinds, because they occur more frequently than storms, will produce more total energy.

APPENDIX A

Instrumentation, Data Storage and Computer Programming

Instrumentation

The instruments used to measure and to store the wave-height data were located north of Kapapa Island and on Moku O Loe (Coconut) Island in Kaneohe Bay. To the north of Kapapa Island, a Vibrotron pressure gauge was installed to measure sea-surface elevations. The pressure gauge rested on the ocean bottom in approximately 8 meters (~26 feet) of water (Fig. 2). Approximately 900 meters (~3000 feet) of single conductor submarine cable connected this pressure gauge to an FM transmitter located on Kapapa Island. Powered by four, 6-volt car batteries, the transmitter broadcasted a vertically polarized signal at 162.175 MHz.

On Coconut Island, this signal was received at the Hawaii Institute of Marine Biology (HIMB). A cable led from the receiver to a digital tape recorder which stored the data on magnetic tape. A telephone line was installed which permitted a check on reception of the audio signal by the tape recorder.

Data Storage

Data were stored on magnetic tape and on disks. Initially, data were recorded on half-size reels (1200 feet) of magnetic tape at 200 BPI, Binary, and 7-track. These reels were usually changed with each transmitter battery change, usually every 2 weeks. The data were then transferred to full-size (2400 feet) reels, at 800 BPI, EBCDIC, and 9-track, or 556 BPI, BCD, and 7-track. Two sets of data were kept in their original form on the half-reels on which they were originally recorded. Thus all the data were kept on 2 full-size reels and 2 half-size reels. All the data were also stored on an IBM 2316 disk pack. The sea-surface elevation values were separated from the rest of the data and stored on still another IBM 2316 disk pack. The two complete sets of data on tape and on disk were to insure against data loss, and the set of separated wave-height values on the other disk was for convenience in calculating the spectra.

Computer Programming

The computer program for calculating the wave-energy spectra (Table 1) is comprised of two main sections: an error correction section to detect and correct bad values, and a "Fast Fourier Transform" section to calculate the spectral values.

The error correction section begins after the data are read for one wave record and stored.

To detect errors, first the sea-surface elevation values were checked against a maximum and a minimum value which were set after a few wave records had been examined. If the maximum or minimum value was exceeded, the bad value was set to the maximum value. Later, in the error correction section, if more than 40 bad values (approximately 1 per cent of the total number of values) were detected by the computer, the program stopped. Forty bad values generally means that all the values are larger than the maximum value. Such a large number of bad values may indicate a systematic instrument error. Next, the differences between successive sea-surface elevation values were calculated; i. e., the first sea-surface elevation value was subtracted from the second sea-surface elevation value, and so on. This first difference may be thought of as describing the slope of the wave--whether the wave is steep or gentle. A distribution curve of these first differences was plotted. The standard deviation of these first differences previously had been calculated and the first differences were limited to ±3 standard deviations (within which should lie 99.73 per cent of the first difference values). This first difference curve should resemble a Gaussian or normal distribution. A large number of values clustered at the endpoints of the curve would indicate that a correction was needed. More than one maximum may indicate systematic instrument error. Last, the difference between consecutive first differences were calculated; i. e., the first 1st difference was subtracted from the second 1st difference, and so on. This second difference describes the curvature of the wave. A distribution curve, which may be Gaussian or skewed, was plotted.

Now the correction of bad values began. If any sea-surface elevation was found to equal the previously set maximum value, that value was replaced with the average of the two sea-surface elevation values on either side. If either a first difference or a second difference value exceeded ±3 standard deviations of its value, the value was corrected. The second difference was checked first and if it was too large, the sea-surface elevation value associated with this second difference was corrected by averaging the two sea-surface elevation values on either side. Then the first difference was checked and the sea-surface elevation values were averaged again if bad values were still found. If the first difference between two sea-surface elevation values was bad, the second value was assumed to be wrong and the values on either side were averaged. For a visual check of the accuracy of these corrections, another first difference distribution curve and a plot of sea-surface elevations versus time were made.

If fewer than five consecutive bad sea-surface elevation values were found, the wave energy spectrum was calculated next. Otherwise, the energy spectrum was not calculated and the computer continued to another wave record.

APPENDIX B

Tables 1 to 3

Table 1

Computer Program

PAGE 001

```
C  JCASE=1,2 GIVES SPECTRUM. JCASE = 3,4,5,6 GIVES LOG SPECTRUM. JCASE=1,3 PLOTS
C   BETWEEN LIMITS XL AND XG READ IN. ALL OTHER JCASE LIMITS CALCULATED FROM
C   THE SPECTRUM.  JCASE = 5 XL IS CALCULATED AND XG=XL+5. JCASE=6 VISE VERSA.
C   THE SPECTRUM. JCASE=5 USES XG=XL(CALCULATED )+5. JCASE=6 GIVES XL=XG(CALC)-5.
C   NOTE THE NEED FOR A PARAMETER CARD.
      INTEGER SUMINT(50)
      DIMENSION FMT(10), F(4100), AC(500), CS(500), PS(500), PL(101),
     1B(50,100), ALOW(50), ALP(50), ADIFF(5000), PPERCT(50)
      DIMENSION TI(4), TX(2), TY(6), PSD(251,2), U(5000)
      DIMENSION R(102), KTEST(6)
      DIMENSION ET(500), TDIFF(5000)
      DIMENSION FA(2100), FB(2100), FC(2100)
      DATA IZEE,IONE/1H ,1H*/, IB/'8'/, STAR/'*'/, BLANK/' '/, W/'W'/
      DATA STAR, BL, EYE / '*', ' ', 'I'/
      DATA TX, TY/'   C','PS  ',' LOG',' ENE','RGY ','(CM*','*2/C',
     1'PS) '/, DOT/'#'/
      DATA CR/'Q'/
      DEFINE FILE 22 (15920,1600,E,IPO)
CCC   READ FORMAT CARD                               CCC
      READ (5,21) N,M,NEST,JCASE, XL, XG
   21 FORMAT (4I5, F5.1, F5.1)
CCCCC                                                CCCCC
CCC   READ CARD FOR DISK RECORD NO.                  CCC
 211  READ (5,217,END=233) LOW, MAX
 217  FORMAT (2I5)
CCCCC                                                CCCCC
C FMX = MAX. ALLOWED VALUE OF RAW DATA, THIS IS SET ARBITRARILY
C FMN - MIN. ALLOWED VALUE OF RAW DATA, THIS IS SET ARBITRARILY
      FMX=160000.
      FMN=140000.
CCC   CLF = CALIBRATION FACTOR FOR DIMENSIONS IN FEET   CCC
CCC   CLM = CALIBRATION FACTOR FOR DIMENSIONS IN METERS   CCC
CCC   CAL = CALIBRATION FACTOR FOR DIMENSIONS IN CENTIMETERS   CCC
      CLF = .000609
      CLM = .000186
      CAL = .0186
CCC   VM, VS, VN, VT ARE USED FOR THE PLOTTING OF THE 'DATA VS. TIME'
C                    CURVES
C   VM AND VN = AMOUNT TO BE SUBTRACTED FROM DATA
C   VS AND VT = SCALING FACTOR
      VM = 138000.
      VS = 200.
      VN = 141000.
      VT = 200.
CCCCC                                                CCCCC
      IPO=LOW
CCCCC                                                CCCCC
C READ 16 DISK RECORDS OF 256 VALUES EACH AND STORE: TOTAL OF 4096 PTS.
      DO 737 I=1,16
      LL=256*(I-1) + 1
      LIM = LL+255
      READ (22'IPO,200,ERR=150) TI, (F(K),K=LL,LIM)
 200  FORMAT (4A4,200F6.0,56F6.0)
 737  CONTINUE
CCCCC                                                CCCCC
      IPOO=IPO-1
      PRINT 352
 352  FORMAT ('1')
      PRINT 569, LOW,IPOO,TI
```

Table 1 (Continued)

Computer Program


```
 569  FORMAT (3X, 'LOW=',I5,5X,'MAX=',I5,5X,4A4)
CCC   Q FLAGS BAD DATA (DATA THAT HAS BEEN CORRECTED BY CORRECTION
C                     ROUTINE) ON DATA VS. TIME PLOT          CCC
C BLANKING OUT Q ARRAY
      DO 26 K=1,N
  26  Q(K) = BLANK
      NS = 0
      ICARD=0
      RG = 980.*980.
      H = 26.*30.48
      HG = H/980.
      SHG = SQRT(HG)
      PI = 3.141593
      TPI = 2.*PI
C CALCULATION OF 1ST DIFFERENCE, MEAN, MAX, MIN
  20  DO 401 I=1,N
      IF(F(I).LE.FMX) GO TO 805
      PRINT 809, I, F(I)
 809  FORMAT(5X,I6,5X,F12.5)
      Q(I) = QR
      F(I)=FMX
      NS = NS+1
      IF(NS.GT.40) GO TO 211
      GO TO 401
 805  IF(F(I).GE.FMN) GO TO 401
      PRINT 809, I, F(I)
      Q(I) = QR
      F(I)=FMX
      NS = NS+1
      IF(NS.GT.40) GO TO 211
 401  CONTINUE
      IGO=0
 8100 IGO = IGO + 1
      AMIN=0
      AMAX=0
      SUMX=0
      SUMXSQ=0
C   ZEROING OF INTERVAL ARRAY
      DO 57 K=1,50
      PPERCT(K)=0
 57   SUMINT(K)=0
      DO 67 I=1,50
      DO 67 K=1,100
 67   B(I,K)=BLANK
      DO 500 I=2,N
      DIFF=F(I) - F(I-1)
      ADIFF(I-1) = DIFF
      IF (DIFF.GT.AMAX) AMAX=DIFF
      IF (DIFF.LT.AMIN) AMIN=DIFF
      SUMX = SUMX + DIFF
      SUMXSQ = SUMXSQ + DIFF*DIFF
 500  CONTINUE
      AN = N-1
      AMEAN = SUMX/AN
C STANDARD DEVIATION = SIGMA
      SIGMA =SQRT((SUMXSQ - (SUMX*SUMX)/AN)/(AN-1))
      ALIMIT=3.*SIGMA
C ONEDIF = VALUE OF DIFFERENCE BETWEEN 2 DATA PTS.
      ONEDIF = ALIMIT
```

Table 1 (Continued)

Computer Program


```
      DFEET = ALIMIT*CLF
      DMETER = ALIMIT*CLM
      FMIN = AMIN*CLF
      DMMIN = AMIN*CLM
      FMAX = AMAX*CLF
      DMMAX = AMAX*CLM
      FMEAN = AMEAN*CLF
      DMMEAN = AMEAN*CLM
      AINT = 6.*SIGMA/50.
      ALOWL=AMEAN-ALIMIT-AINT
      DO 340 I=1,50
      ALOWL = ALOWL + AINT
      ALOW(I) = ALOWL
 340  AUP(I) = ALOW(I) + AINT - .1
      KL = N-1
      DO 515 K=1,KL
      L= (AMEAN + ALIMIT + ADIFF(K))/AINT + 1.
      IF (L.GE.1.AND.L.LE.50) GO TO 250
      IF (L.LT.1) L=1
      IF(L.GT.50) L=50
 250  SUMINT(L)=SUMINT(L) + 1
 515  CONTINUE
C    NEAREST .2%, I.E., .1% AND ABOVE ARE INCLUDED IN NEXT .2%
      DO 333 K=1,50
      PP=1000.*(SUMINT(K)/AN) +.5
      IF (PP.GE.1.5) GO TO 301
      PPERCT(K)=0
      GO TO 333
 301  MCM=PP/200
      PP=PP - 200.*MCM
      IPCT = PP/2. + .5
      PPERCT(K) = IPCT/5.
      B(K,IPCT) = STAR
      IF (MCM.GT.0) B(K,IPCT) = W
 333  CONTINUE
C    PRINT HEADINGS FOR 1ST DIFFERENCE GRAPH
      PRINT 351
 351  FORMAT ('1',1X,'1ST DIFFERENCE',4X,'NUM   PCT 0',24X,'5',23X,
     1'10',.3X,'15',23X,'20'//)
C PRINT 1ST DIFFERENCE GRAPH
      PRINT 350, (ALOW(K),AUP(K),SUMINT(K),PPERCT(K),(B(K,L),L=1,100),K=
     11,50)
 350  FORMAT (1X,2F8.1,I6,F6.1,2X,100A1)
      PRINT 367, AMIN, AMAX, AMEAN, SIGMA, T1, N
 367  FORMAT (//10X,'MIN =',F8.1,5X,'MAX =',F7.1,5X,'MEAN =',F7.1,5X,
     1'SIGMA =',F7.1,'  RECORD BEGAN ',+A4, 5X, 'N =',I4)
      PRINT 605, FMIN,DMMIN,FMAX,DMMAX,FMEAN,DMMEAN,DFEET,DMETER
 605  FORMAT(/1X,'MIN =',F6.2,'FT,',1X,F6.2,'M',3X,'MAX =',F6.2,'FT,',1X
     1,F6.2,'M',3X,'MEAN =',F7.4,'FT,',1X,F7.4,'M',3X,'MAX ALLOWED CHANG
     1E IN HT =',F6.2,'FT,',1X,F6.2,'M')
      GO TO (8101,8102), IGO
 8101 SUMX = 0
C    CALCULATE 2ND DIFFERENCE AND PLOT
      SUMXSQ=0
C    ZEROING OF INTERVAL ARRAY
      DO 507 K=1,50
      PPERCT(K)=0
 507  SUMINT(K)=0
      DO 607 I=1,50
```

Table 1 (Continued)

Computer Program


```
      DO 607 K = 1,100
 607  B(I,K)=BLANK
      KC = N-2
      DO 501 I=1,KC
      TDIF = ADIFF(I+1) - ADIFF(I)
      TDIFF(I) = TDIF
      SUMX = SUMX + TDIF
      SUMXSQ = SUMXSQ + TDIF*TDIF
 501  CONTINUE
      FZ = KC
      AMEAN = SUMX/FZ
      SIGMA =SQRT((SUMXSQ - (SUMX*SUMX)/FZ)/(FZ-1))
C TWODIF = 2ND DIFFERENCE; DIFFERENCE OF DIFFERENCE
      TWODIF=3.*SIGMA
      AINT = 6.*SIGMA/50.
      ALCWL=AMEAN-TWODIF-AINT
      DO 502 I=1,50
      ALCWL = ALCWL + AINT
      ALCW(I) = ALCWL
 502  AUP(I) = ALOW(I) + AINT - .1
      DO 503 K=1,KC
      L= (AMEAN + TWODIF + TDIFF(K))/AINT + 1.
      IF (L.GE.1.AND.L.LE.50) GO TO 675
      IF (L.LT.1) L=1
      IF(L.GT.50) L=50
 675  SUMINT(L)=SUMINT(L) + 1
 503  CONTINUE
C   NEAREST .2%. I.E., .1% AND ABOVE ARE INCLUDED IN NEXT .2%
      DO 633 K=1,50
      PP=1000.*(SUMINT(K)/FZ) +.5
      IF (PP.GE.1.5) GO TO 631
      PPERCT(K)=0
      GO TO 633
 631  MCM=PP/200
      PP=PP - 200.*MCM
      IPCT = PP/2. + .5
      PPERCT(K) = IPCT/5.
      B(K,IPCT) = STAR
      IF (MCM.GT.0) B(K,IPCT) = W
 633  CONTINUE
C   PRINT HEADINGS FOR 2ND DIFFERENCE GRAPH
      PRINT 651
 651  FORMAT('1',19X,'NUM   PCT 0',24X,'5',23X,'10',23X,'15',23X,'20'//)
C PRINT 2ND DIFFERENCE GRAPH
      PRINT 650, (ALOW(K),AUP(K),SUMINT(K),PPERCT(K),(B(K,L),L=1,100),K=
     11,50)
 650  FORMAT (1X,2F8.1,I6,F6.1,2X,100A1)
      PRINT 596
 596  FORMAT (25X,'2ND DIFFERENCE GRAPH')
CCC IN THESE CORRECTIONS, ONLY F(I)'S ARE CHANGED; THE 1ST AND 2ND
C   DIFFERENCES (ADIFFAND SECD) ARE CALCULATED FROM THE ORIGINAL F(I)'S
C   AND ARE NOT CHANGED AFTER F(I)'S ARE CORRECTED
      PRINT 352
      JCTR=0
      PRINT 973
 973  FORMAT (21X,'F(I-1)',7X,'F(I)',7X,'F(I+1)',4X,'I',8X,'OLOF',12X,
     1'ADIFF OR SECD')
C   F HAS 4096 PTS,  ADIFF HAS 4095 PTS,  TDIFF HAS 4094 PTS
C   ADIFF(4095) IS SET EQUAL TO ADIFF(4094) BECAUSE I AM CHECKING ONLY
```

Table 1 (Continued)

Computer Program

PAGE 005

```
C      TO THE 4095TH DATA PT.; THEREFORE, IF THE DIFFERENCE BETWEEN THESE
C      2 PTS IS GT. TWODIF, THEN F(4095) WOULD NEED TO BE CORRECTED BY
C      AVERAGING F(4094) AND F(4096).  HOWEVER, IN MY LOOP, I AM LOOKING
C      ONLY AS FAR AS F(4095).
       ADIFF(KL)=ADIFF(KL-1)
       KT = 0
       DO 402 I=2,KL
       JC = 0
       SECD = TDIFF(I-1)
       SECD= ABS(SECD)
       IF(F(I).NE.FMX) GO TO 420
       JC = JC + 1
       F(I) = (F(I-1) + F(I+1))*.5
       Q(I) = QR
       PRINT 403, F(I-1), F(I), F(I+1), I
  403  FORMAT (16H LIMIT EXCEEDED , 3F12.1,I6)
C  THIS OLDF IS EITHER THE ORIGINAL F(I) OR THE F(I) CORRECTED BECAUSE
C    IT IS GREATER THAN FMX
 420   OLDF=F(I)
       IF(SECD.LE.TWODIF) GO TO 421
       JC = JC + 1
       F(I) = (F(I-1) + F(I+1))*.5
       Q(I) = QR
       PRINT 404, F(I-1), F(I), F(I+1), I, OLDF, SECD
  404  FORMAT (16H 2ND DIFFERENCE , 3F12.1,I6,F12.1, 6X, F12.1)
C    IF THE 1ST DIFFERENCE BETWEEN 2 DATA PTS IS BAD, I AM ASSUMING THAT
C      THE 2ND DATA PT IS THE CAUSE OF THE BADNESS
 421   IF(ABS(ADIFF(I-1)).LT.ONEDIF) GO TO 520
C  THIS OLDF CAN BE THE ORIGINAL F(I) OR THE F(I) CORRECTED BECAUSE THE
C    SECOND DIFFERENCE IS GREATER THAN TWODIF OR THE F(I) CORRECTED
C    BECAUSE IT IS GREATER THAN FMX AND ITS SECOND DIFFERENCE IS GT 2DIF
       OLDF=F(I)
       JC = JC + 1
       F(I)=.5*(F(I-1)+F(I+1))
       Q(I) = QR
       JCTR = JCTR+1
       PRINT 405, F(I-1), F(I), F(I+1), I, OLDF, JCTR, ADIFF(I-1)
 405   FORMAT(16H 1ST DIFFERENCE , 3F12.1, I6, F12.1, I6, F12.1)
 520   IF(JC.EQ.0) GO TO 402
       KT = KT + 1
C IF THERE ARE 5 OR MORE CONSECUTIVE BAD VALUES, KT IS .GE.5 AND THE
C SPECTRUM IS NOT CALCULATED
       IF(KT.GE.5) GO TO 402
       IF(KT.GT.1) GO TO 521
 522   KTEST(KT) = I
       GO TO 402
 521   IF(KTEST(KT-1).EQ.(I-1)) GO TO 522
C IF THERE ARE LESS THAN 5 CONSECUTIVE BAD VALUES, KT IS SET BACK TO
C ZERO AND THE SEARCH FOR 5 CONSECUTIVE BAD VALUES BEGINS AGAIN
       KT = 0
 402   CONTINUE
       IF(IGO.EQ.1) GO TO 8100
C  PLOTS COUNTS VS. TIME IN TWO CURVES; EACH CURVE CONSISTS OF N/2 PTS.
 8102 NN=N/2
       PRINT 352
       DO  409 I=1,NN
       DO 442 MZ=1,101
 442   R(MZ)=BLANK
       IPA = (F(I)-VM)/VS
```

Table 1 (Continued)

Computer Program


```
      NNN=I*NN
      IPB = (F(NNN)-VN)/VT
      IF(IPB.GE.0.AND.IPB.LE.100.) GO TO 749
      IF(IPB.LT.0.) NIPB=IPB/100.
      IPB=-IPB + 100*NIPB
      R(IPB)=W
      GO TO 750
 749  R(IPB)=DOT
 750  R(IPA)=STAR
 409  PRINT 408, Q(I), I, Q(NNN), NNN, F(I), F(NNN), (R(MZ),MZ=1,101)
 408  FORMAT (1X,A1,I4,1X,A1,I4,2F8.0,2H |,101A1,1H|)
      IF(KT.GE.5) GO TO 211
C  CALCULATE AVERAGE
      AV=0.
      DO 291 I=1,N
 291  AV=AV + F(I)
      AV=AV/N
      PRINT 24, AV
  24  FORMAT ('0AVERAGE VALUE OF F = ', E12.5)
      PRINT 352
C   CALCULATE SPECTRUM
C  CALIBRATION FACTOR IS .0186 (IN CM)
      DO 937 I=1,N
C F(I) BECOMES CALIBRATED VALUE, ITS UNITS ARE CM; THE SPECTRUM IS
C ENERGY IN SQ.CM/CYCLE PER SECOND
 937  F(I) = (F(I)-AV)*CAL
      CALL FOURC3(F,4096,1,2049,2,FA,FB,FC)
      CALL SMFC(FC,PS,2049,8,NEST)
CCCCC                                                       CCCCC
C   DF = FREQUENCY INTERVAL BETWEEN SPECTRAL ESTIMATES
      DF = 1./(2.*(NEST-1.)*2.)
CCCCC                                                       CCCCC
      DO 8 I = 2,100
    8 PL(I) = BL
      DO 9   I = 1,101,50
    9 PL(I) = EYE
      IF(JCASE.LE.2)GO TO 11
CCC   PUNCHES CARDS WITH RAW SPECTRAL VALUES (WITHOUT TAKING LOG
C               AND WITHOUT CORRECTING FOR DEPTH)    CCC
      PUNCH 567, LOW, IPOO, TI
 567  FORMAT (2I5,4A4)
      DO 554 I=1,NEST,6
      IUPA = I+ 5
      ICARDA = I/6 + 1
 554  PUNCH 555, (PS(K),K=I,IUPA), ICARDA
 555  FORMAT (6E12.5, 9X, I3)
CCC   THIS PORTION MAKES DEPTH CORRECTION AND TAKES LOG    CCC
C SIGMA**2 = G*K*TANH(K*H)
C BETA**2 = ALPHA*TANH(ALPHA)
C ALPHA = K*H
C BETA = SIGMA*SQRT(H/G)
C SIG = FREQUENCY (CYCLES/SEC)
C SIGMA = FREQUENCY (RADIANS/SEC) = 2*PI*SIG
      SIG = 0.
      PUP = 0.
      QSM = 0.
      DO 645 I=1,NEST
      BETA = TPI*SIG*SHG
      AKH = ALPHA(BETA)
```

Table 1 (Continued)

Computer Program


```
      COSHK = (EXP(AKH) + EXP(-AKH))/2.
C     ET(I) IS DEPTH CORRECTED SPECTRAL ESTIMATE
      ET(I) = PS(I)*COSHK*COSHK
      PUM = PUM + ET(I)
      QSM = QSM + PS(I)
      PS(I) = ALOG10(ABS(PS(I)) + 1.E-30)
      ET(I) = ALOG10(ABS(ET(I)) + 1.E-30)
      SIG = SIG + DF
  645 CONTINUE
CCCCC                                                   CCCCC
   11 IF(JCASE.EQ.1.OR.JCASE.EQ.3)GO TO 13
      PM = -1.E30
      PG = 1.E30
      DO 12  I=1,NEST
      PM = AMAX1(PM, ET(I))
   12 PG = AMIN1(PG, ET(I))
      XL = PG
      XG = PM
      IF(PM.LE.3.0.AND.PG.GE.-2.0) XG = 3.0
   13 CONTINUE
      IF (JCASE.EQ.5) XG = XL+5.
      IF (JCASE.EQ.6) XL = XG-5.
      RANGE = 100./(XG-XL)
      PRINT 22, N, NEST, XL, XG, JCASE, TI
   22 FORMAT (///' NO. POINTS =',I5,' NO. ESTIMATES = ',I3,' XL = ',
     1E12.5,' XR = ',E12.5,' JCASE = ',I2,'   RECORD BEGAN ',4A4)
      DO 14  I = 1,NEST
      KK = (PS(I) - XL) * RANGE +1.
      IF (KK.LE.1.) KK=1
      IF (KK.GE.101) KK = 101
      DUMMY = PL(KK)
      PL (KK) = STAR
      LL = (ET(I)-XL)*RANGE + 1.
      IF(LL.LE.1) LL=1
      IF (LL.GE.101) LL=101
      DUM = PL(LL)
      PL(LL) = DOT
      IMN=I-1
      PRINT 23, IMN, PS(I), ET(I), PL
   23 FORMAT (1X, I3, 1X, E11.5, 1X, E11.5, 1X, 101A1)
      PL(LL) = DUM
   14 PL(KK) = DUMMY
CCC   PRINTS SUM OF ENERGY   CCC
      PRINT 772, QSM, PUM
  772 FORMAT (3X,'SUM OF ENERGY AT DEPTH = ',E12.5,7X,'SUM OF ENERGY AT
     1SURFACE = ',E12.5)
      PRINT 352
      GO TO 211
  150 PRINT 410
  410 FORMAT (3X, 'ERROR IN READING DISK')
      GO TO 211
  233 STOP
      DEBUG SUBCHK
      END
      SUBROUTINE FOURC3(F,LEN,JL,JU,JCASE,FA,FB,FC)
      DIMENSION F(4100),FA(2100),FB(2100),Y(4098),FC(2100)
      DIMENSION AA(2), BB(2), JNT(16), G(2)
      COMPLEX X(4098), A, B, W, Z1, ZR
      EQUIVALENCE(G,W),(A,AA),(B,BB),(X,Y)
```

Table 1 (Continued)

Computer Program


```
      ZR=(1.,0.)
      ZI=(0.,1.)
      PRINT 30,LEN,JL,JU,JCASE
   30 FORMAT('0SUBROUTINE FOURC3 CALLED WITH LEN = ',I5,' JL = ',I4,
     1 ', JU = ',I4,', AND JCASE = ',I2)
      IF(JCASE.EQ.2)GO TO 116
      DO 115 J=1,LEN
  115 Y(J)=F(J)
      GO TO 15
  116 AV=0.
      DO 4 J=1,LEN
    4 AV=AV+F(J)
      XL=LEN+1
      AV=AV/(XL-1.)
      DO 5 J=1,LEN
      XJ=J*2
      ARG=3.1415927*(XJ/XL-1.)
    5 Y(J)=(F(J)-AV)*(.54+.46*COS(ARG))*1.56
   15 L=LEN-1
      DO 20 I=1,16
      L=L/2
      IF(L.EQ.0)GO TO 16
   20 CONTINUE
      STOP
   16 LX=2**I
      ZLZ=2./FLOAT(LEN)
      LLX=LX-LEN
      N=I-1
      L=LX/2
      ZL=L
      OZL=1./ZL
      PIOL=3.1415927*OZL
      DO 11 I=1,N
   11 JNT(I)=2**(N-I)
      SUM=0.
      DO 8 I=1,LEN,2
    8 SUM=SUM+Y(I)-Y(I+1)
      LEN1=LEN+1
      DO 13 I=LEN1,LX
   13 Y(I)=0.
      Y(LX+1)=SUM*ZLZ
      Y(LX+2)=0.
      DO 40 LAYER=1,N
      NBLOCK=2**(LAYER-1)
      LBLOCK=L/NBLOCK
      LBHALF=LBLOCK/2
      NW=0
      DO 40 IBLOCK=1,NBLOCK
      LSTART=LBLOCK*(IBLOCK-1)
      ARG=-2.*PIOL*FLOAT(NW)
      G(1)=COS(ARG)
      G(2)=SIN(ARG)
      DO 25 I=1,LBHALF
      J=I+LSTART
      K=J+LBHALF
      A=X(K)*W
      X(K)=X(J)-A
   25 X(J)=X(J)+A
      DO 32 I=2,N
```

Table 1 (Continued)

Computer Program


```
      IF(AND(JNT(I),NW).EQ.0.)GO TO 40
   32 NW=NW-JNT(I)
   40 NW=NW+JNT(I)
      NW=0
      DO 80 K=1,L
      NW1=NW+1
      IF(NW1.LE.K)GO TO 55
      B=X(NW1)
      X(NW1)=X(K)
      X(K)=B
   55 DO 70 I=1,N
      IF(AND(JNT(I),NW).EQ.0.)GO TO 80
   70 NW=NW-JNT(I)
   80 NW=NW+JNT(I)
      W=CEXP(PIOL*ZI)
      X(1)=ZR*(Y(1)+Y(2))*ZLZ
      LL=L/2+1
      DO 90 I=2,LL
      J=L-I+2
      A=.5*(ZR*(Y(2*I-1)+Y(2*J-1))+ZI*(Y(2*J)-Y(2*I)))
      B=.5*(ZR*(Y(2*I-1)-Y(2*J-1))-ZI*(Y(2*J)+Y(2*I)))*W**(I-1)
      X(I)=(A+ZI*B)*ZLZ
      Y(2*J-1)=(AA(1)+BB(2))*ZLZ
   90 Y(2*J)=(BB(1)-AA(2))*ZLZ
      LX=LX+2
      L=L+1
      DO 91 I=JL,JU
      FA(I)=Y(2*I-1)
      FB(I)=Y(2*I)
   91 FC(I)=FA(I)**2+FB(I)**2
      PETURN
      OEBUG SUBCHK
      END
      SUBROUTINE SMFC(C,D,N,M,N1)
      DIMENSION C(2100), D(300)
      CK=0.
      IF(M/2*2.EQ.M) CK=.5
      M1=M/2
      N1=1+(N-1-M1)/M
      PRINT 21,N,M,N1
   21 FORMAT('OSUBROUTINE SM FC CALLED WITH N= ',I5,', M= ',I2,    ',NUMB
     1ER OF COEFFICIENTS RETURNED IS ',I4)
      D(1)=C(1)
      DO 1 J=1,M1
    1 D(1)=C(1)+C(J+1)
      D(1)=D(1)-CK*C(M1)
      DO 2 I=2,N1
      K=(I-1)*M+1
      D(I)=C(K)
      DO 3 J=1,M1
    3 D(I)=D(I)+C(K+J)+C(K-J)
    2 D(I)=D(I)-CK*(C(K+M1)+C(K-M1))
      RETURN
      DEBUG SUBCHK
      END
      FUNCTION ALPHA(BETA)
      TEST=1.E-05
      BB=BETA*BETA
      IF(BETA.LE.1.) A=BETA
```

Table 1 (Continued)

Computer Program


```
      IF(BETA.GT.1.) A=BB
   30 X=EXP(A)
      Y=EXP(-A)
      Z=(X-Y)/(X+Y)
      CC=BB-A*Z
      IF(ABS(CC).LT.TEST) GO TO 50
      SECH=2./(X+Y)
      ALP=A-CC/(-Z-A*SECH*SECH)
      A=ALP
      GO TO 30
   50 ALPHA=A
      RETURN
      END
```

Table 2

A Daily Summary of Gales, Storms, Smallcraft Warnings and the Number of Wave Energy Spectra

Legend:

G. Gale, wind speed greater than 33 knots.

S Storm, wind speed greater than 47 knots.

TS Tropical storm, wind speed greater than 33 knots.

T Typhoon, wind speed greater than 64 knots (a hurricane of the East Asia sector).

H Hurricane, wind speed greater than 64 knots.

SCW Smallcraft warning.

GW Gale warning, put into effect when wind speeds are 34-47 knots.

· A wave energy spectrum.

* Weather data from 0200 HST National Weather Service surface analyses and weather records. Other weather data are from First Weather Wing and Fleet Weather Central 0200 HST surface analyses.

Table 2. (Continued) A Daily Summary of Gales, Storms, Smallcraft Warnings and the Number of Wave Energy Spectra

JANUARY						
					22 * G(46N,174W)—— S(42N,148E)——	23 * —(41N,171W)—— —G(38N,156E)——
24 * —(41N,170W) —(44N,168E)——	25 * G(49N,145W) —(42N,168E) G(41N,166W)——	26 ● * SCW S winds G(41N,150E)—— G(34N,173W) —(38N,160W)	27 ● * GW S winds —(48N,160E)—— G(52N,150W) G(27N,169W)——	28 ● * SCW SW-WSW winds —(48N,163E)—— —(33N,162W)——	29 * —(40N,162E) —(38N,153W)——	30 * G(47N,161E) —(47N,150W)——
31 * S(41N,160E) G(54N,149E) —(51N,153W)						

Table 2. (Continued) A Daily Summary of Gales, Storms, Smallcraft Warnings and the Number of Wave Energy Spectra

FEBRUARY	1	2	3	4	5	6
	GW for S winds G(37N,153E) G(58N,154W)	G(45N,152E) G(38N,167E) S(43N,178W)	G(37N,156E) (45N,175W)	(48N,173W)	(51N,174W)	G(39N,160E) G(50N,177E)
7	**8**	**9**	**10**	**11**	**12**	**13**
S(54N,160W) (50N,180)	G(55N,170W) (48N,177E)	G(51N,137W) (47N,179W)	G(35N,168E) (50N,175W)	(44N,172W) S(53N,154W)	(48N,168W) G(27N,147E) G(56N,149W)	(51N,156W) (29N,138E)
14	**15**	**16**	**17 ⊙**	**18 ⊙⊙**	**19 ⊙**	**20 ⊙⊙**
G(55N,146W) (32N,157E)	(58N,144W) (36N,180) G(37N,144E)	(42N,169W) S(38N,155E)	SCW for S winds G(43N,138E) (54N,150W) (35N,175E) G(57N,170W)	(42N,150E) (40N,171W)	(43N,165E) (47N,164W) High surf warnings	SCW for NE winds (44N,179E) (55N,156W) for N & W shores
21 ⊙	**22 ⊙**	**23 ⊙**	**24**	**25 ⊙**	**26**	**27**
(46N,173E) G(36N,179W) G(57N,150W)	(43N,170W) (58N,146W)	G(51N,135W) G(42N,145E)	S(51N,148E)	G(37N,163W) (52N,150E)	(36N,163W) G(53N,161E)	SCW for E winds (36N,165W) (52N,170E) G(30N,174E) G(31N,151E)
28						
(42N,162W) G(49N,146E) (30N,177W) S(37N,159E)						

Table 2. (Continued) A Daily Summary of Gales, Storms, Smallcraft Warnings and the Number of Wave Energy Spectra

MARCH	1 S(46N,162E)— G(30N,175W) G(57N,151W)—	2 —(46N,154E)— G(34N,130E)— —S(58N,149W)—	3 —G(43N,162E) —(38N,144E)— —(57N,141W)— G(39N,170W)—	4 SCW for ENE winds —S(40N,149E)— —G(59N,140W) —(44N,167W)—	5 ●● G(51N,175W) —(43N,158E)— —(47N,151W)—	6 ● —(48N,159E)— —(51N,136W)
7 ● G(53N,170W)— —(49N,160E)—	8 ● —(52N,153W)— —G(48N,166E)—	9 —(56N,138W) —(51N,171E)— G(50N,165W)—	10 —(50N,176W)— —(54N,147W)	11 G(44N,150E) —(50N,165W) G(43N,166E) S(47N,139W)—	12 SCW for NE winds G(47N,173W)— —(52N,134W)	13 —S(50N,147W)—
14 G(38N,157E) —(52N,135W) G(48N,175E)—	15 G(36N,144W)— —S(52N,172W)—	16 —(34N,140W) —(51N,166W)—	17 G(40N,163E)— —(59N,171W)	18 —S(50N,179E)—	19 SCW for S winds— —G(53N,172E) G(48N,150E) G(24N,150E) G(37N,149W)	20 ●● G(51N,156E) G(47N,166E) G(21N,137E)— G(26N,161E) G(33N,156W)
21 ●● G(54N,165E) S(39N,162W) —(20N,139E)—	22 ●● SCW for S winds— G(48N,152E) G(21N,175W)— —(20N,142E) G(44N,146W)—	23 ●●● —(25N,169W)— —(51N,136W)—	24 ●● —(33N,150W)— G(43N,170E)— —(53N,134W)	25 ● SCW for NE winds— —(39N,136W)— —(56N,179E)—	26 G(30N,169E) —S(47N,126W) —(58N,174W)—	27 G(39N,165W) —(56N,169W)—
28 G(52N,137W) G(53N,161E)— —(52N,159W)	29 ● —(55N,174E)	30 ● G(54N,146E)	31 G(55N,164E) G(52N,150W)			

Table 2. (Continued) A Daily Summary of Gales, Storms, Smallcraft Warnings and the Number of Wave Energy Spectra

APRIL				1° G(50N,140E) G(55N,178W) G(55N,144W)	2°° (54N,142E) 51N,159W)	3 NO DATA (56N,145E) (54N,154W)
4 NO DATA (57N,165E) (57N,150W)	5 NO DATA SCW for ENE winds G(50N,139W) GW for ENE winds	6 NO DATA (56N,138W)	7 NO DATA S(43N,159E)	8 NO DATA (47N,166E) G(54N,139W)	9 NO DATA (50N,171E) (53N,140W) G(42N,149E)	10 G(55N,174W) (53N,136W) (40N,153E)
11° G(46N,148W)	12 (46N,142W) G(48N,178W) TS Vera(14N,133E)	13 G(50N,158E)	14 S(59N,150W) T (16N,128E)	15 G(50N,165E)	16° G(51N,136W) S(55N,175W)	17 G(47N,149E) T (24N,129E)
18	19 SCW for NE winds S(55N,174E)	20 G(51N,166W)	21° S(54N,150W) G(43N,172E) G(52N,130E)	22 G(55N,146W) (44N,179W) (55N,143E)	23 (45N,173W) G(44N,152E) TS Wanda(12N,124E)	24° (48N,164W) (51N,153E)
25 G(45N,154E) (57N,161W) (57N,144E)	26 (49N,161E) G(44N,170W)	27 * (50N,170E) G(43N,154E)	28 * G(44N,157E)	29° * (47N,169E)	30 * (49N,176W) G(41N,137W) TS (13N,111E)	

Table 2. (Continued) A Daily Summary of Gales, Storms, Smallcraft Warnings and the Number of Wave Energy Spectra

30 * (56N,163W)	31 ⊙ * S(52N,159W) G(51N,167E)	MAY				1 ⊙ G(40N,129W) G(52N,164W) G(38N,152E) T Wanda(14N,111E) T Amy(9N,147E)
2 (38N,127W) (57N,153W) (39N,166E)	3 (41N,180) TS(20N,110E) TS Babe(16N,118E)	4	5 ⊙ G(45N,149E) G(43N,168W)	6 (47N,160E) (57N,153W) TS(22N,129E)	7 (50N,180) G(37N,152E) TS(33N,156E)	8 (50N,167W) (43N,167E)
9 S(48N,152W)	10 G(52N,150W)	11	12 G(53N,140W)	13 (58N,152W) G(38N,162W)	14 (45N,145W)	15 S(47N,132W)
16 ⊙ G(52N,157W) G(48N,136E)	17 (48N,145W) (52N,137E) G(42N,163E)	18 (43N,177W)	19 (47N,166W) TS Carla(16N,128E)	20 S(56N,163W)	21 G(45N,167E) TS(21N,126E)	22 (49N,178W)
23 (52N,163W) TS Agatha (14N,103W)	24 G(48N,180) (16N,102W)	25 G(47N,140E) T Dinah(12N,128E)	26 (50N,147E)	27 (48N,163E) G(52N,151W)	28 (49N,176E) TS Emma(6N,132E)	29 * (53N,173W) TS (19N,109E)

Table 2. (Continued) A Daily Summary of Gales, Storms, Smallcraft Warnings and the Number of Wave Energy Spectra

JUNE		1 S(57N,157W)	2 ○○	3 G(49N,166W)----	4 ----(45N,151W) G(44N,137E)---	5 SCW for ENE winds-- ----(45N,150E)
6 ---------- G(52N,160W) G(46N,169E)---	7 ----(44N,163W)---	8 ----(52N,153W)---	9 SCW for ENE winds ----(55N,149W)	10 ---------- G(34N,167E)----	11 ---------- ----(40N,178E)-- G(45N,144E)--	12 ○ ----(44N,170W) ----(47N,157E)----
13 ----(52N,167E)---	14 ----(56N,172E) TS Freda(17N,125E	15 G(37N,163E) ---------- TS Bridget(13N,94W)--	16 ----T (19N,117E)--- H (16N,97W)----	17 ○ ----T (21N,115E) ----H (17N,102W)	18 ○ G(44N,162E)---	19 ----(50N,167E) G(40N,150E)
20 ○	21	22	23	24 G(48N,134W) TS Gilda(12N,127E)-	25 ○ ----------	26 ○ -T (17N,116E)----
27 ----T (19N,111E)	28 ○	29 G(44N,171E)	30			

Table 2. (Continued) A Daily Summary of Gales, Storms, Smallcraft Warnings and the Number of Wave Energy Spectra

JULY				1	2 G(56N,167E) TS Harriet(10N,129E)---	3 TS Carlotta(12N,
4 ----T (15N,117E)-- 114W)---	5 TS Ivy(24N,135E)-- TS Denise(15N,112W)	6 G(46N,170E)--- --T (17N,108E) --TS (17N,126W)	7 SCW for ENE winds- -----(53N,172E) --TS (36N,138E) ---H (13N,119W)---	8 G(41N,150E)	9 TS Elenor(14N,121W)	10° G(40N,170E)--- TS Jean(12N,137E)- -TS(14N,138W)---
11 ----(55N,179W)--- ----(15N,130W) TS Kim(16N,113E)- --H (17N,143W)---	12° SCW for NE winds- ------(58N,180)	13° G(41N,155E)--- --T (11N,129E)--- -TS (19N,105E) -TS (17N,153W)	14 -----(46N,166E)	15	16 TS Lucy (15N,132E)	17 ---T (16N,131E)--- --TS (18N,110E) TS Mary(28N,162E)-
18	19 NO DATA TS Francene (13N,112W)---	20 NO DATA ----(36N,162W)	21 NO DATA T Nadire(17N,137E)	22° --TS (23N,113E)	23 -TS (19N,131W)	24 TS Georgette(16N,
25 119W)---	26 ----T (25N,116E)	27 -----(22N,129W)	28 TS Hilary(12N,116W)	29 --H (13N,117W)---	30 SCW for ENE winds-	31 ---H (15N,122W) TS Olive(23N,138E)

Table 2. (Continued) A Daily Summary of Gales, Storms, Smallcraft Warnings and the Number of Wave Energy Spectra

AUGUST						
1 SCW for ENE winds G(41N,178W) T Olive(24N,136E)---- H Hilary(14N,124W)---- H Ilsa(14N,105W)----	2°	3 SCW for ENE winds	4 ---------- ---------- --TS (19N,135W)-- ----------	5 --TS (36N,131E) ---------- --TS (22N,115W)---	6 --TS (20N,141W) --TS (23N,121W)	7 G(46N,175E) G(45N,145E) TS Jewel(16N,106W)-
8 ---TS(17N,109W) TS Polly(25N,130E)						

Table 3

Average Total Energy for Various Weather Conditions

Type of Event	Average Total Energy (cm^2)	Average Total Energy in Peak: Peak Freq. (milliHz)	Average Total Energy in Peak: Average Total Energy (cm^2)	Average Total Energy for 180-250 MilliHz (cm^2)
Gale to the Northwest	791	50-180	687	62
Low to the Northwest		40-60 40-64 42-65	23	
Storm to the North	2029	60-110	1397	168
Strong Tradewinds	3013			512
Weak Tradewinds	1262			325
Strong Southerly Winds	703			73

APPENDIX C

Figures 1 to 66

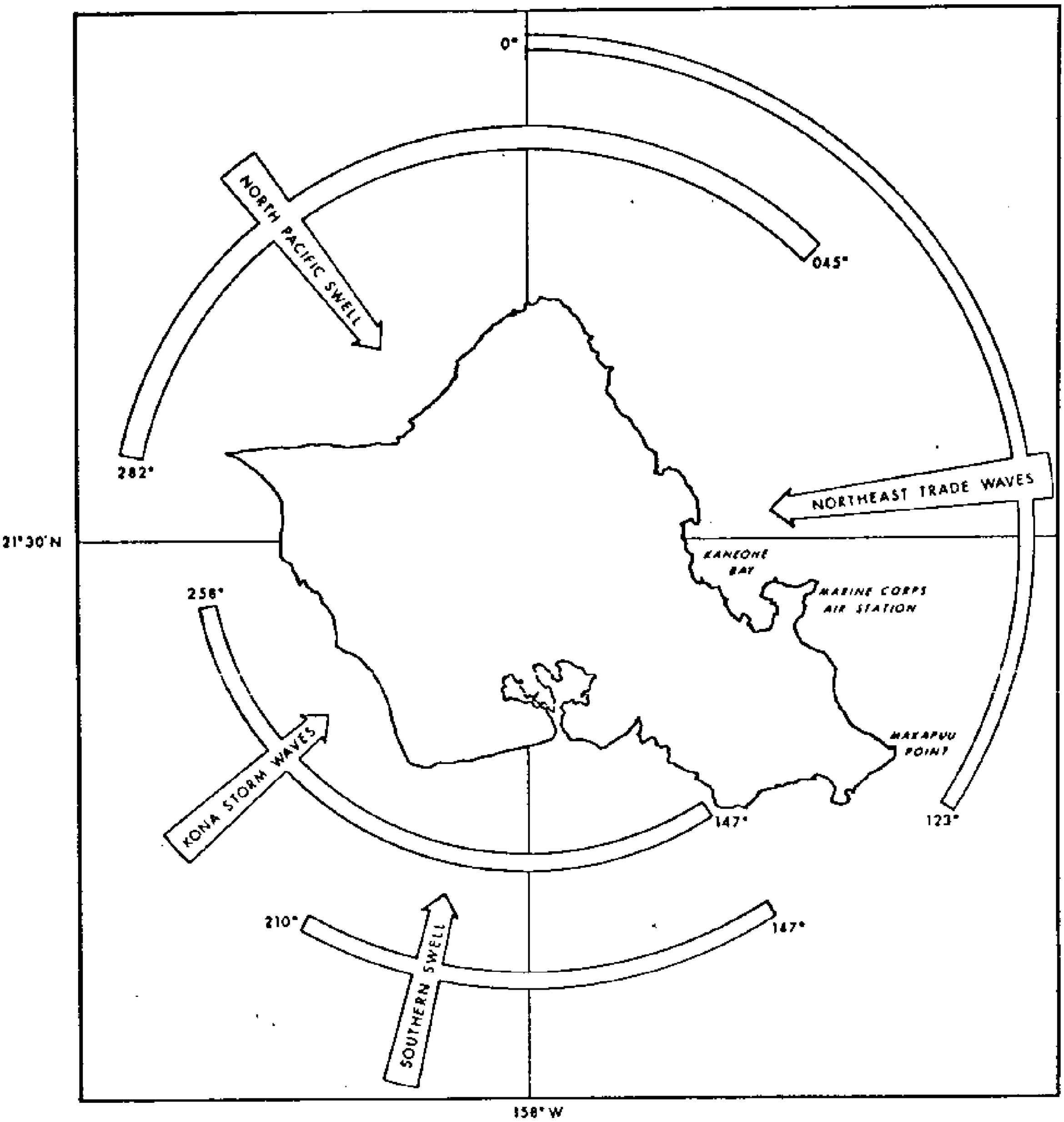

Figure 1. Waves approaching Kaneohe Bay (after Moberly and Chamberlain, 1964, Fig. 1).

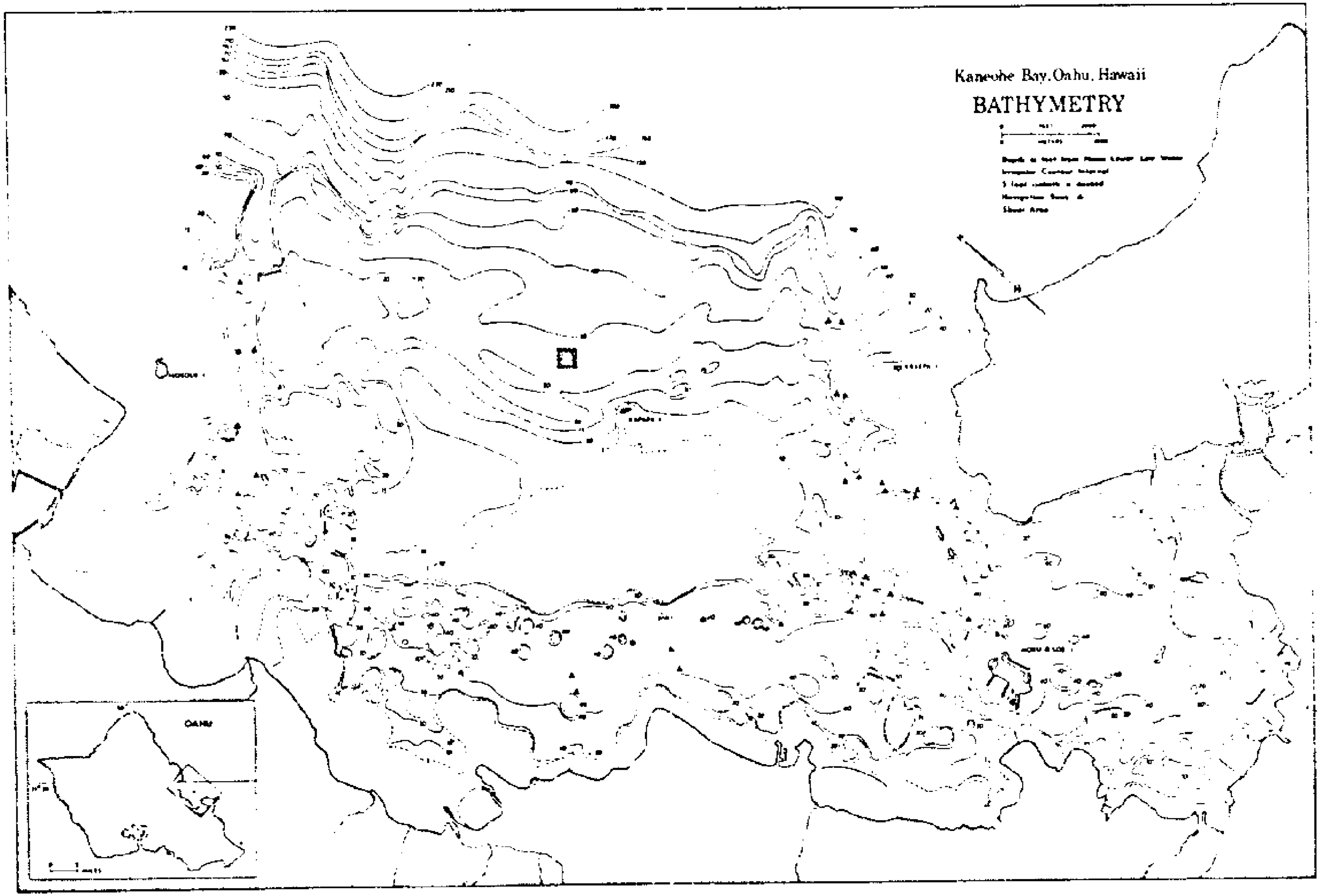

Figure 2. Bathymetry of Kaneohe Bay (after Roy, 1970, Fig. 1) and location of pressure gauge (indicated by dark square).

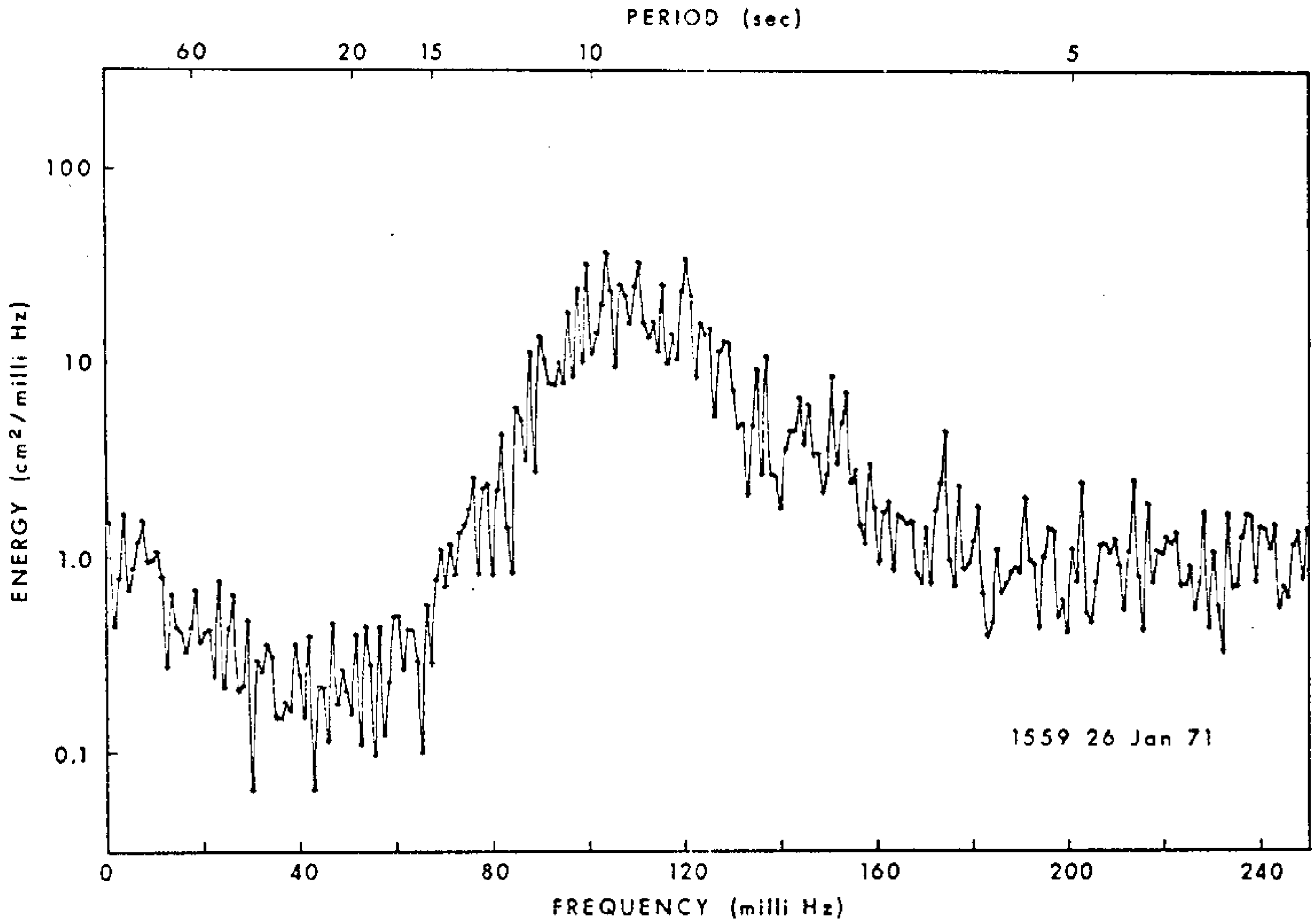

Figure 3. Wave energy spectrum.

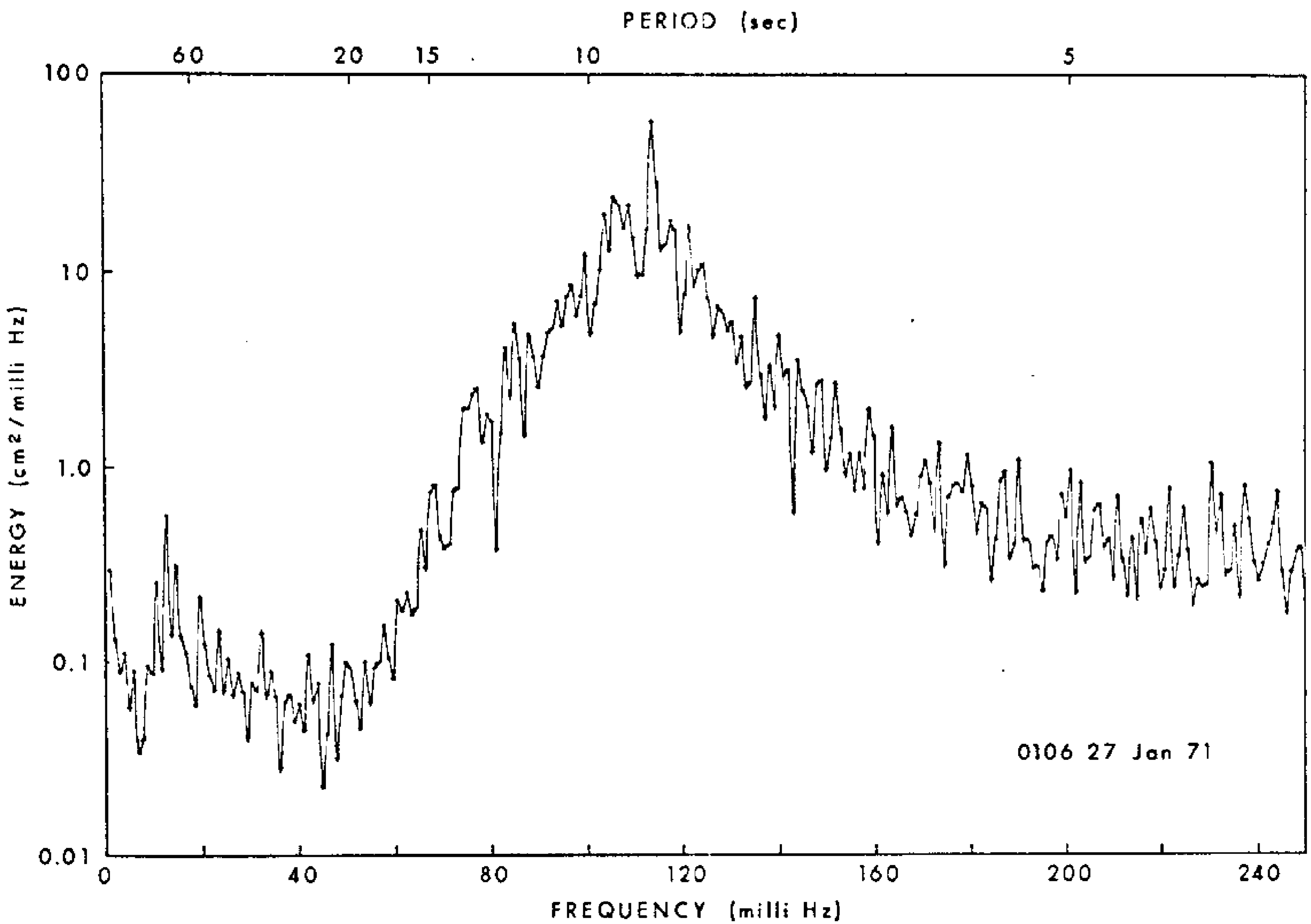

Figure 4. Wave energy spectrum.

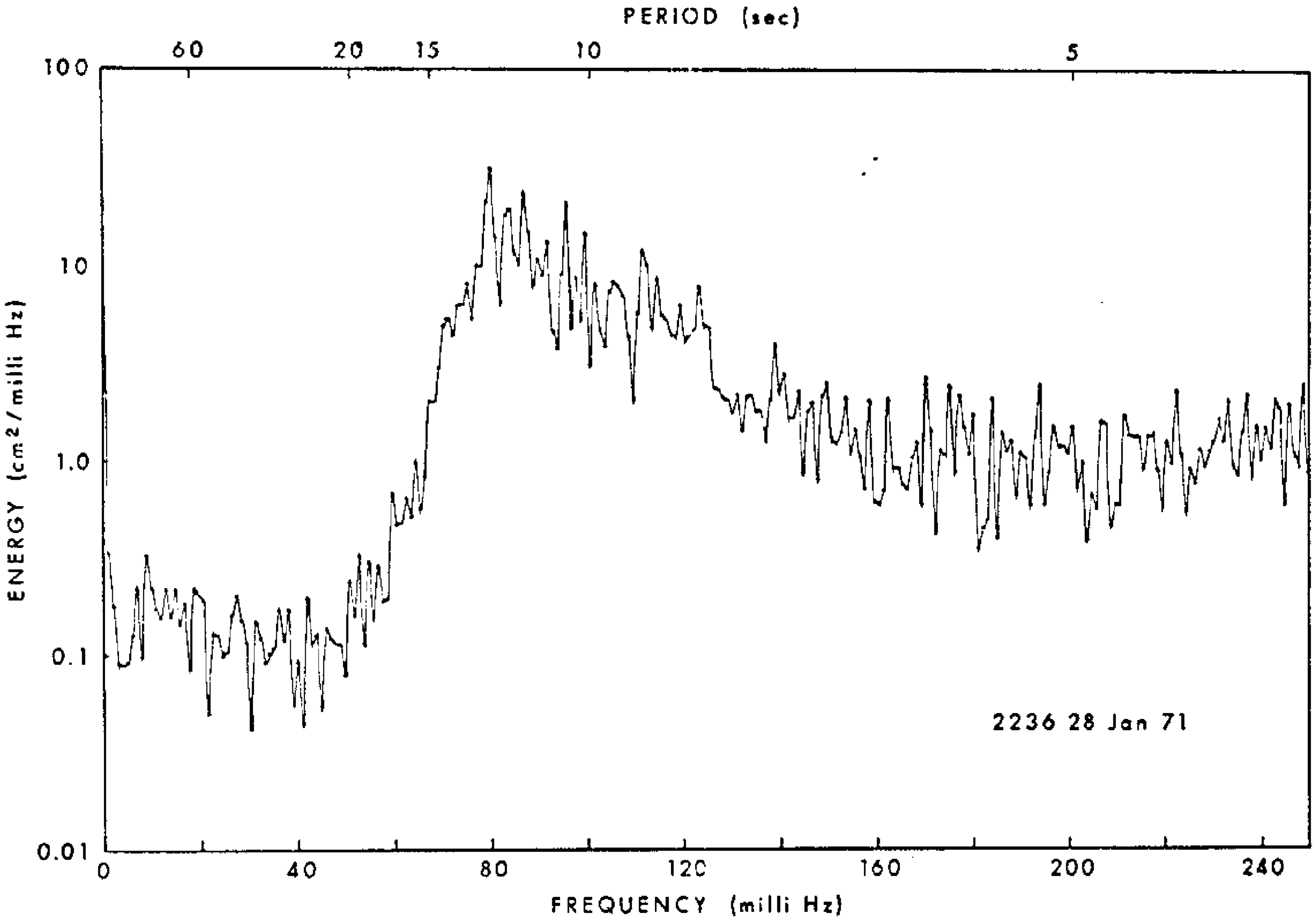

Figure 5. Wave energy spectrum.

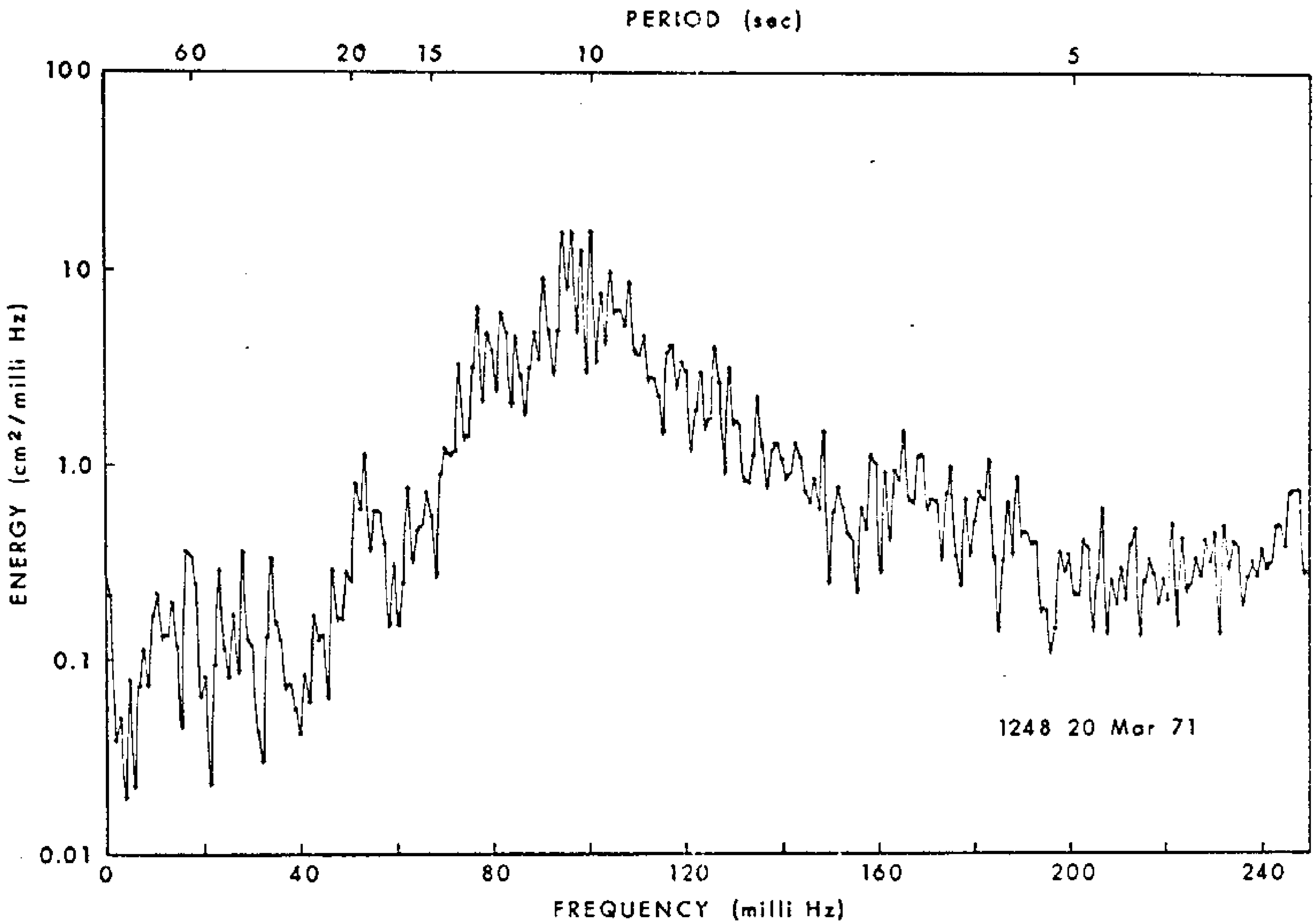

Figure 6. Wave energy spectrum.

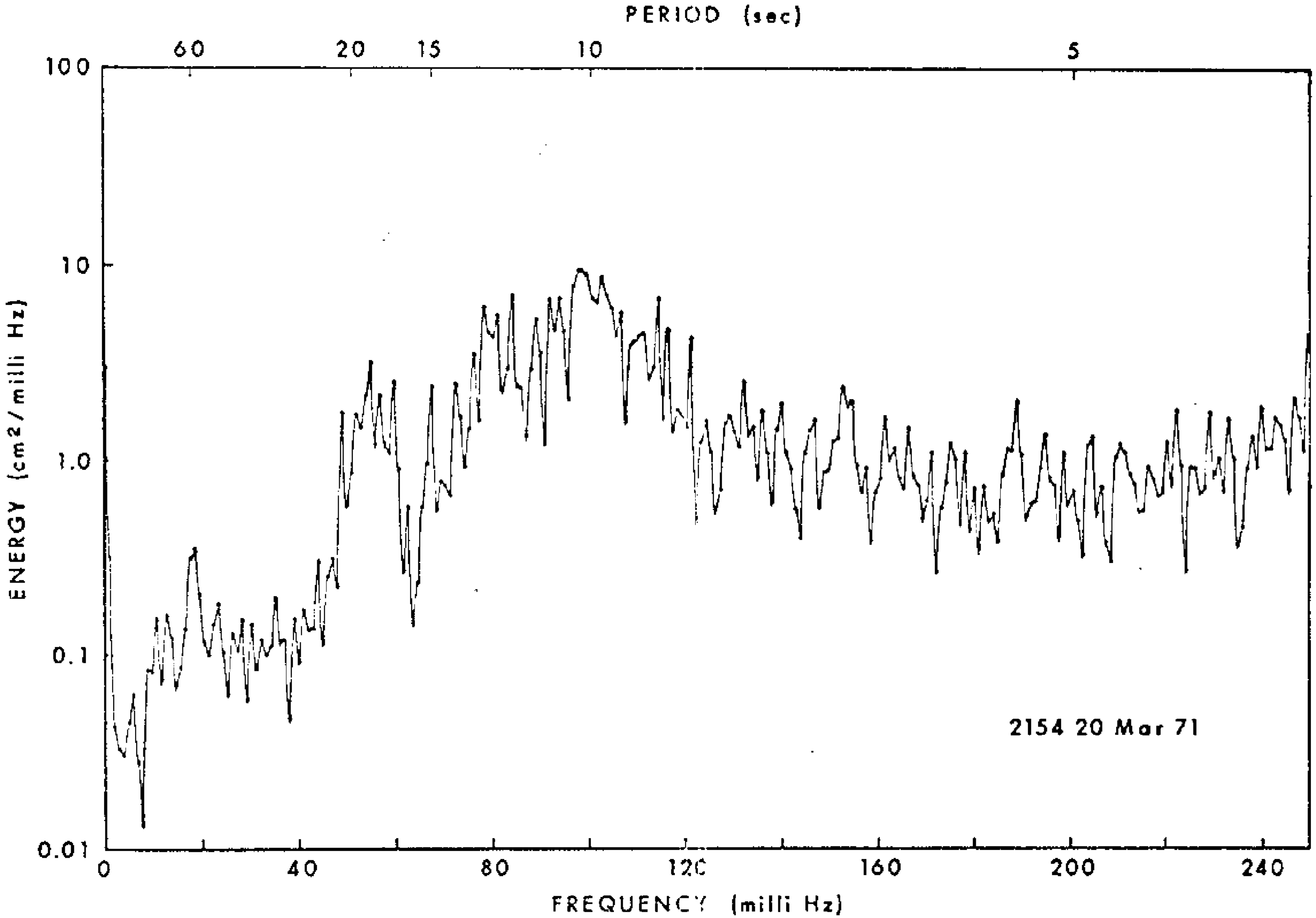

Figure 7. Wave energy spectrum.

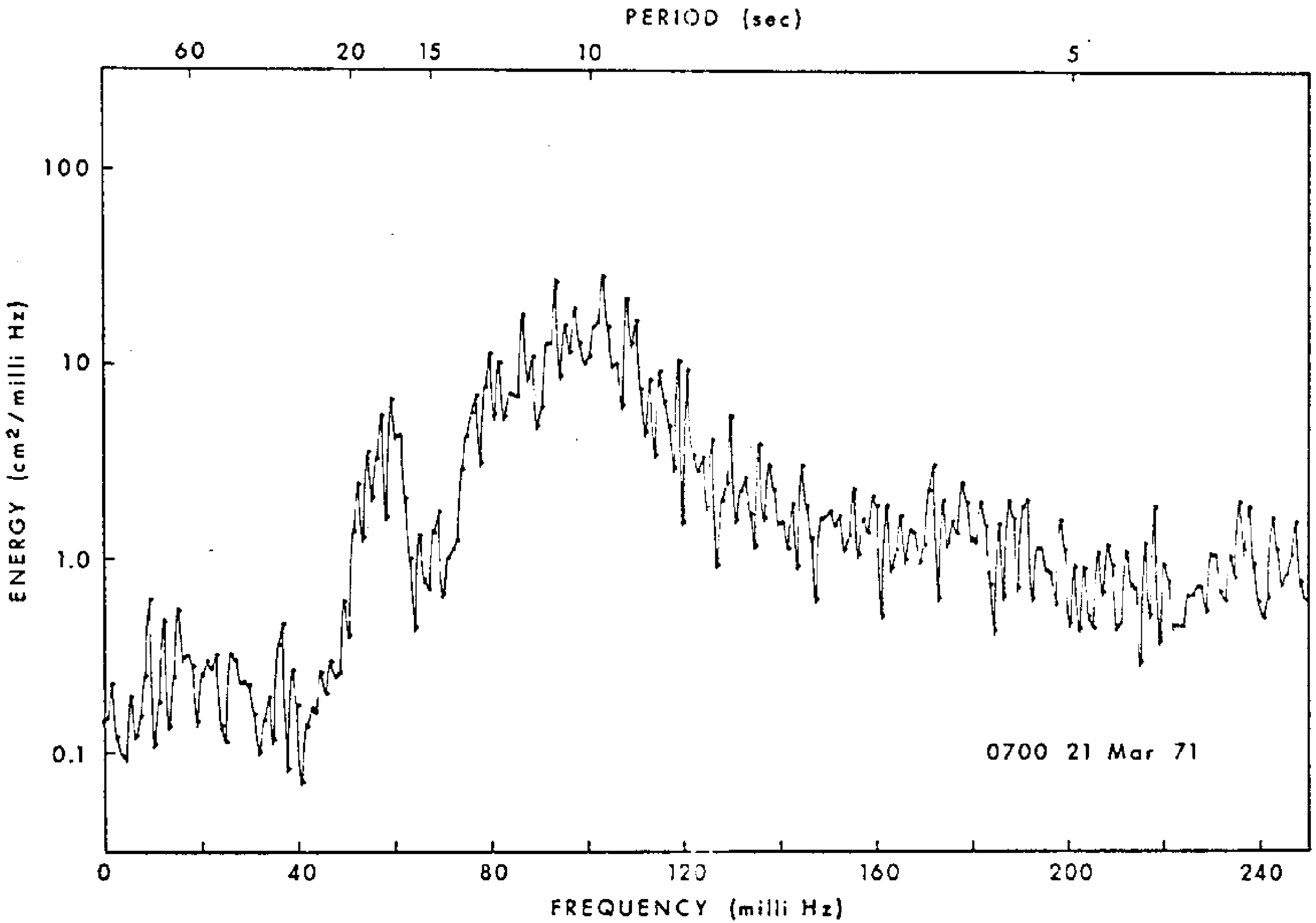

Figure 8. Wave energy spectrum.

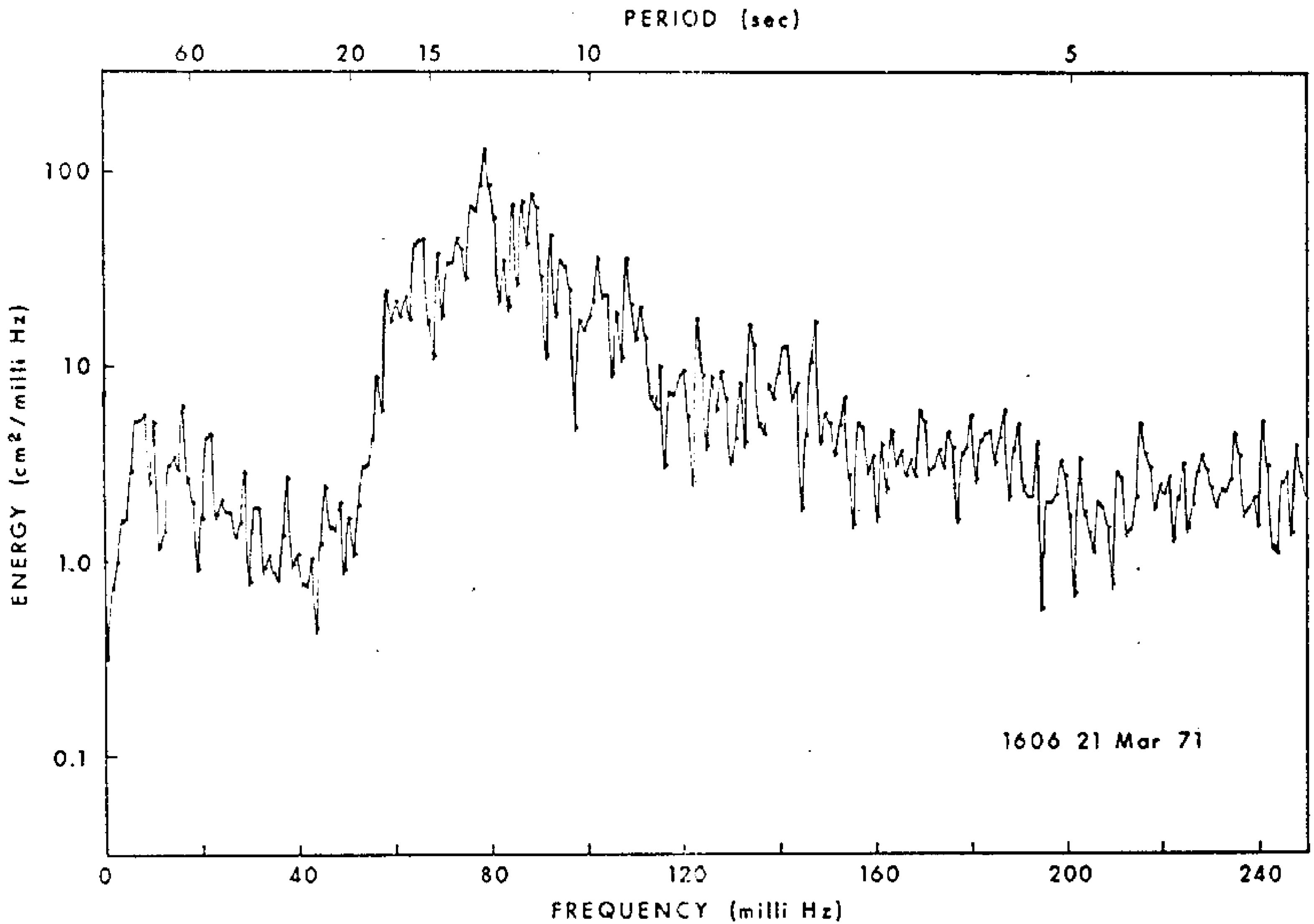

Figure 9. Wave energy spectrum.

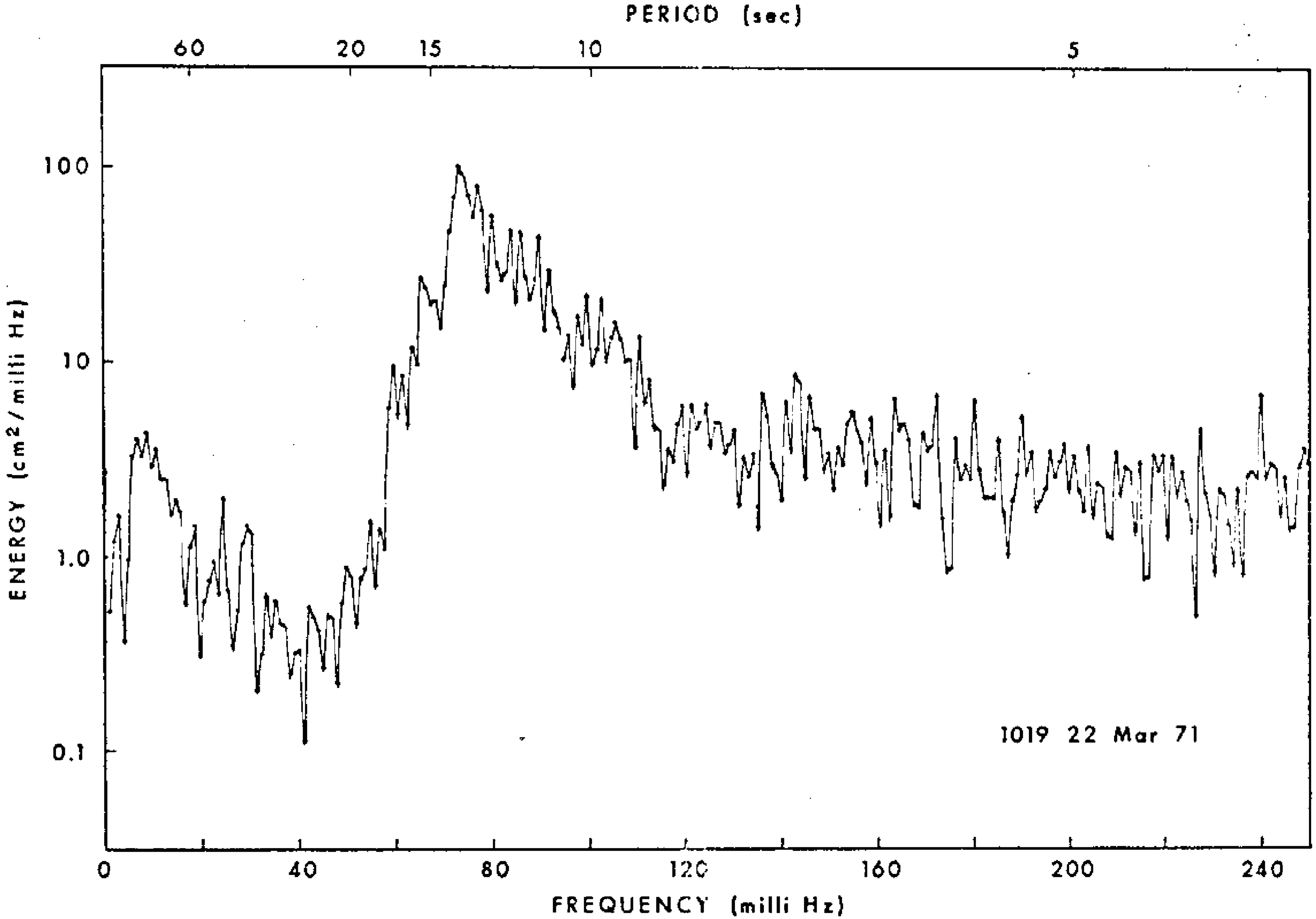

Figure 10. Wave energy spectrum.

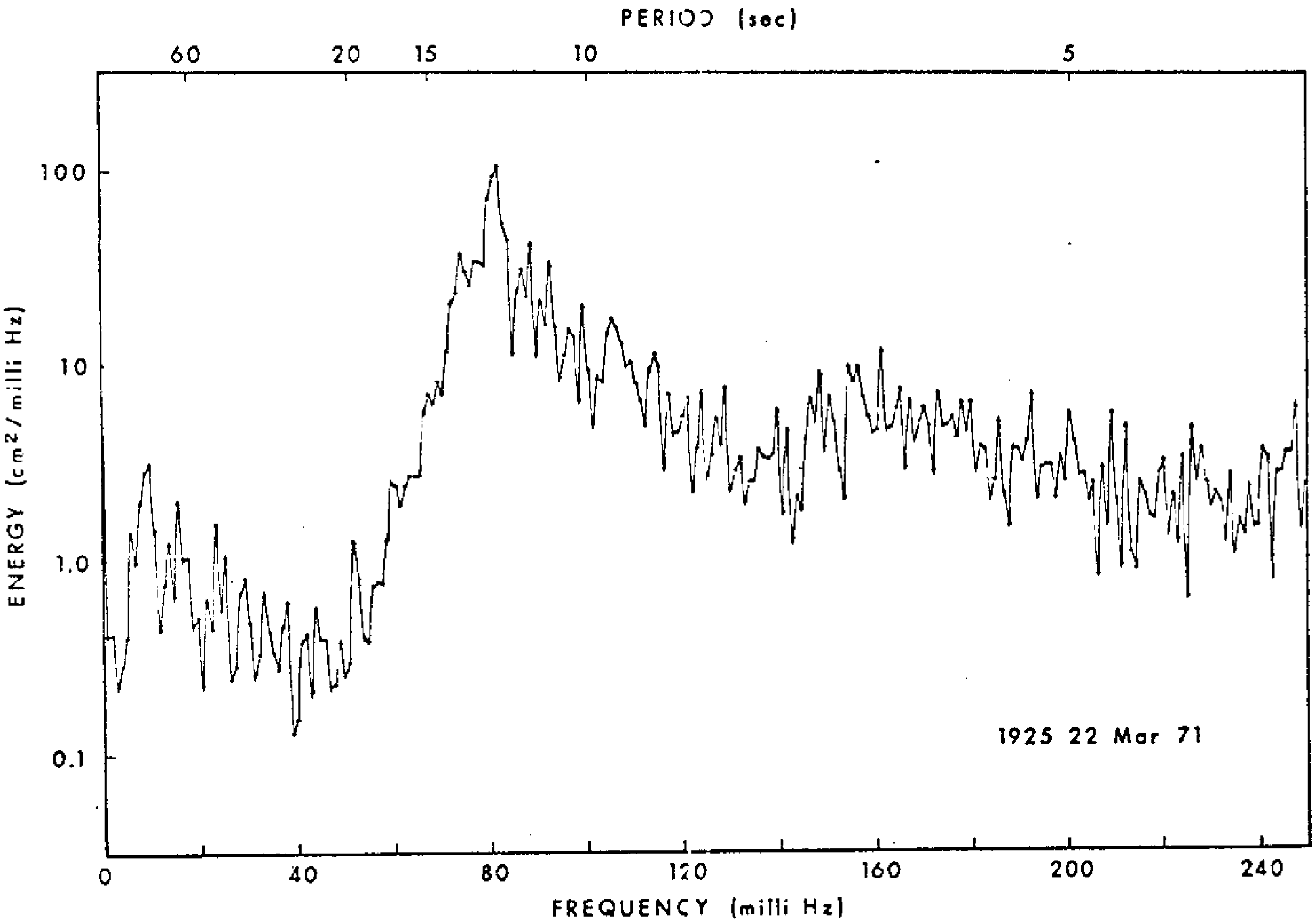

Figure 11. Wave energy spectrum.

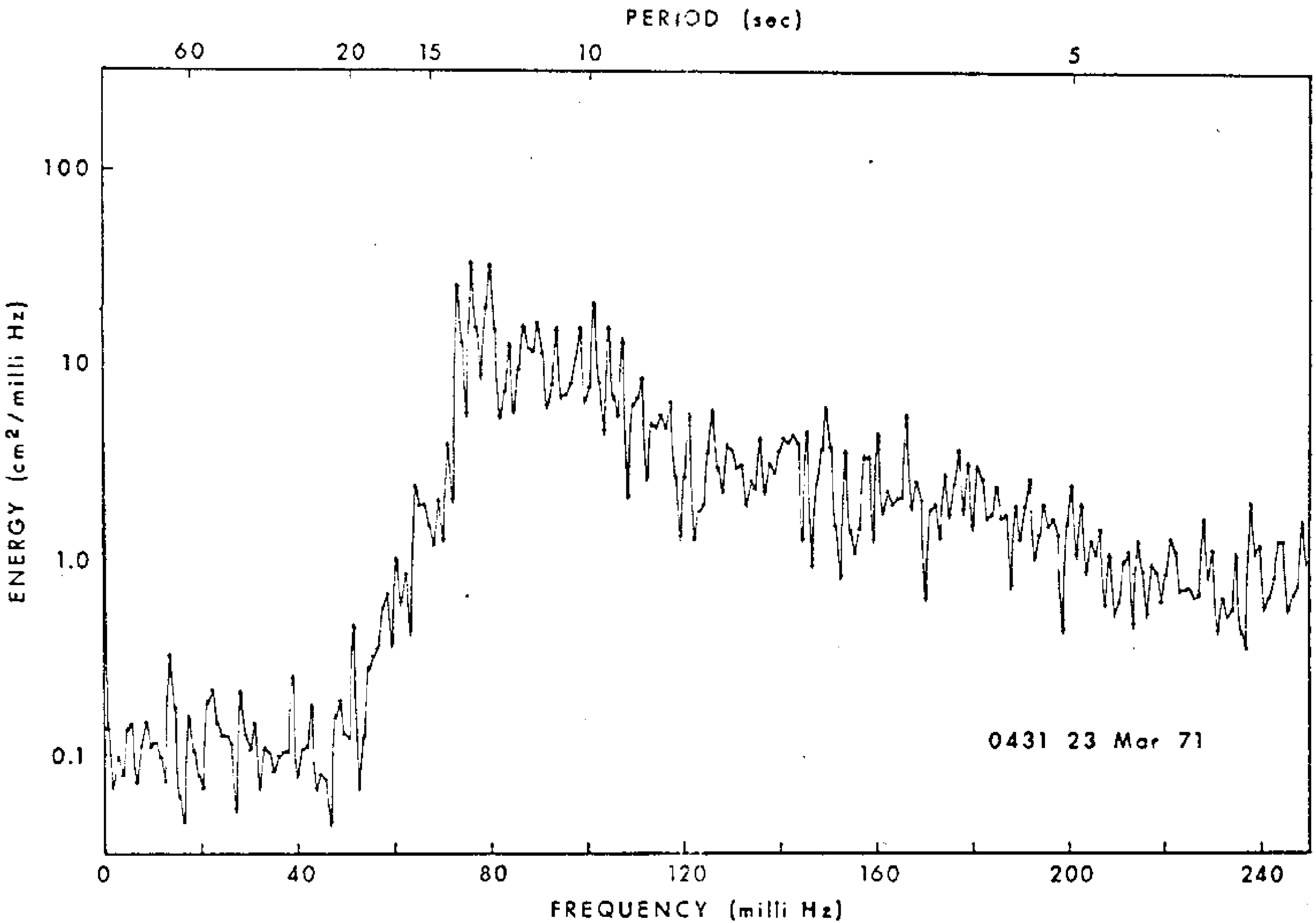

Figure 12. Wave energy spectrum.

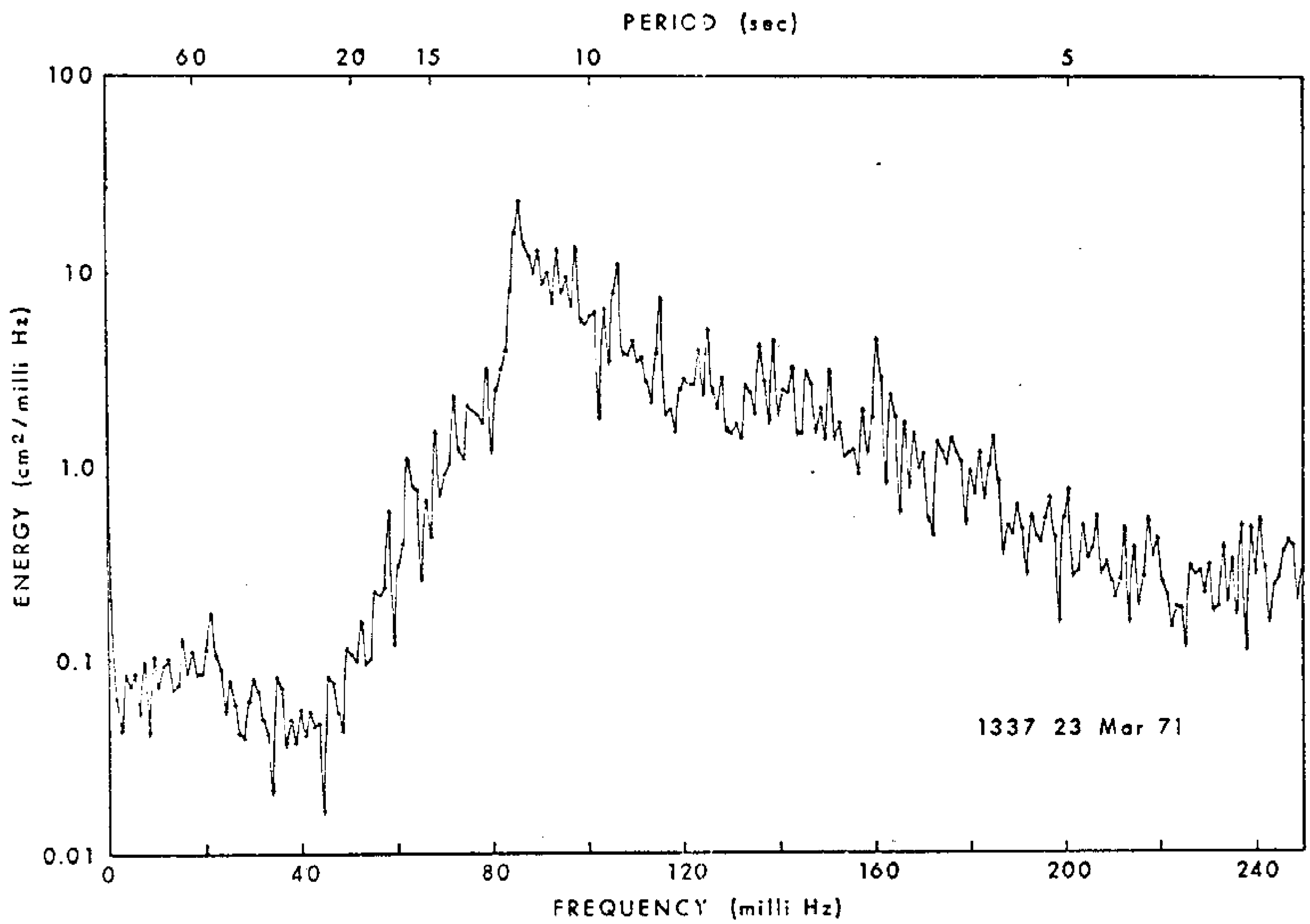

Figure 13. Wave energy spectrum.

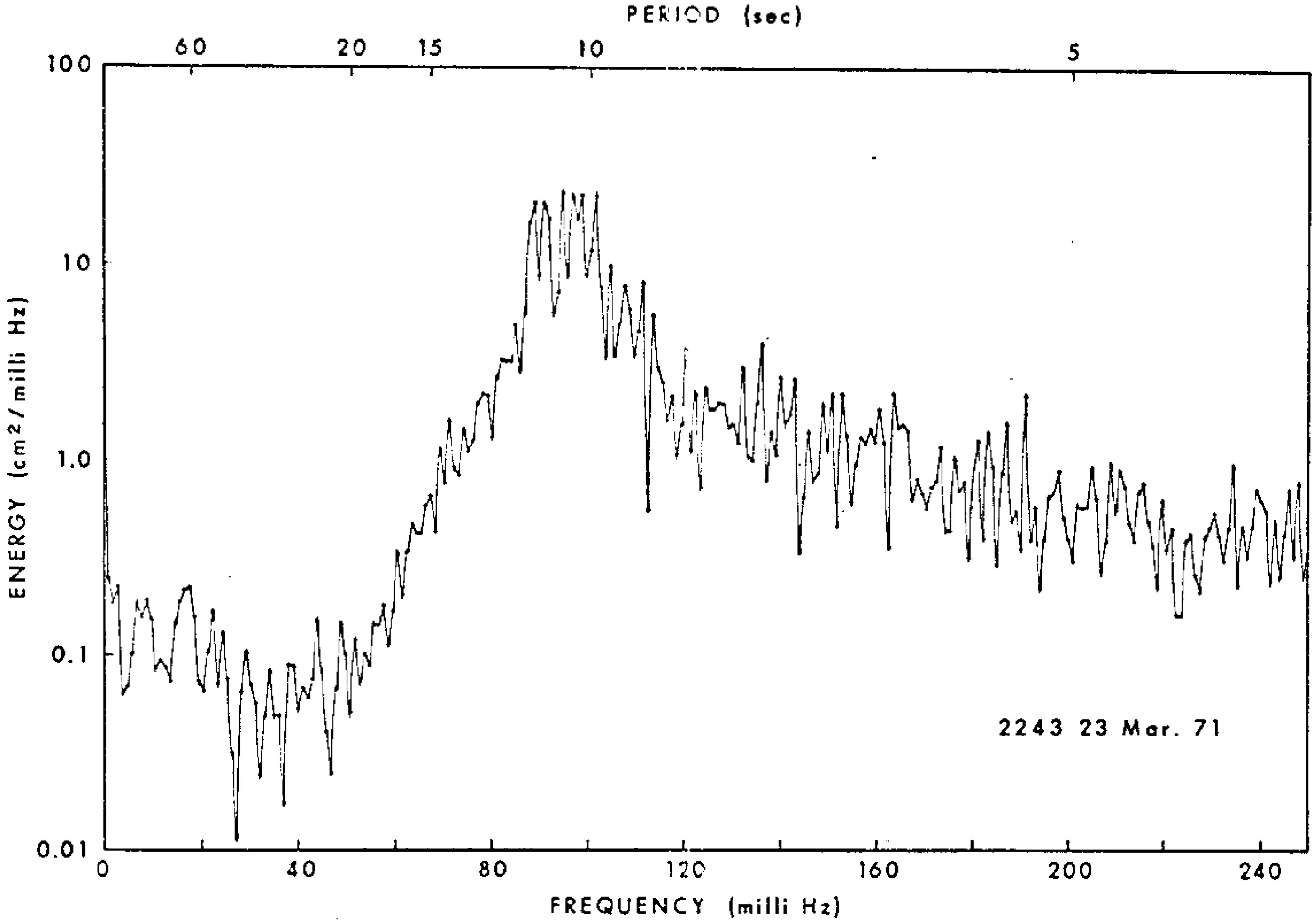

Figure 14. Wave energy spectrum.

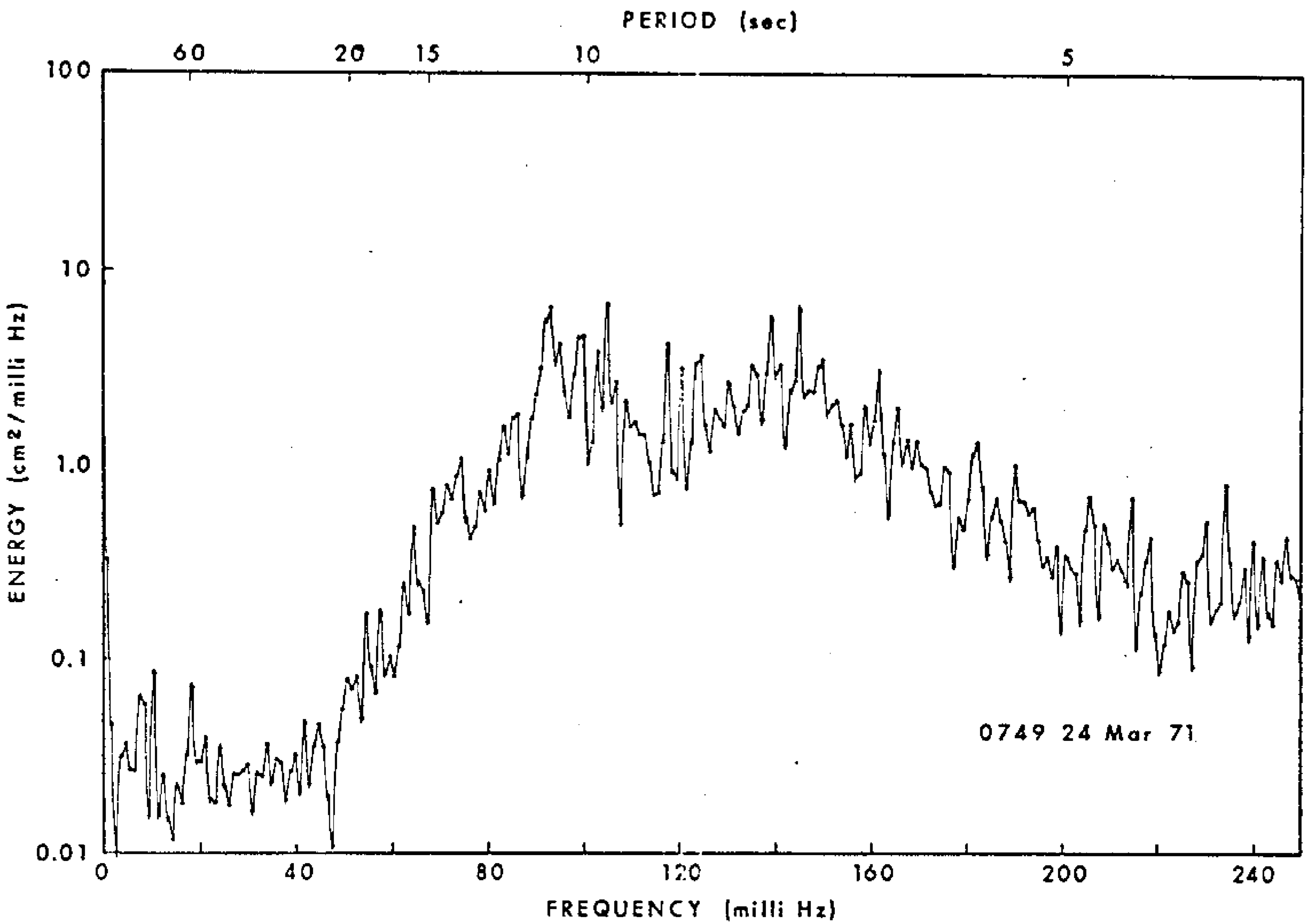

Figure 15. Wave energy spectrum.

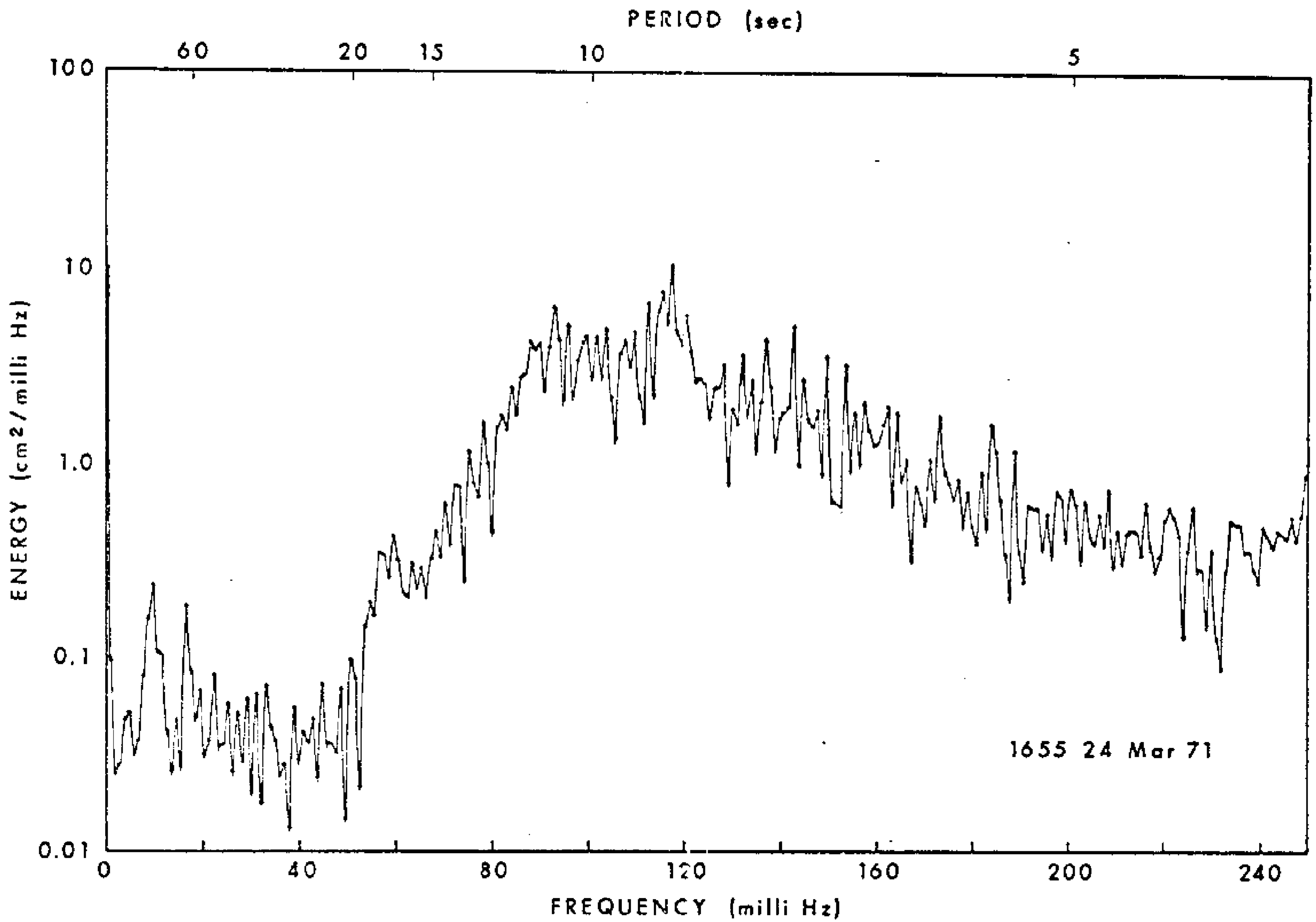

Figure 16. Wave energy spectrum.

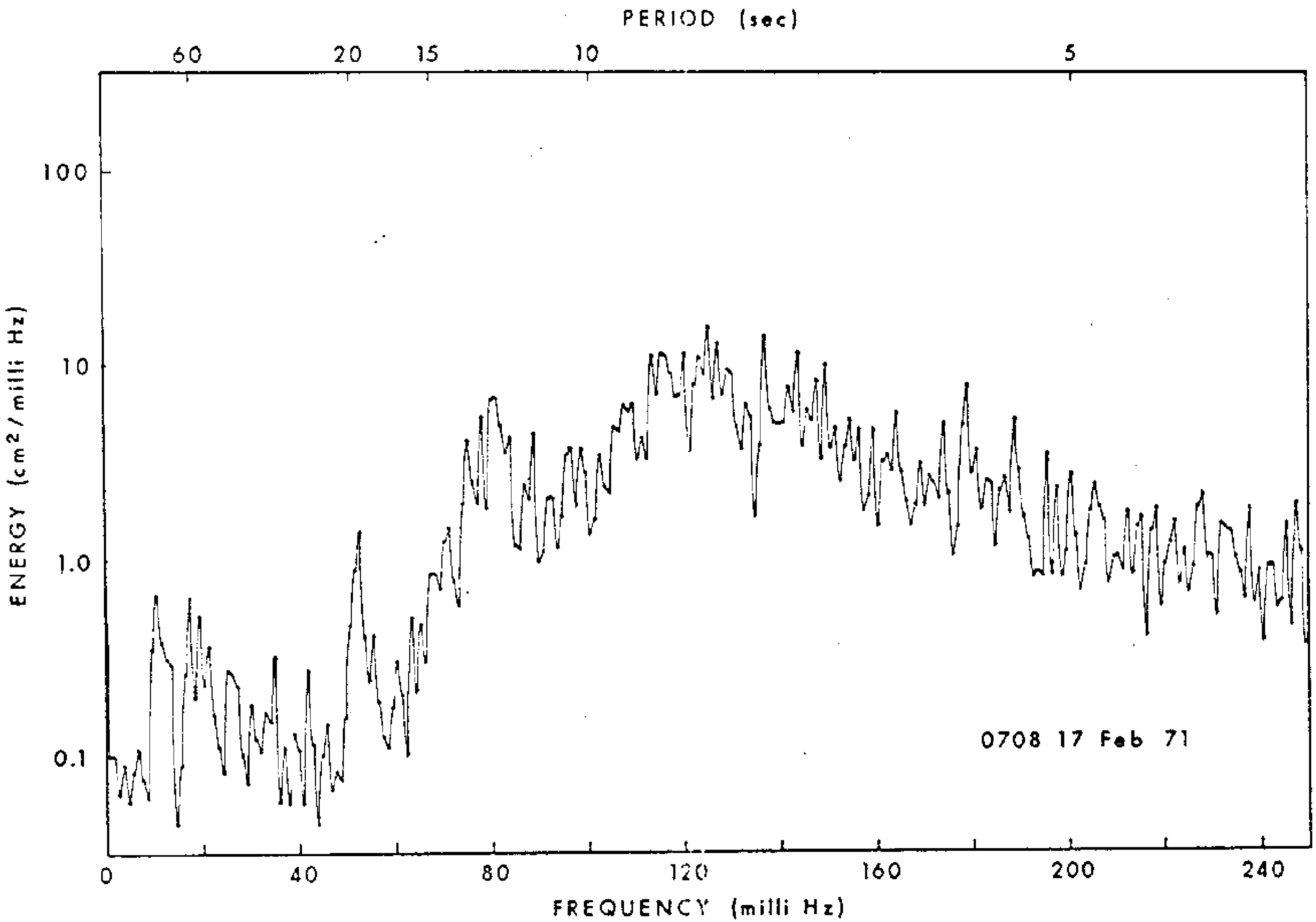

Figure 17. Wave energy spectrum.

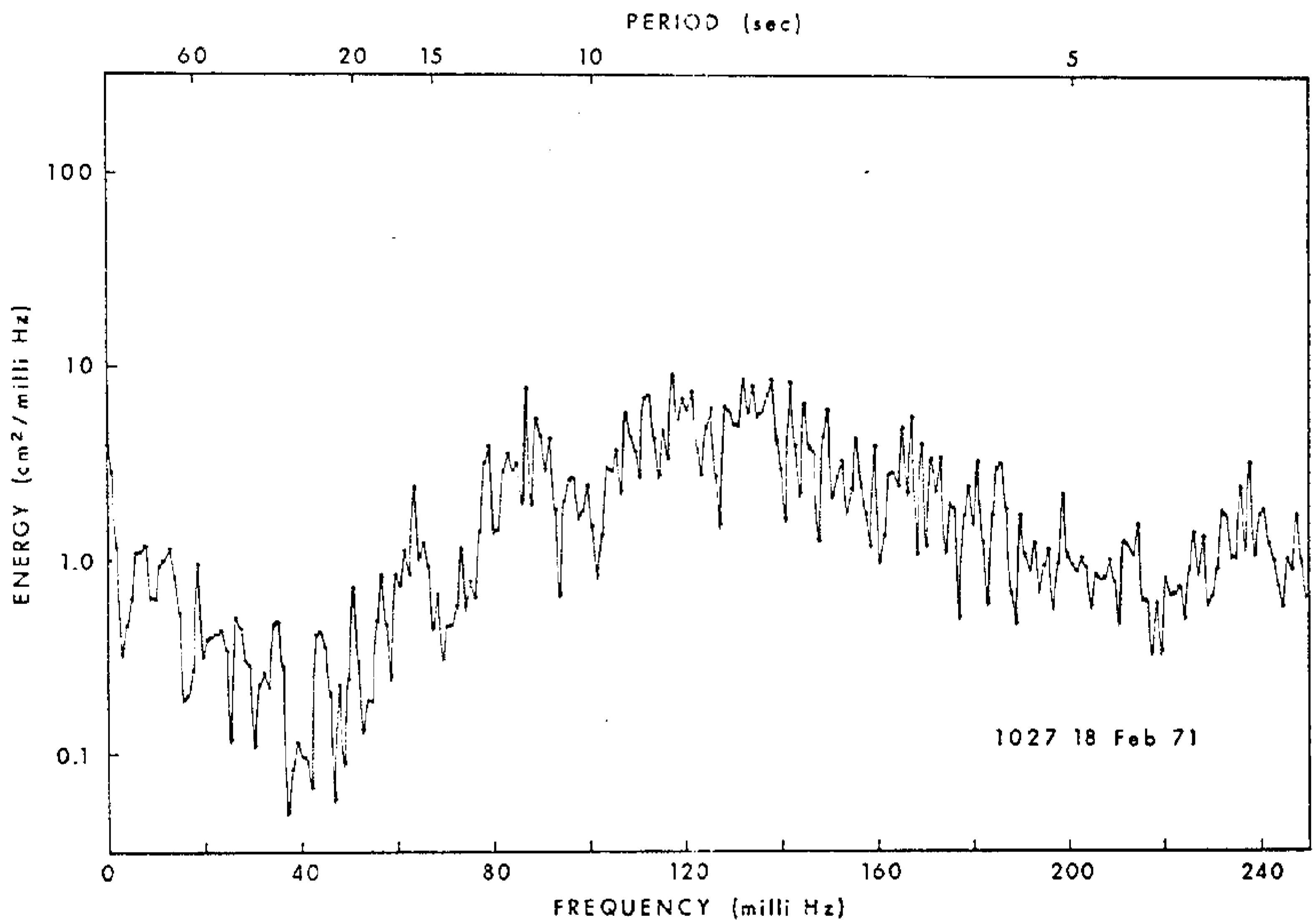

Figure 18. Wave energy spectrum.

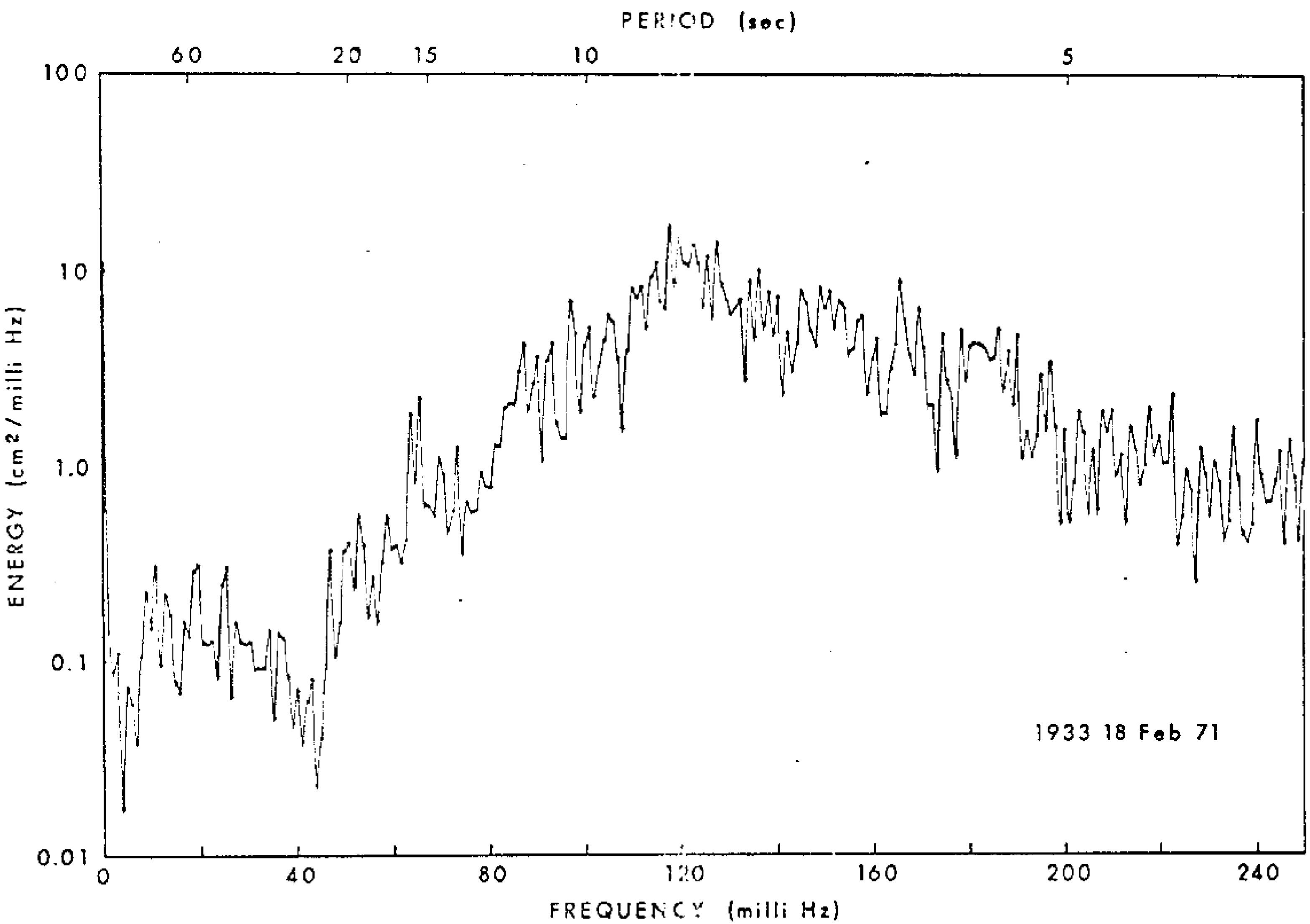

Figure 19. Wave energy spectrum.

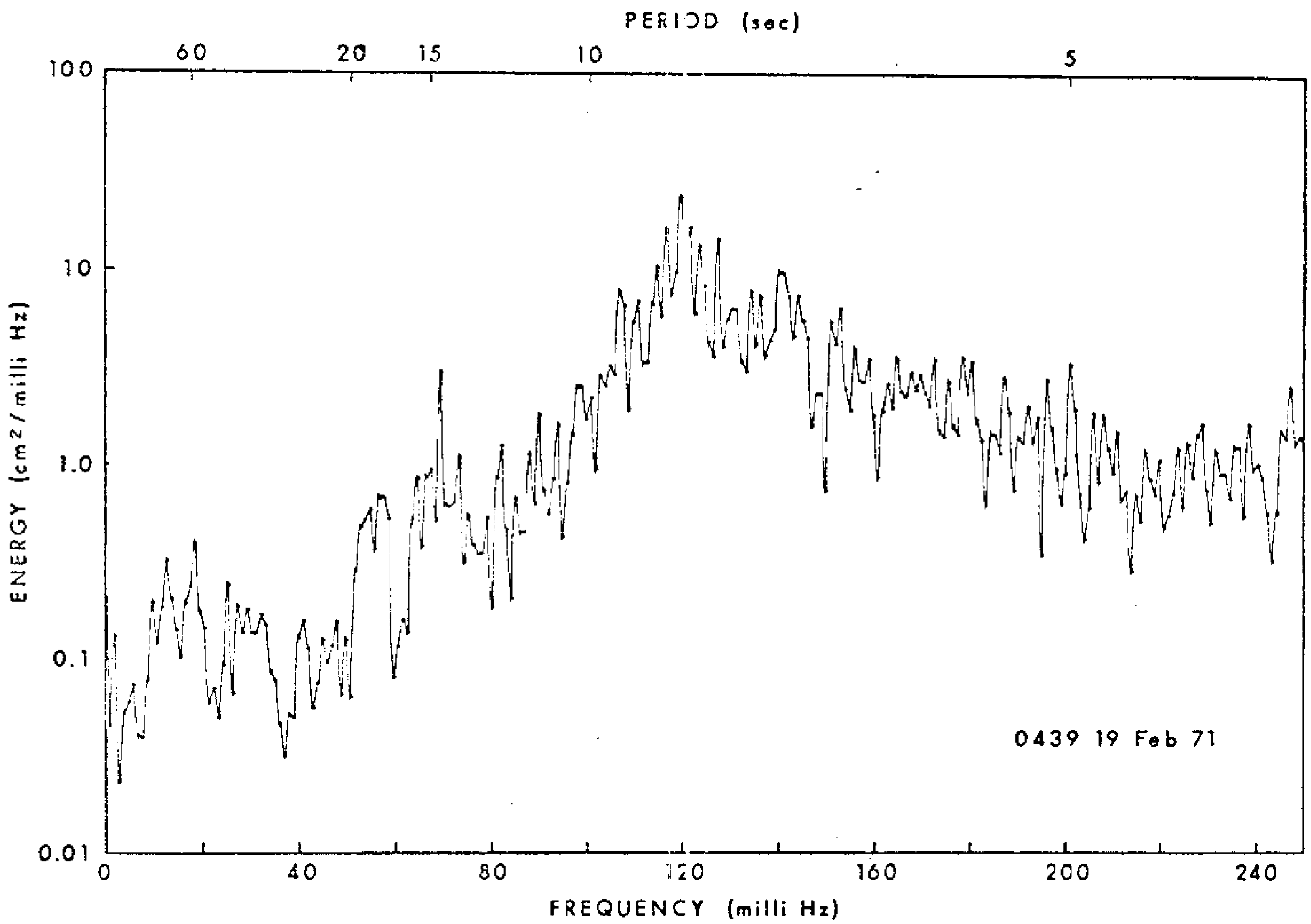

Figure 20. Wave energy spectrum.

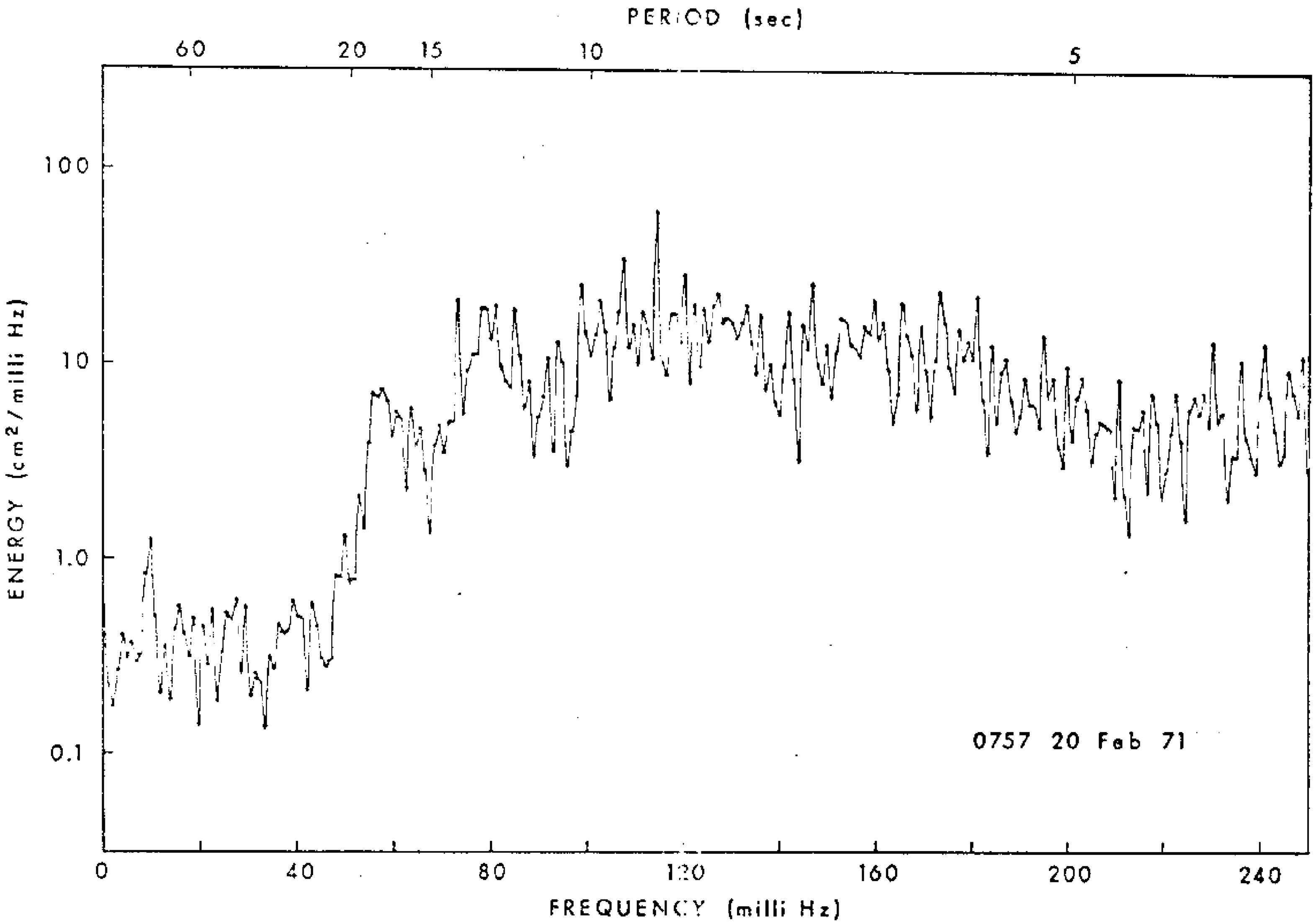

Figure 21. Wave energy spectrum.

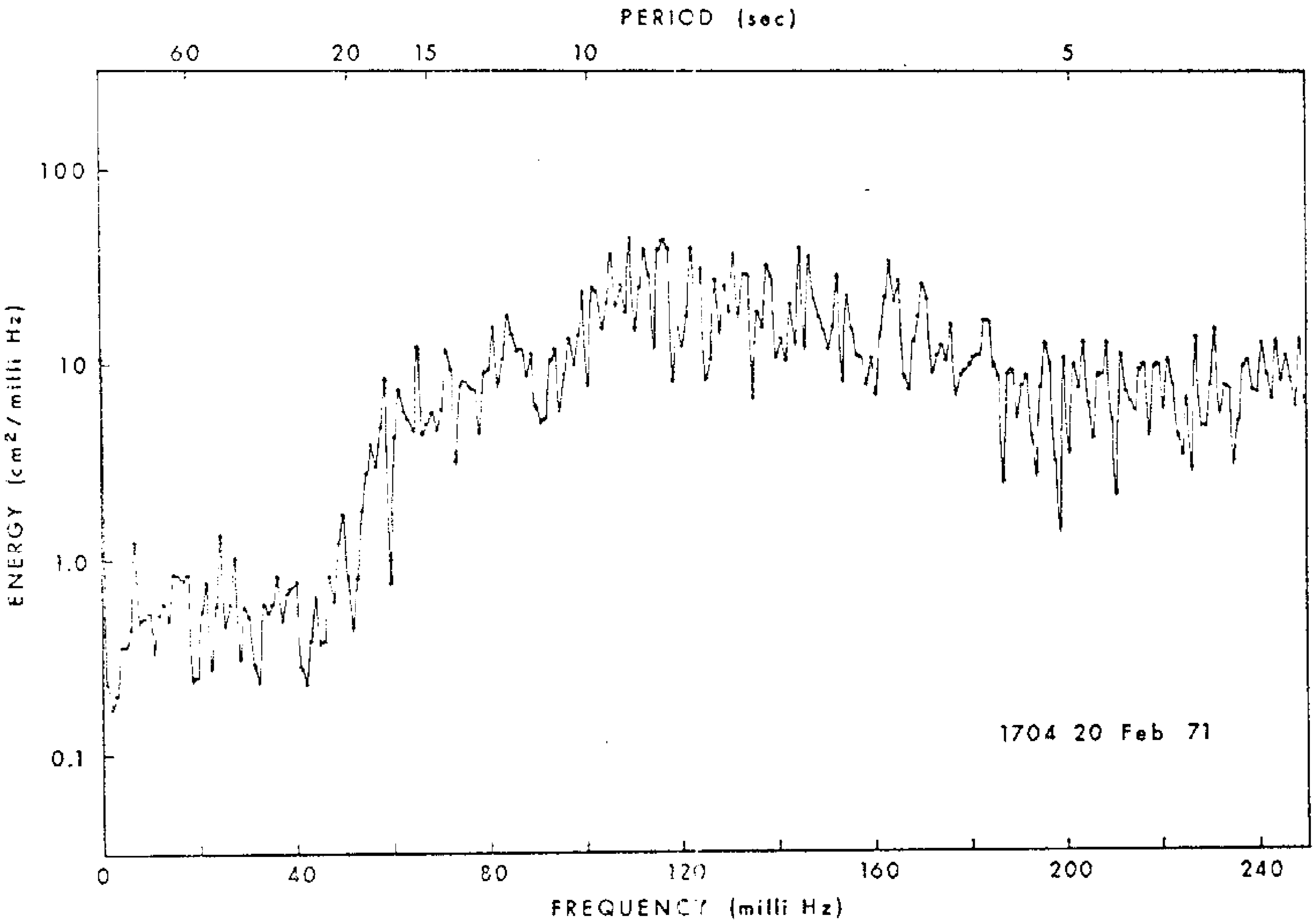

Figure 22. Wave energy spectrum.

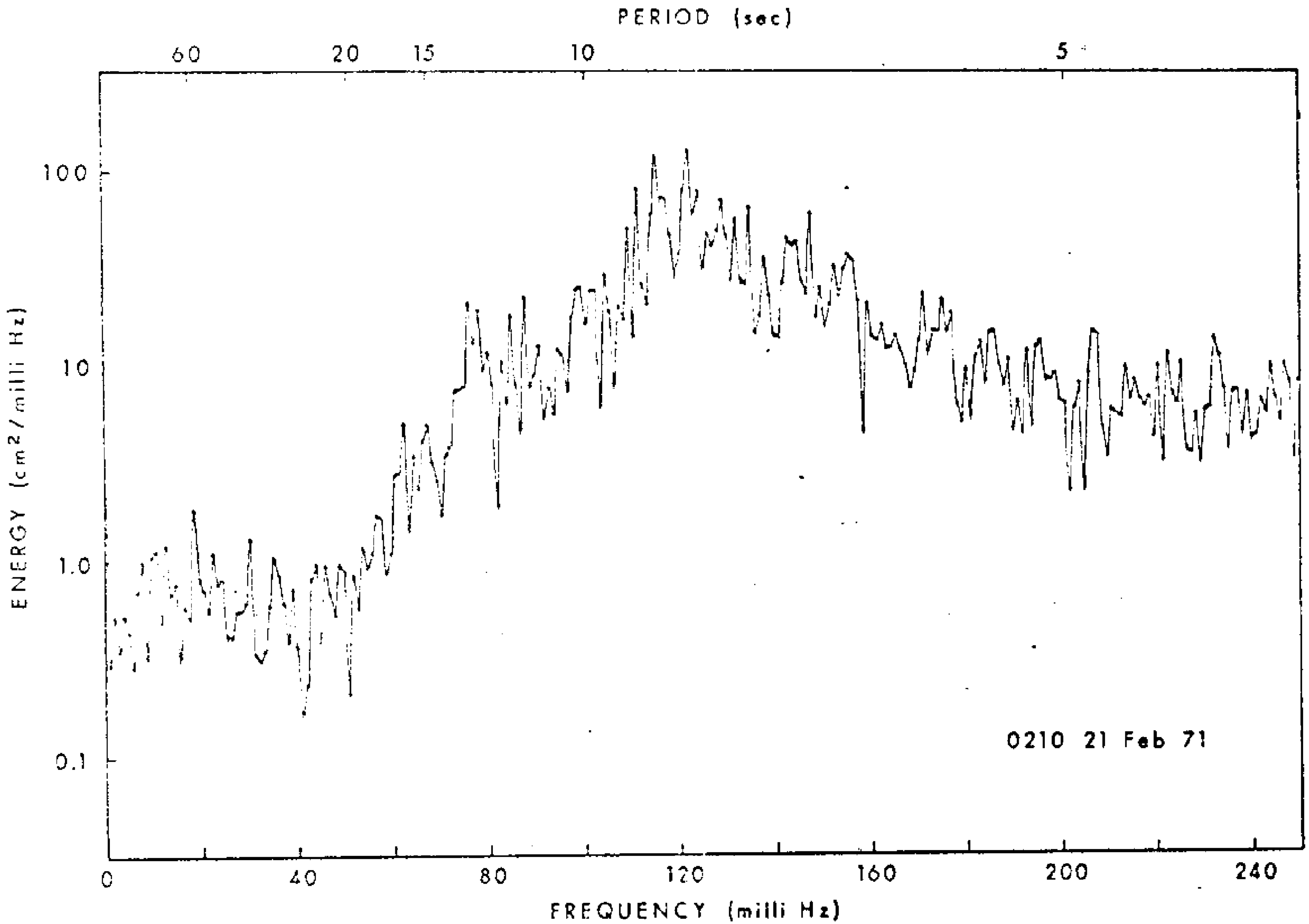

Figure 23. Wave energy spectrum.

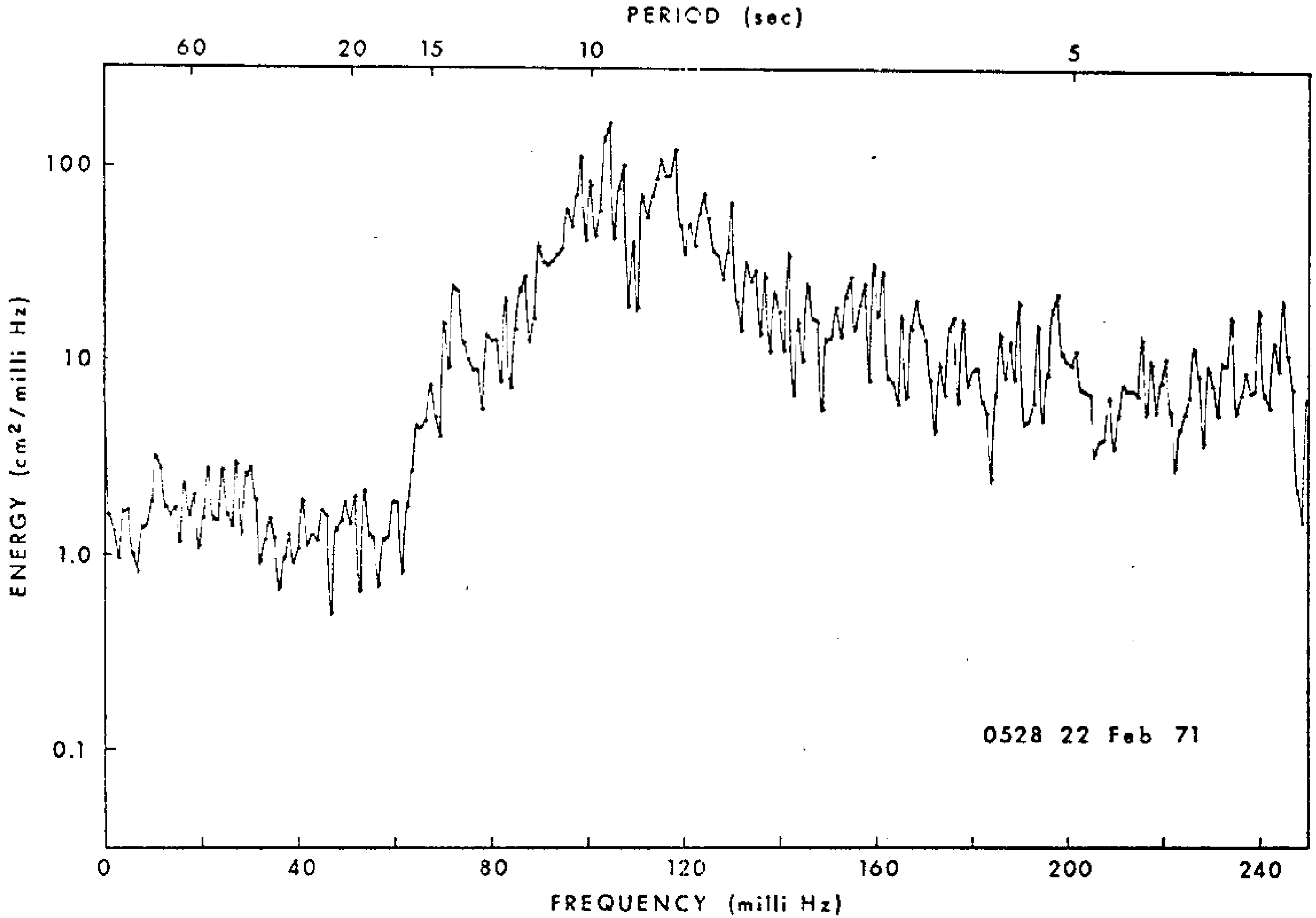

Figure 24. Wave energy spectrum.

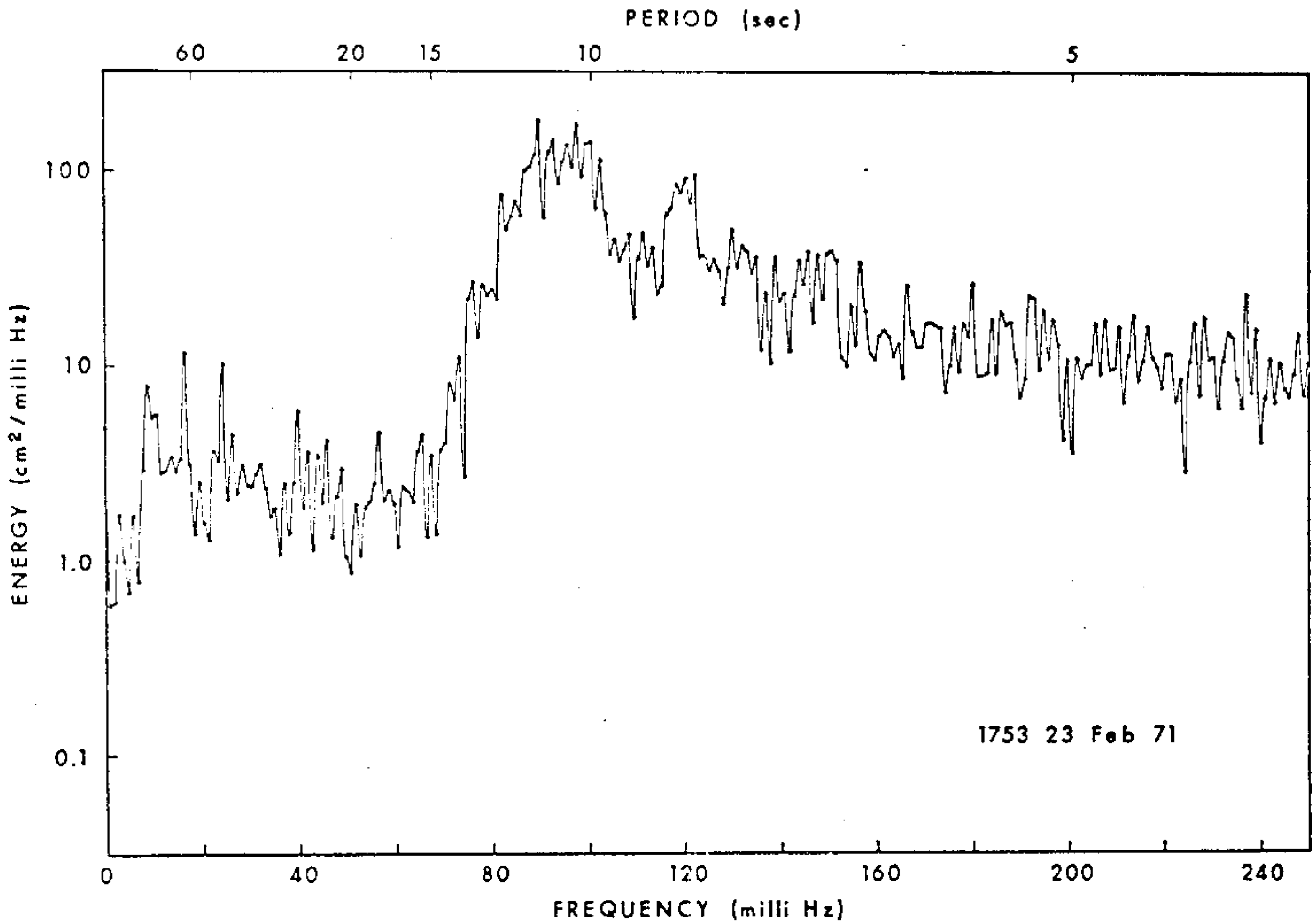

Figure 25. Wave energy spectrum.

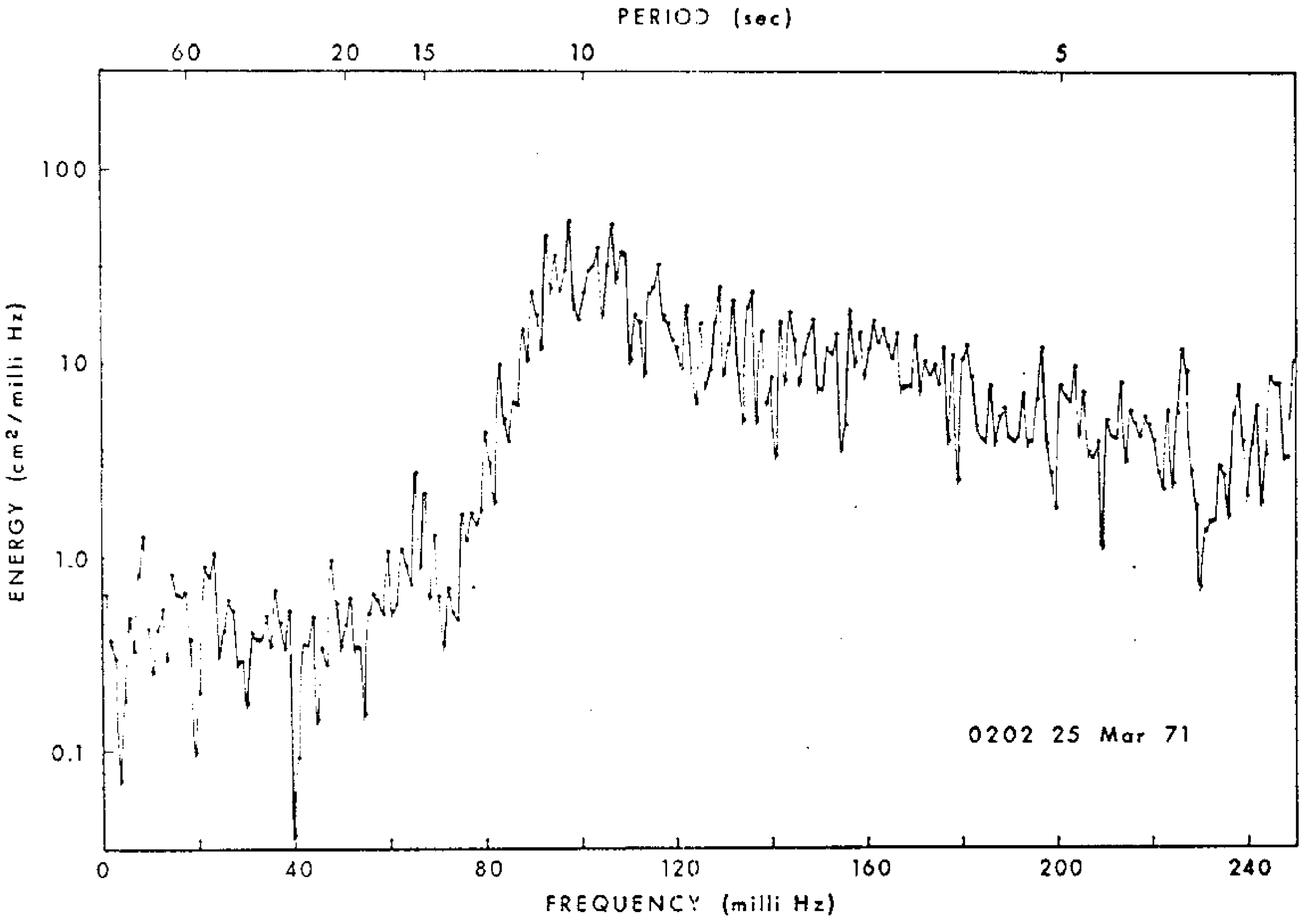

Figure 26. Wave energy spectrum.

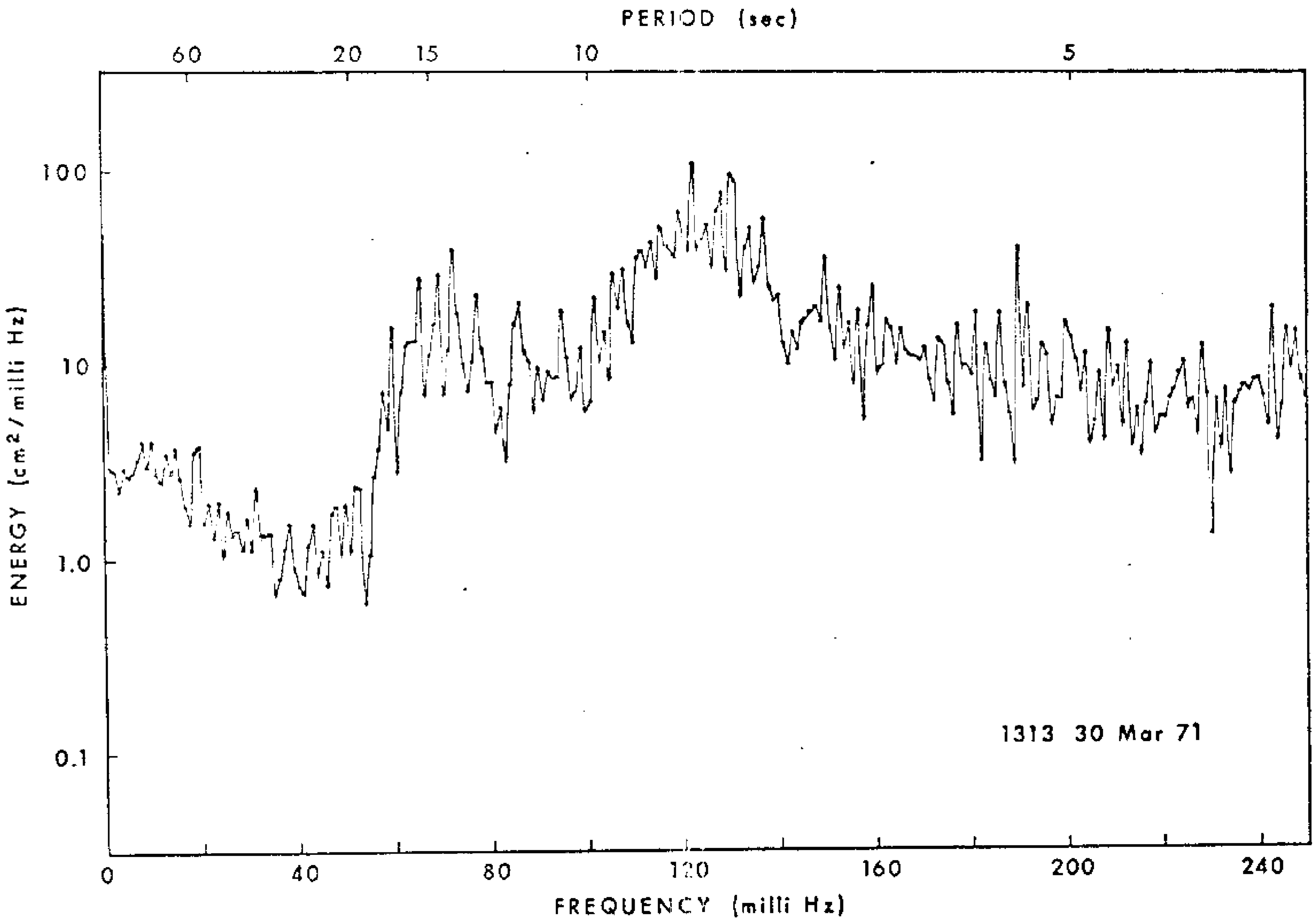

Figure 27. Wave energy spectrum.

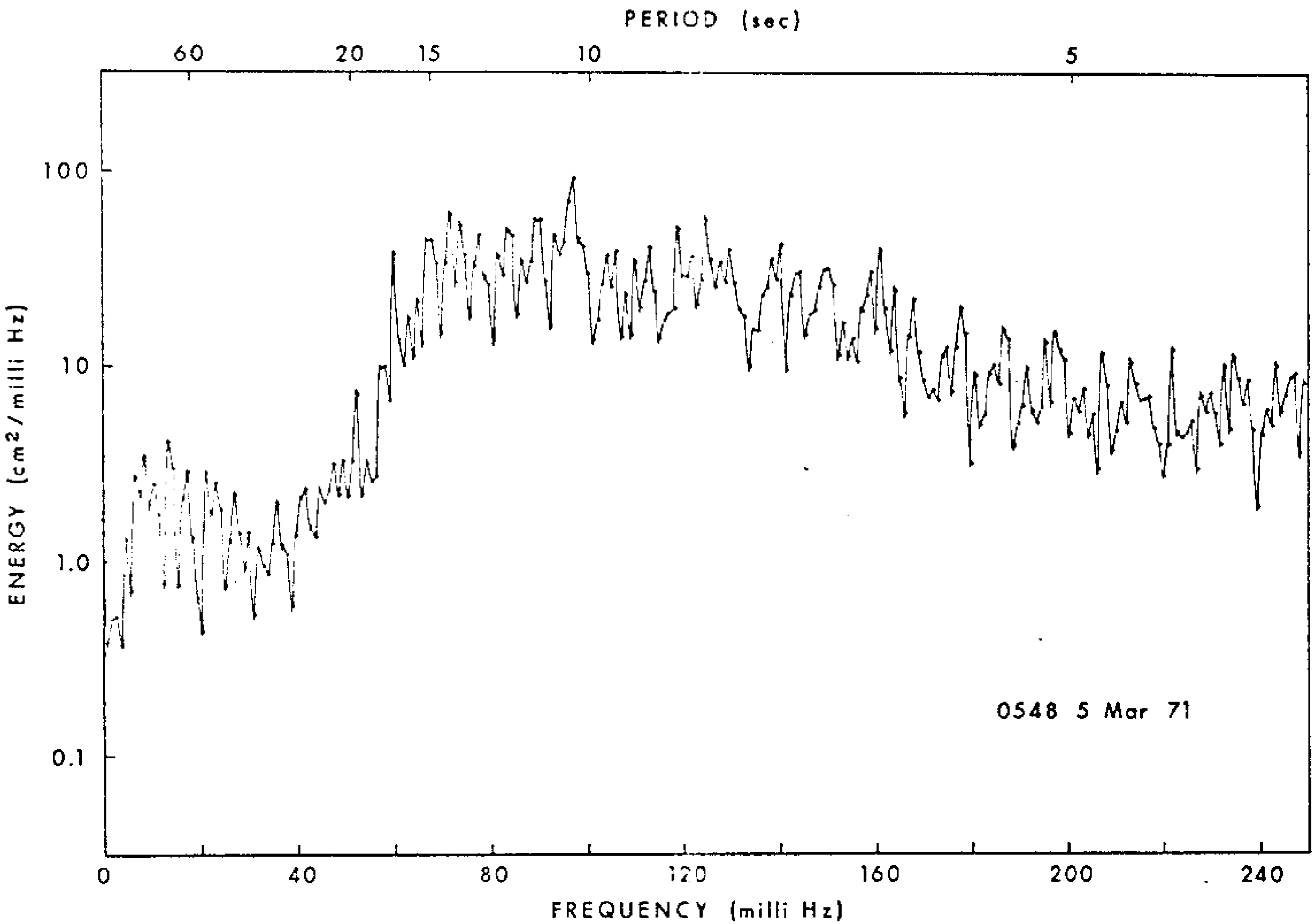

Figure 28. Wave energy spectrum.

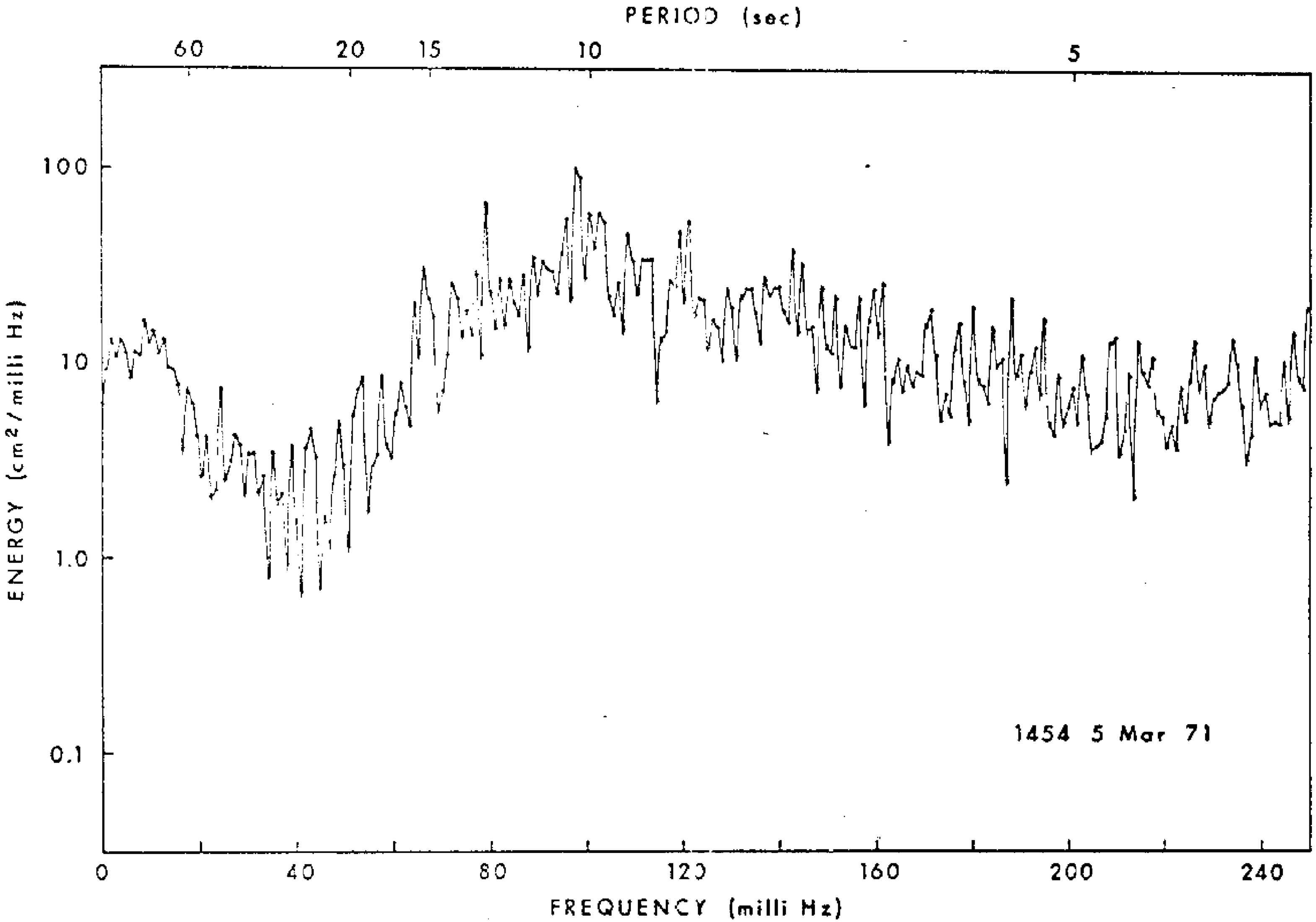

Figure 29. Wave energy spectrum.

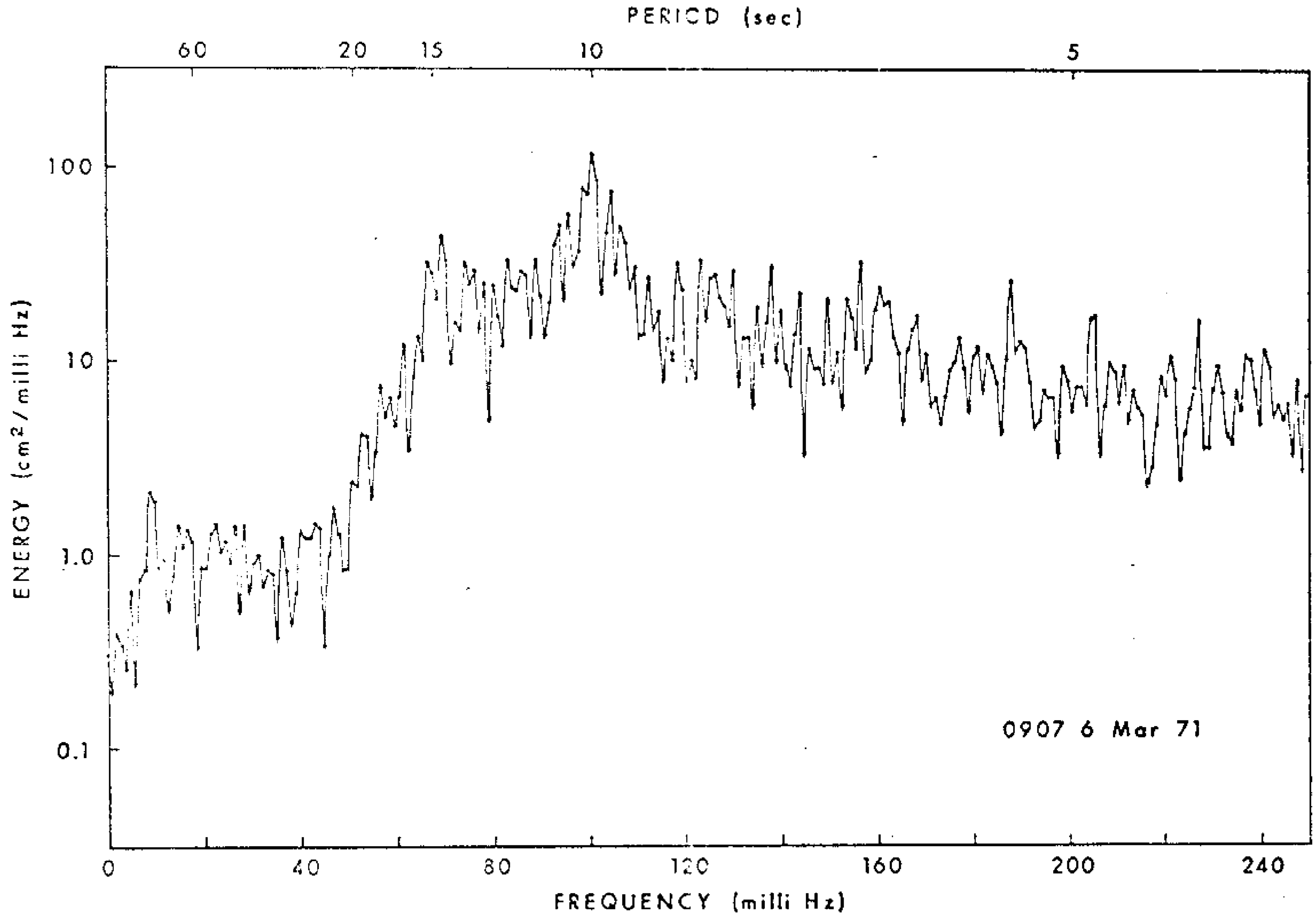

Figure 30. Wave energy spectrum.

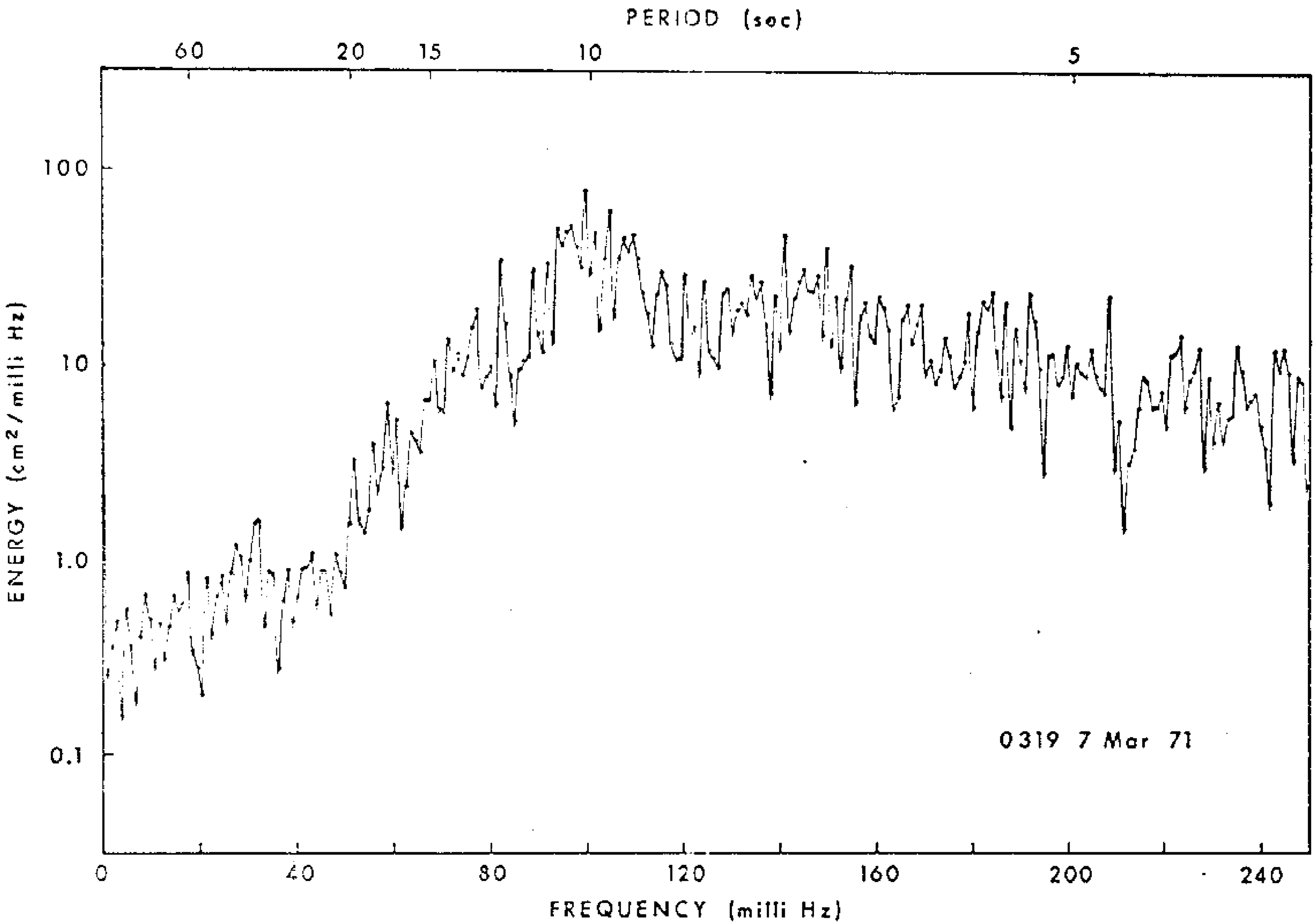

Figure 31. Wave energy spectrum.

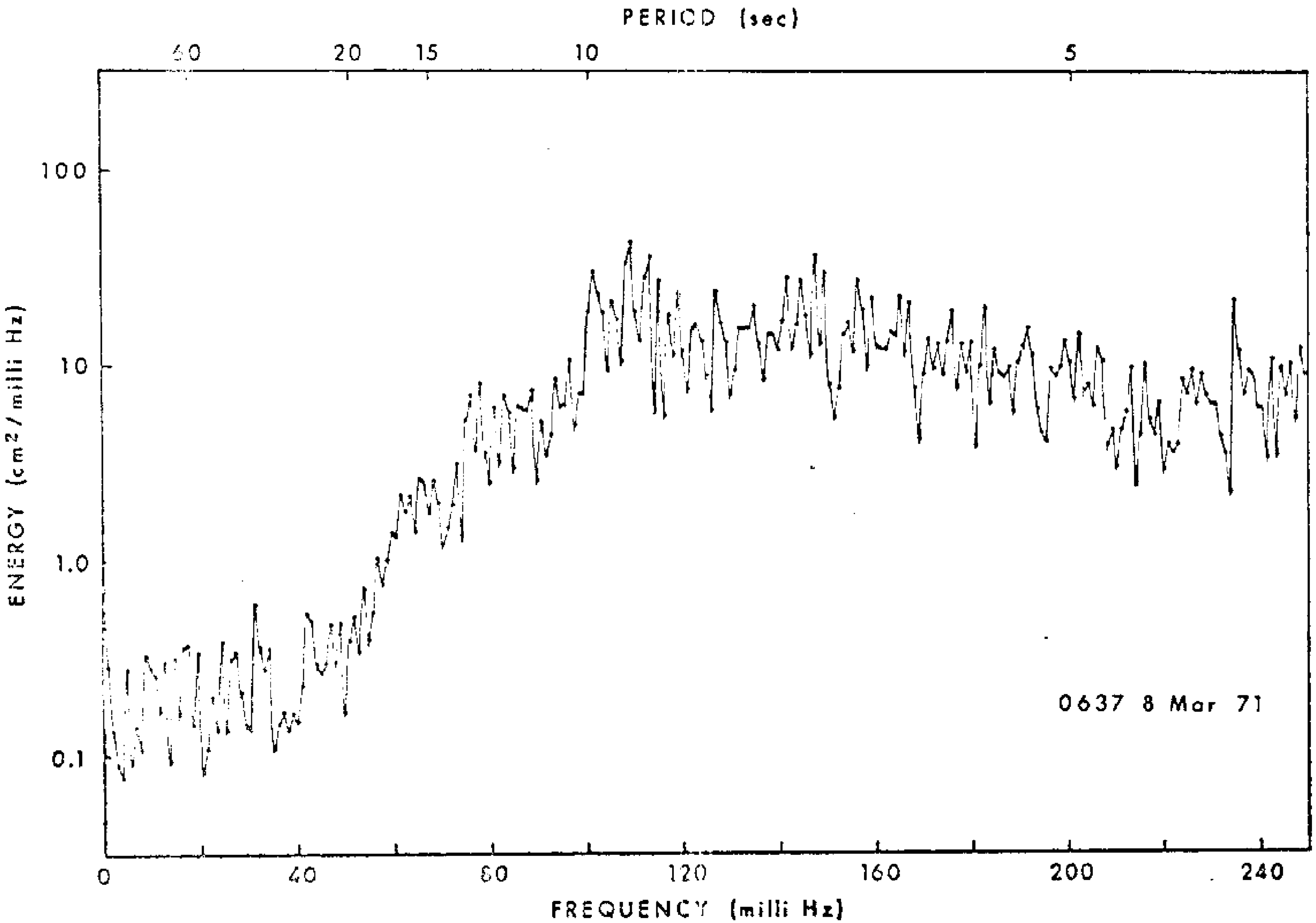

Figure 32. Wave energy spectrum.

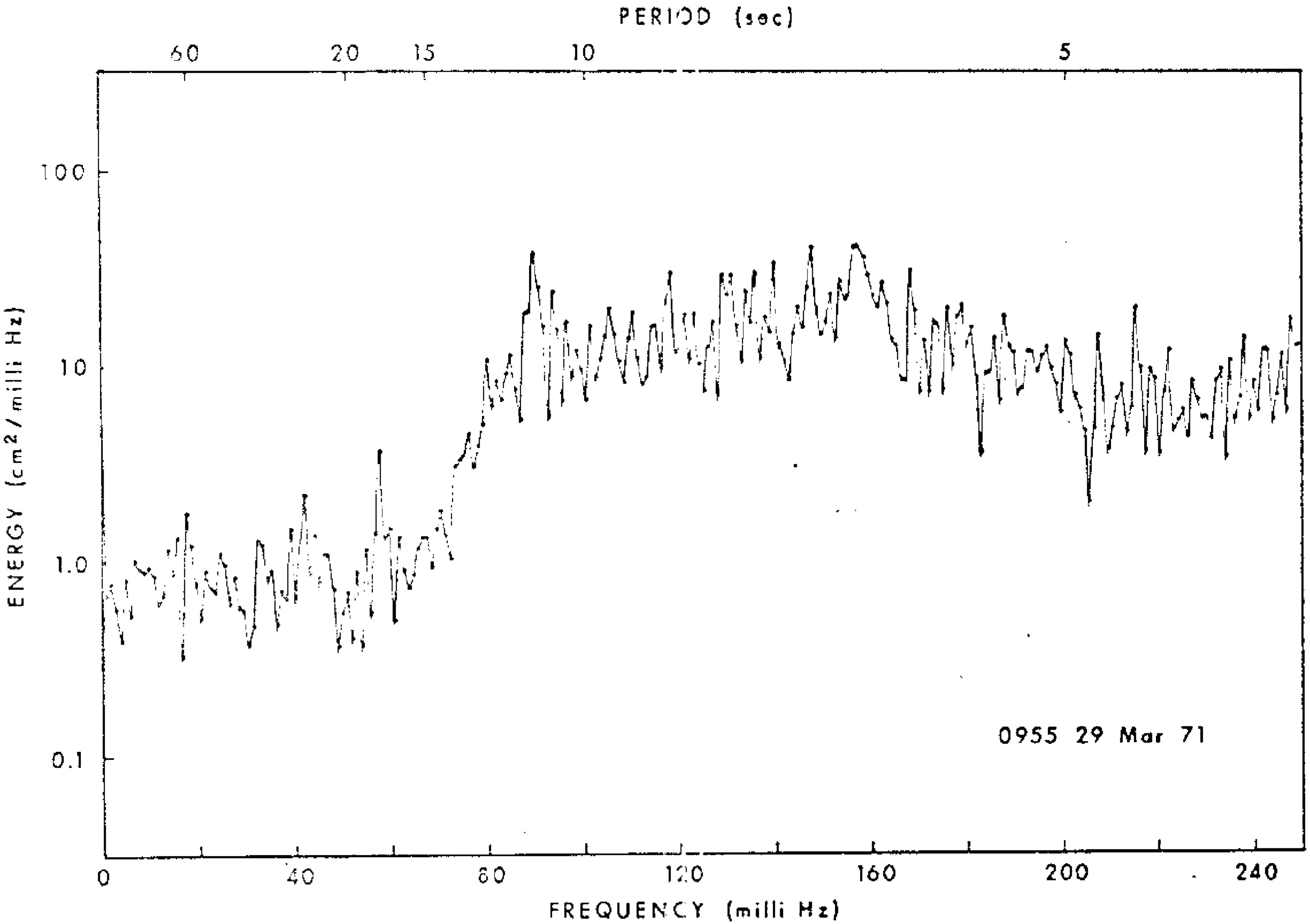

Figure 33. Wave energy spectrum.

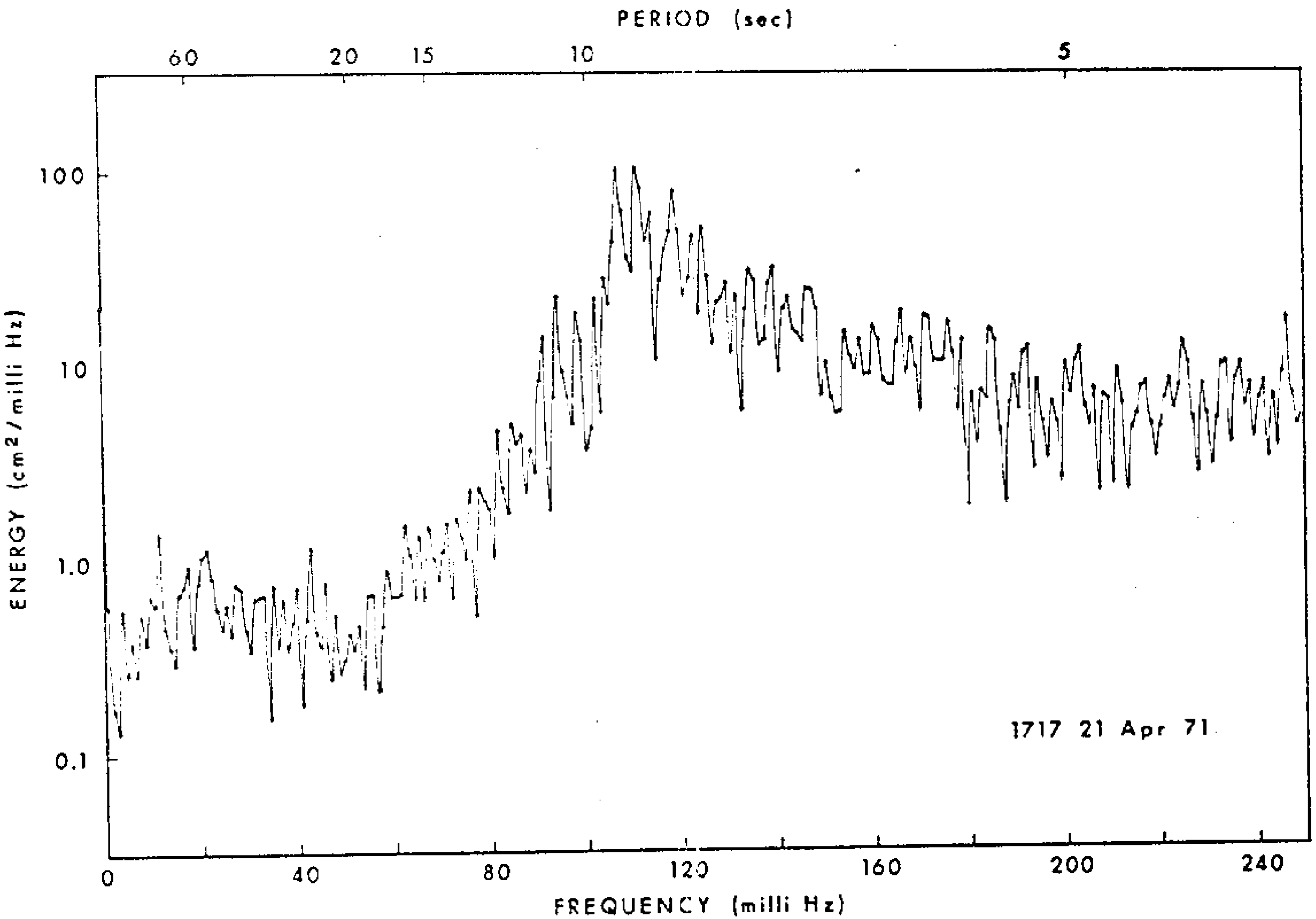

Figure 34. Wave energy spectrum.

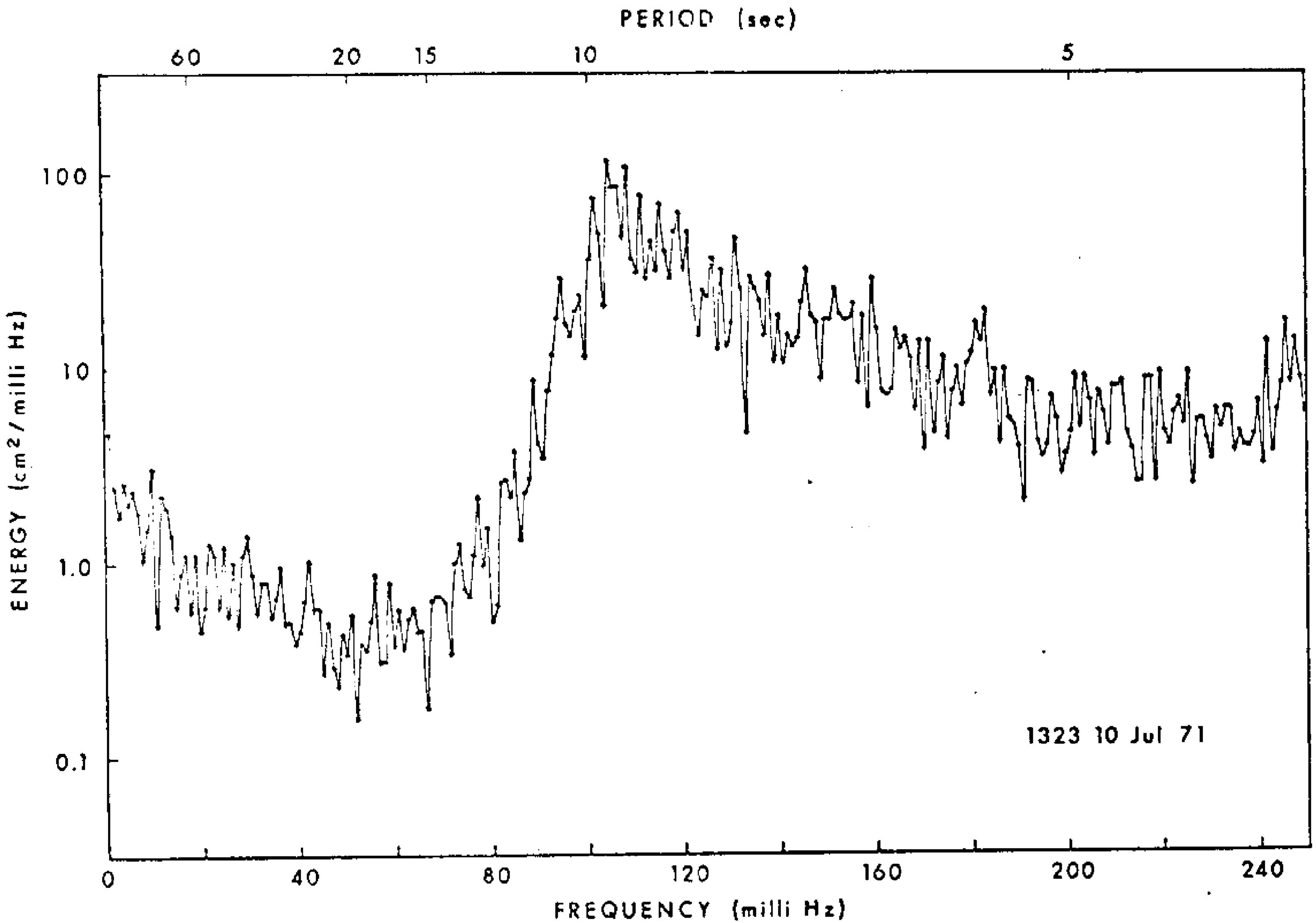

Figure 35. Wave energy spectrum.

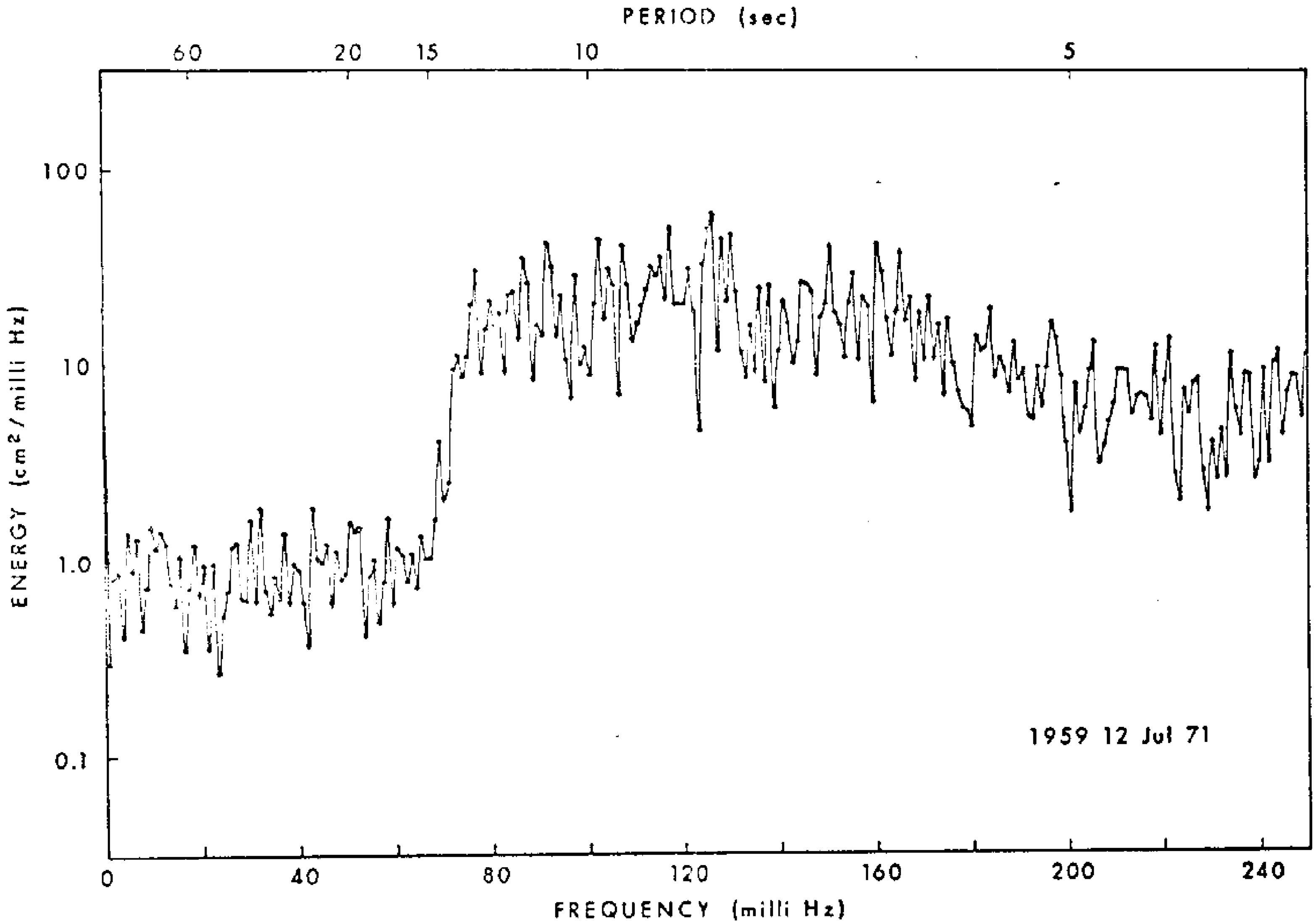

Figure 36. Wave energy spectrum.

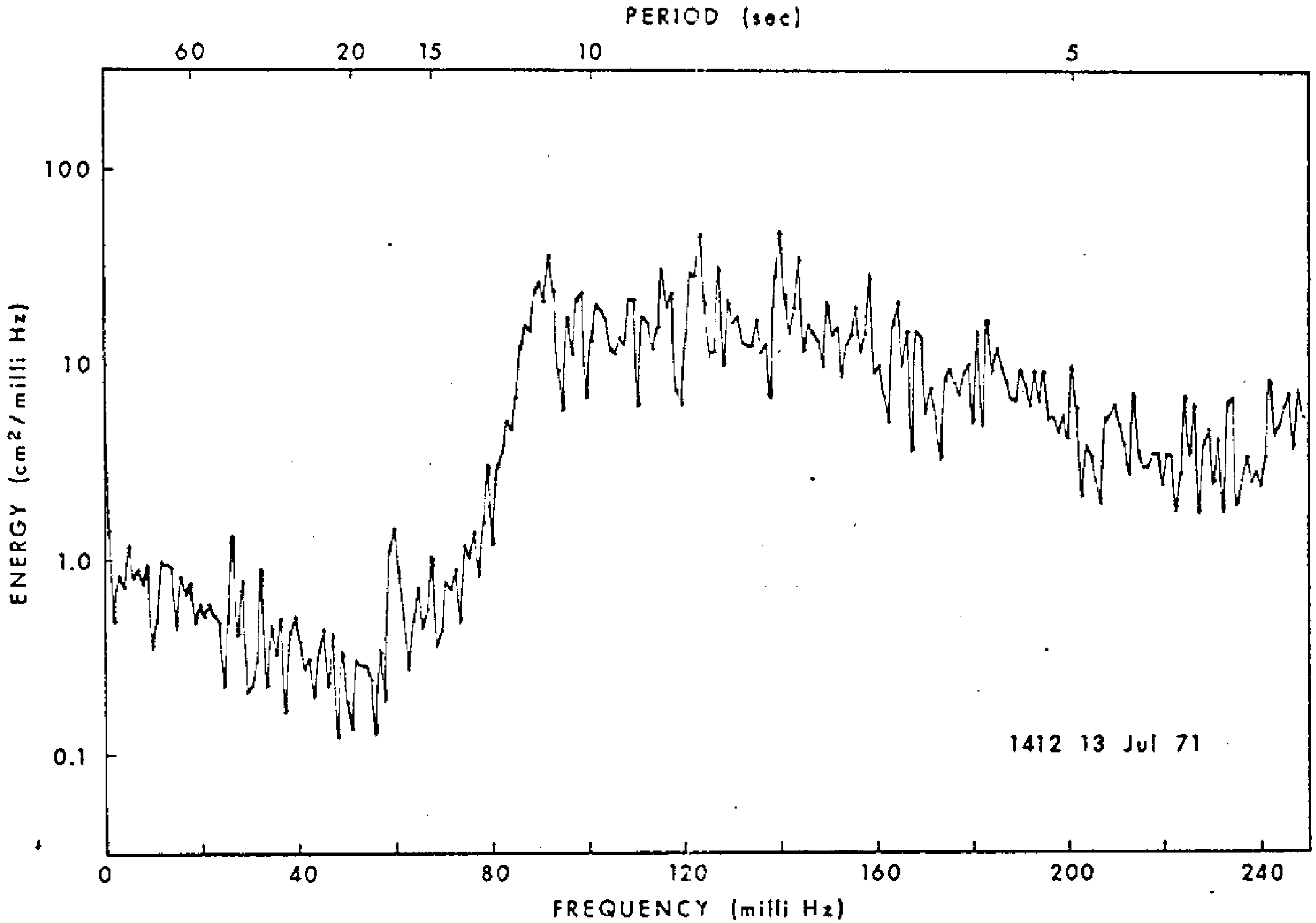

Figure 37. Wave energy spectrum.

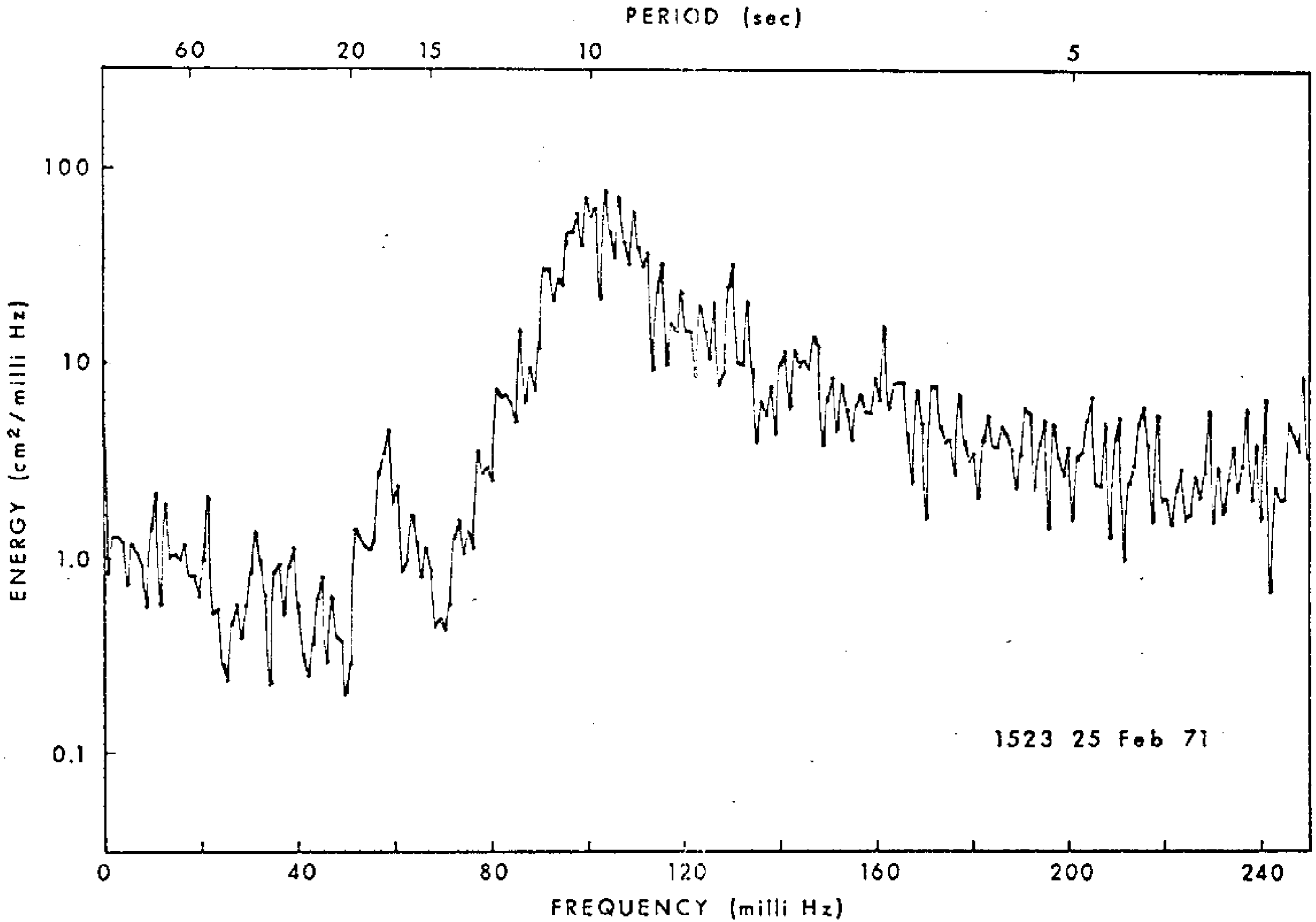

Figure 38. Wave energy spectrum.

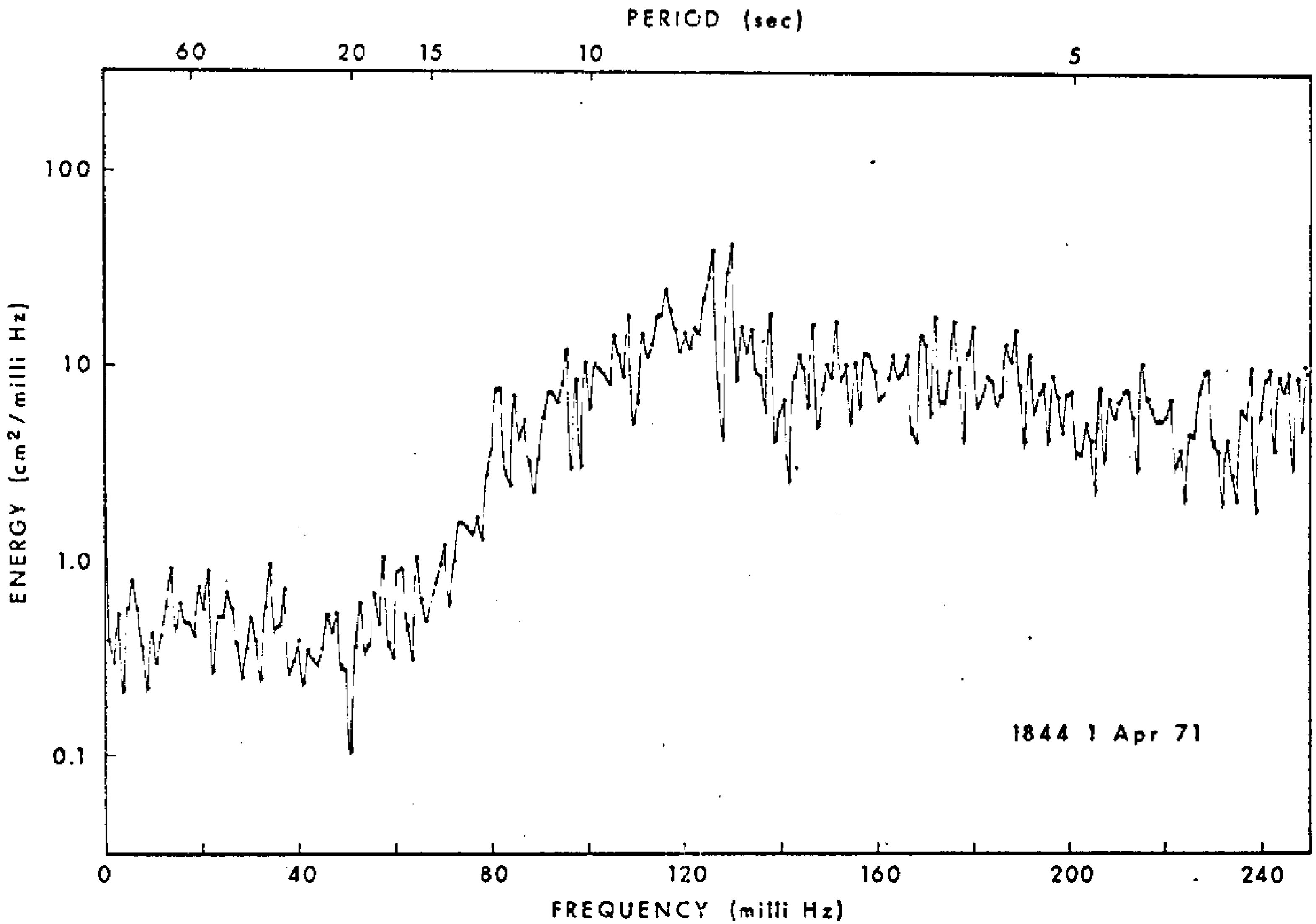

Figure 39. Wave energy spectrum.

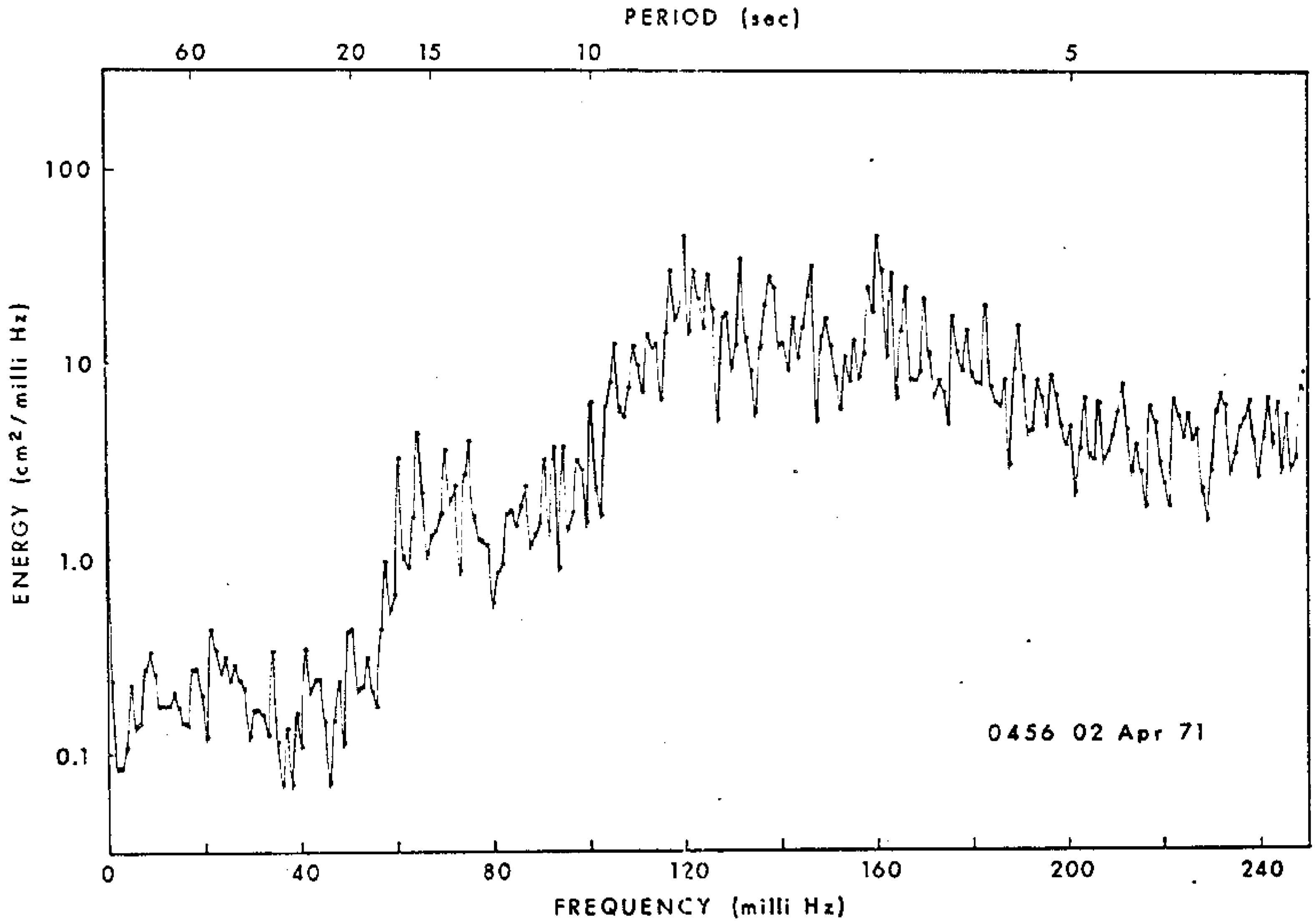

Figure 40. Wave energy spectrum.

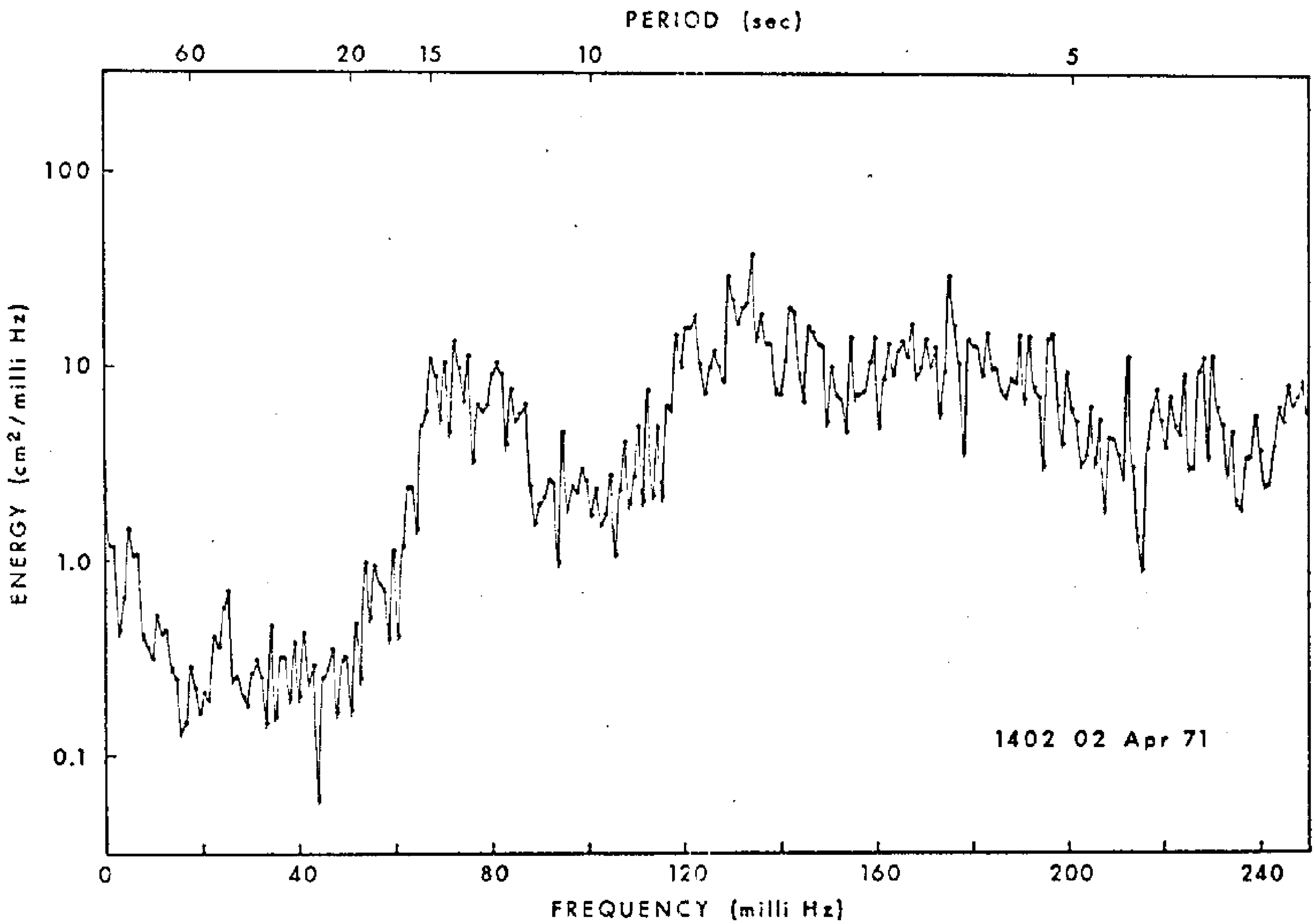

Figure 41. Wave energy spectrum.

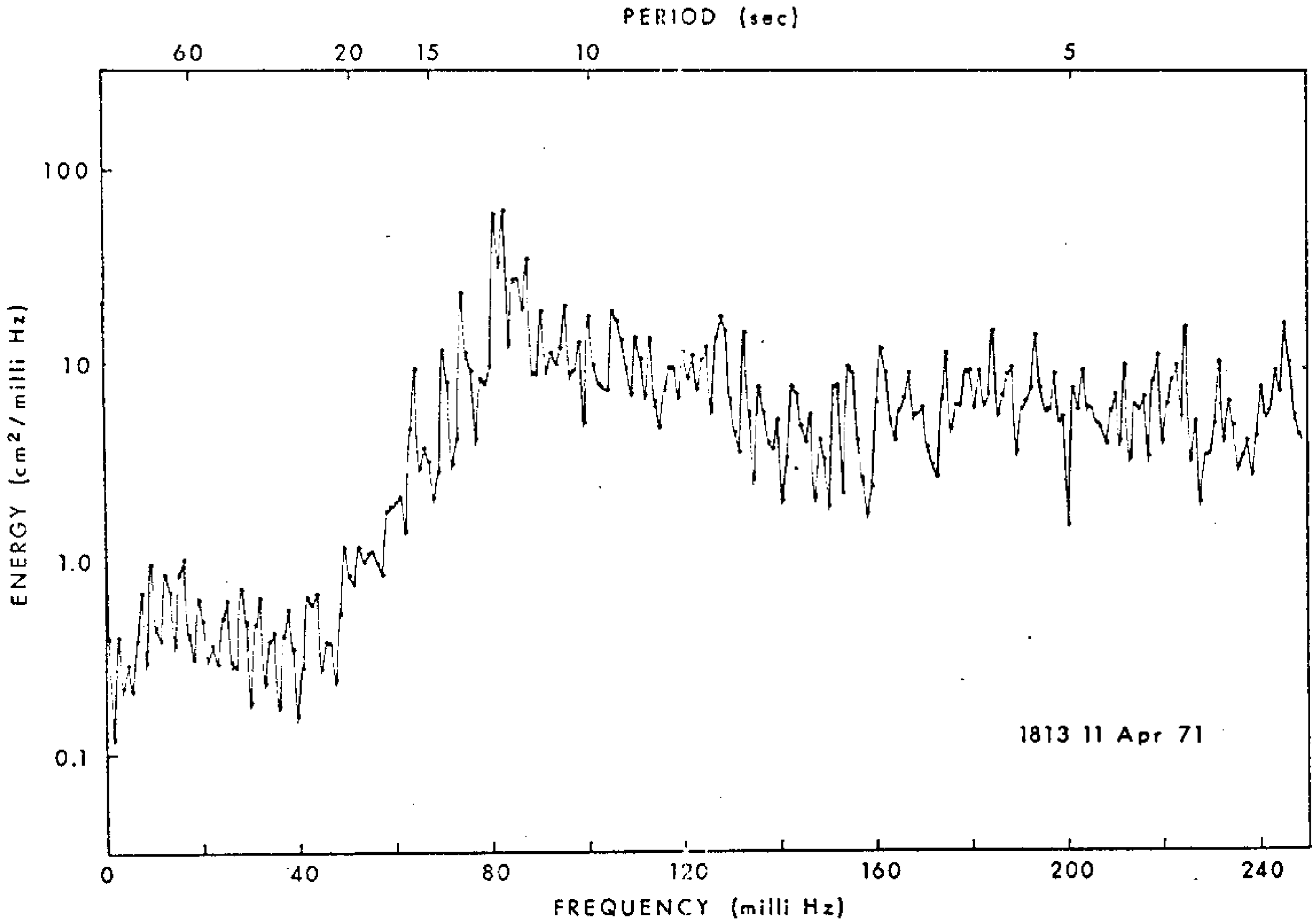

Figure 42. Wave energy spectrum.

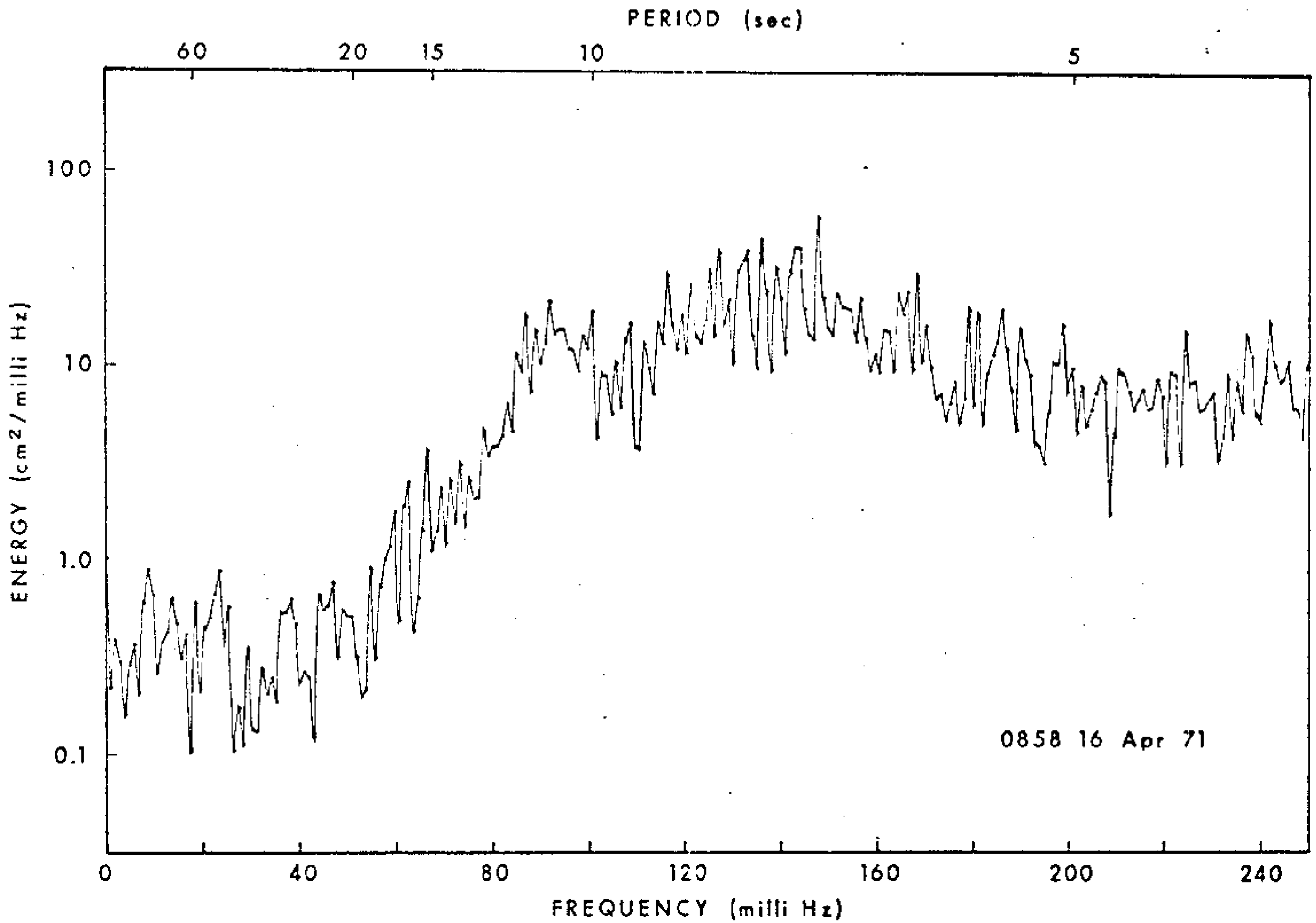

Figure 43. Wave energy spectrum.

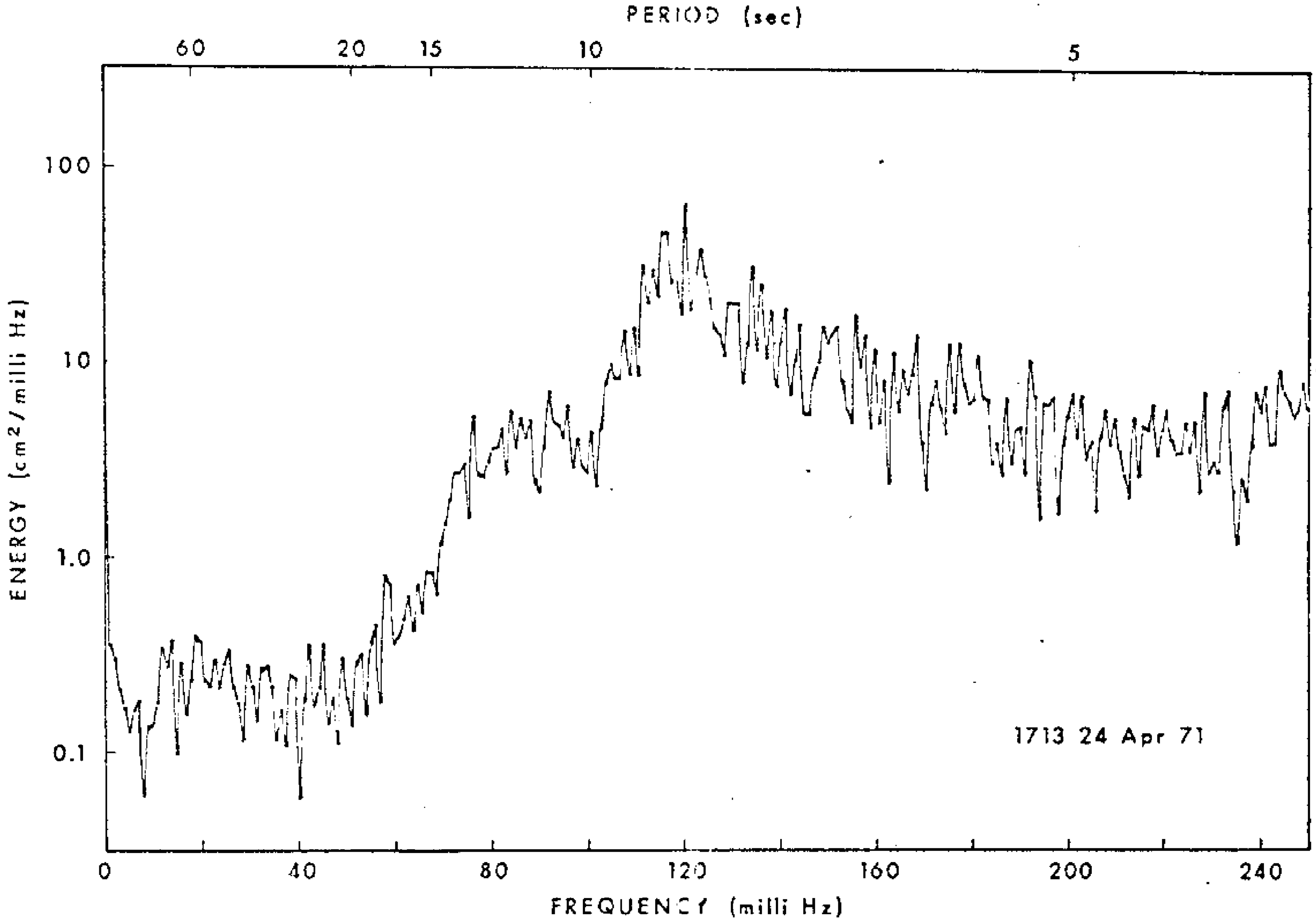

Figure 44. Wave energy spectrum.

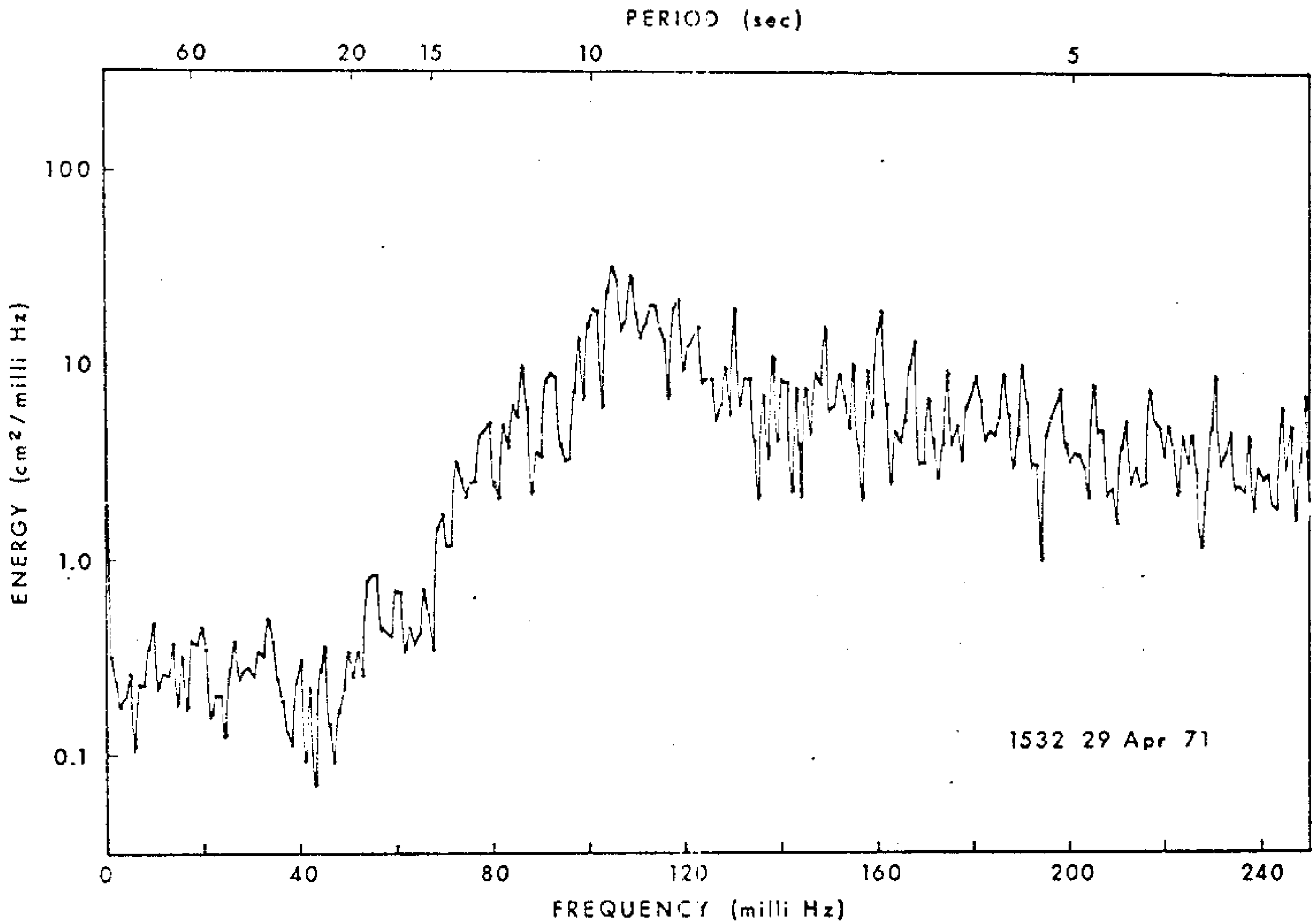

Figure 45. Wave energy spectrum.

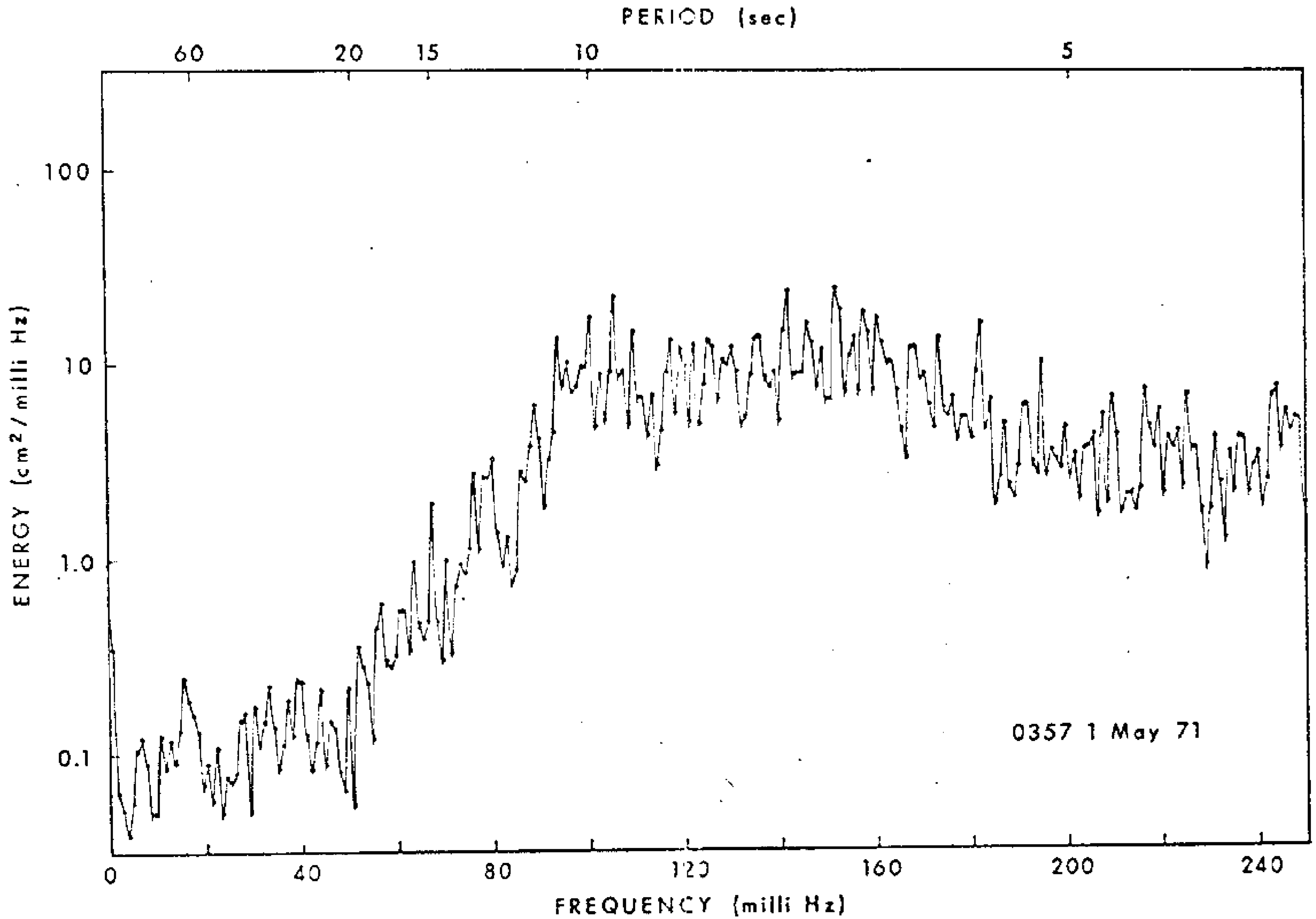

Figure 46. Wave energy spectrum.

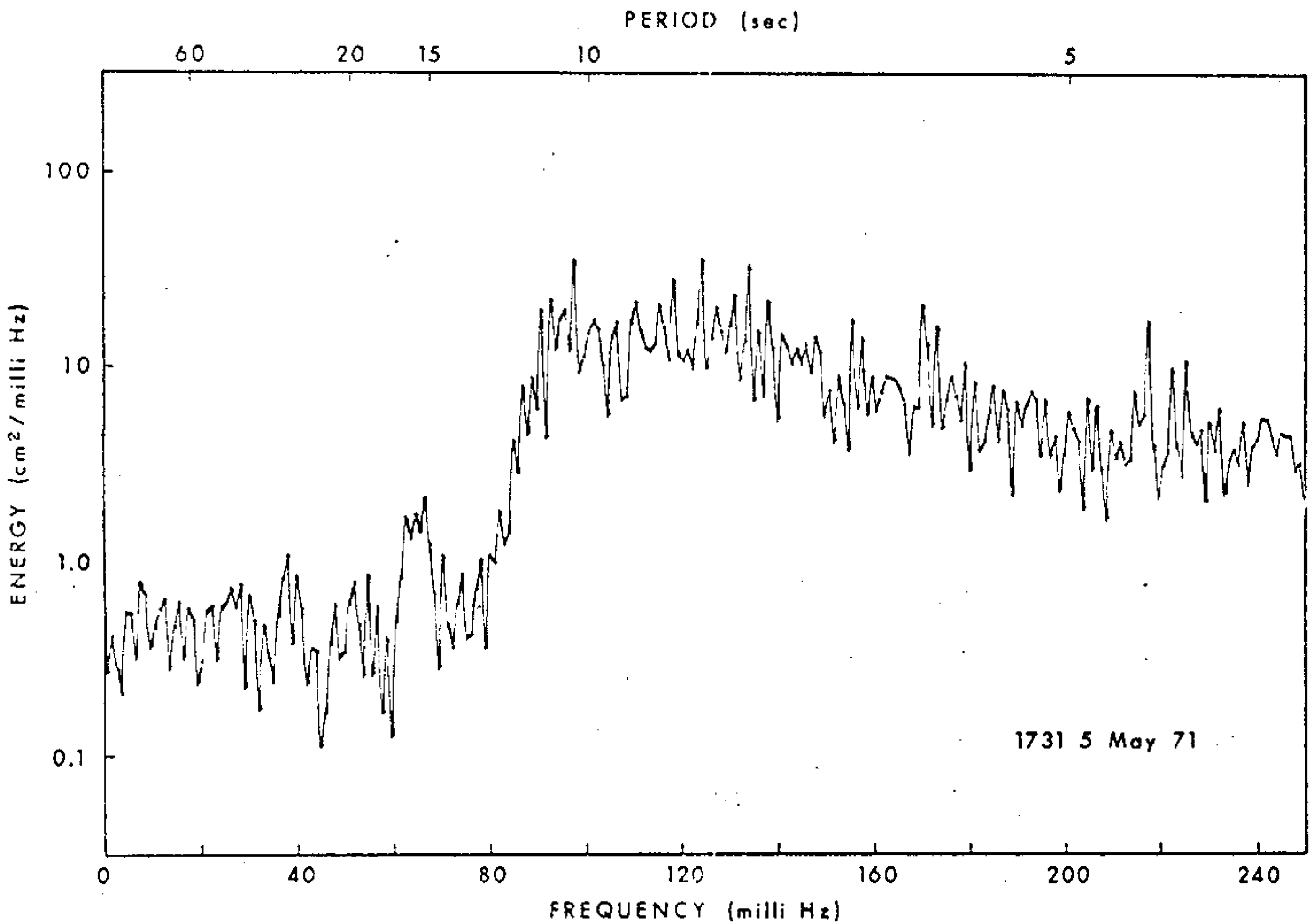

Figure 47. Wave energy spectrum.

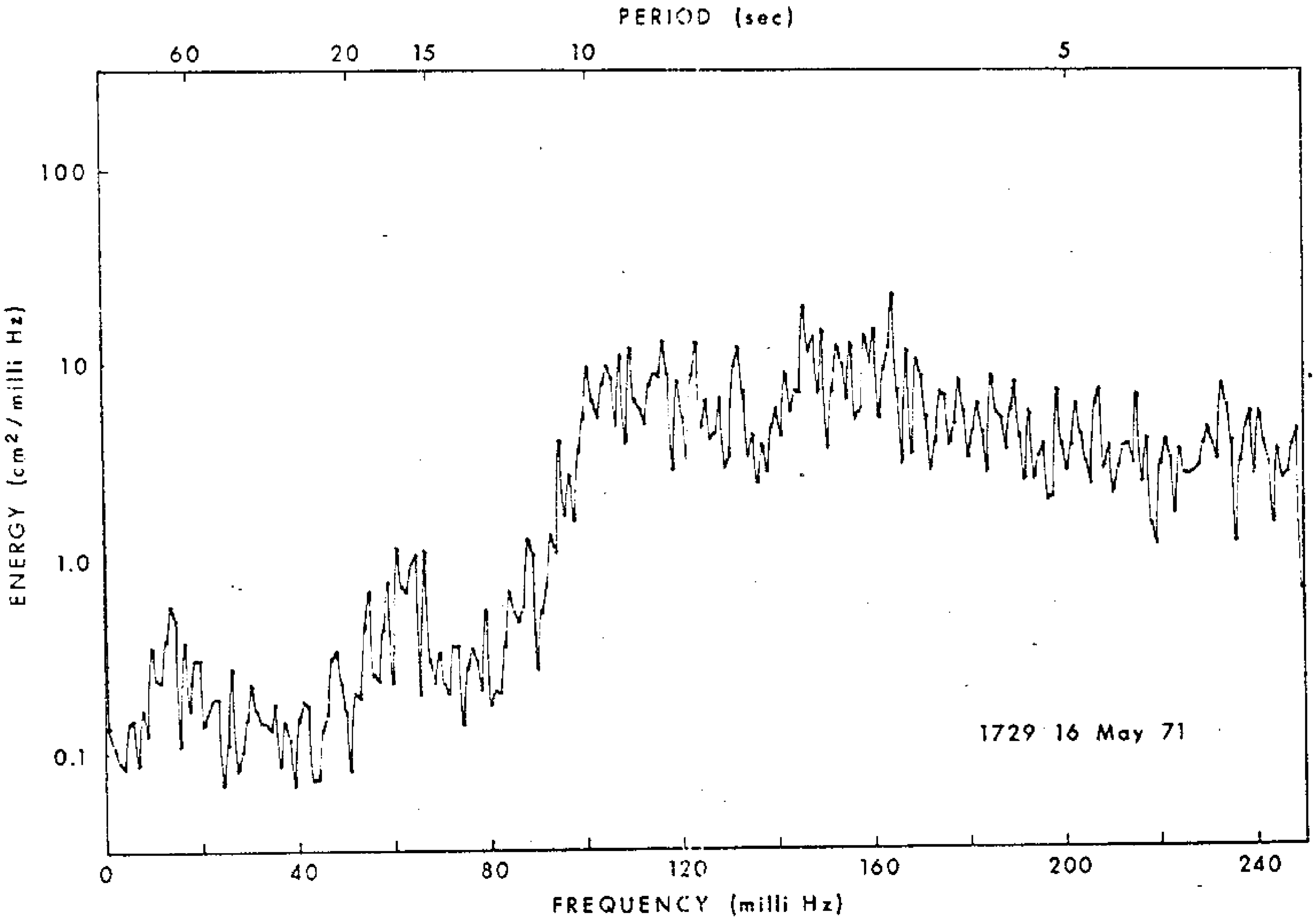

Figure 48. Wave energy spectrum.

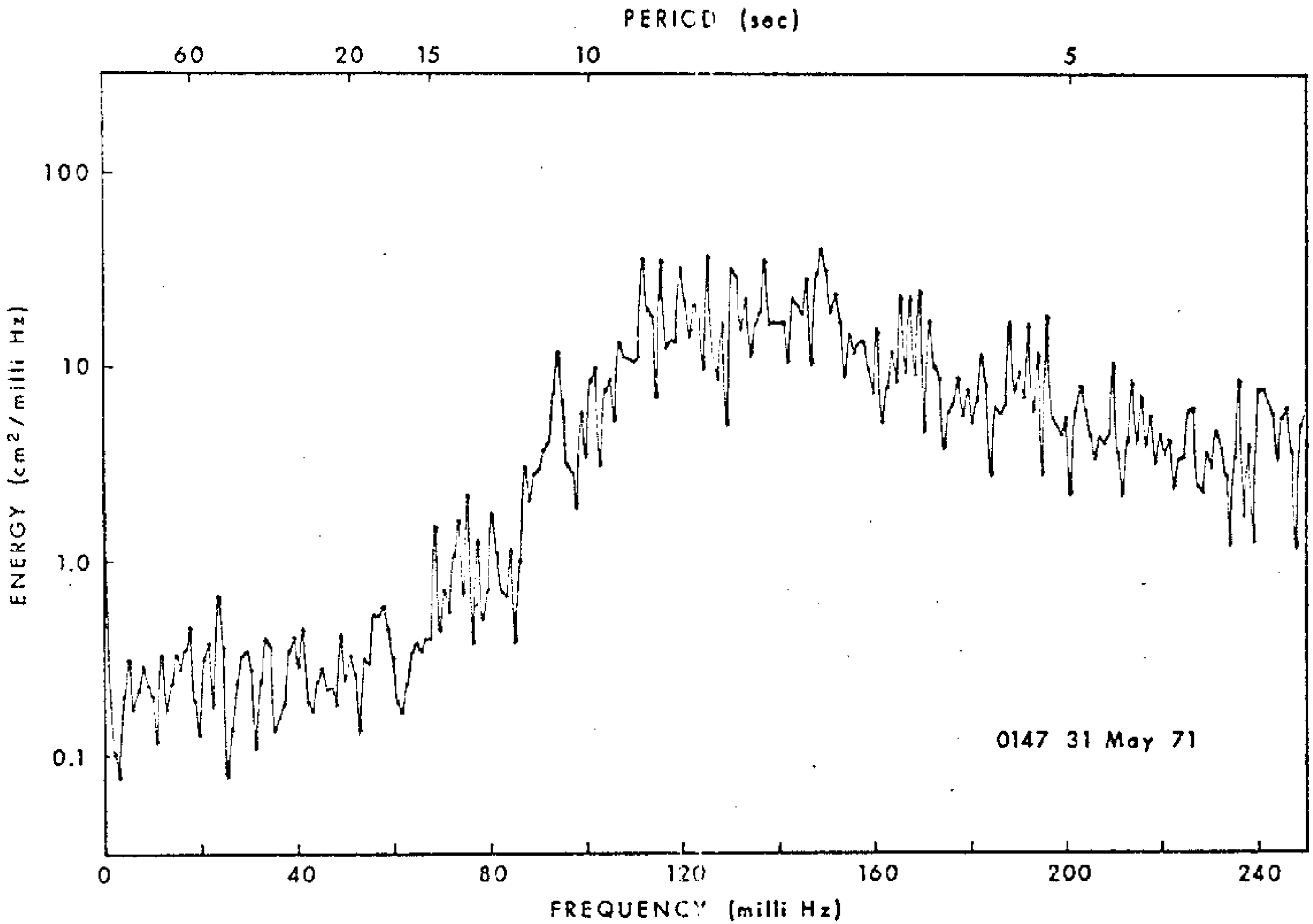

Figure 49. Wave energy spectrum.

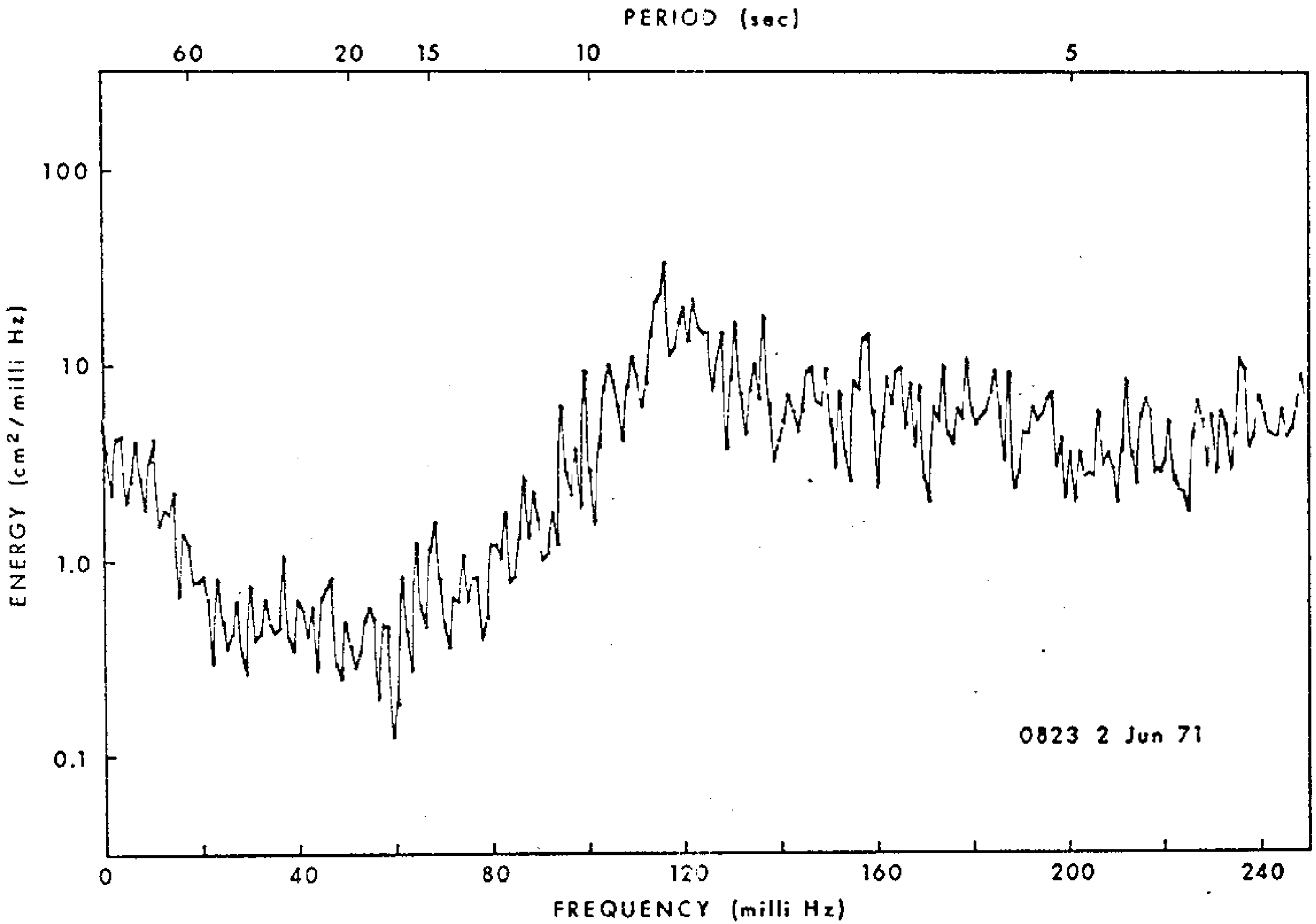

Figure 50. Wave energy spectrum.

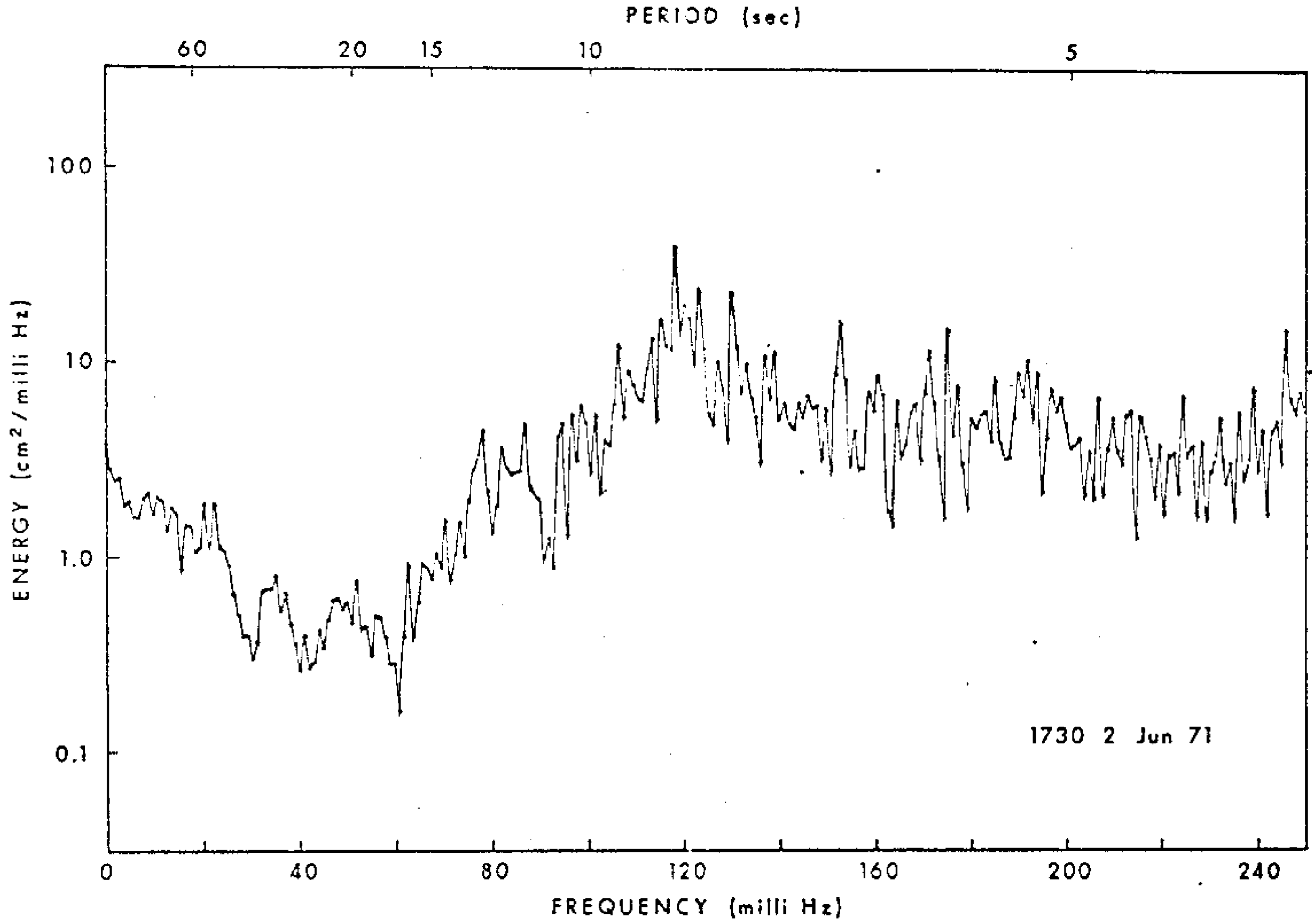

Figure 51. Wave energy spectrum.

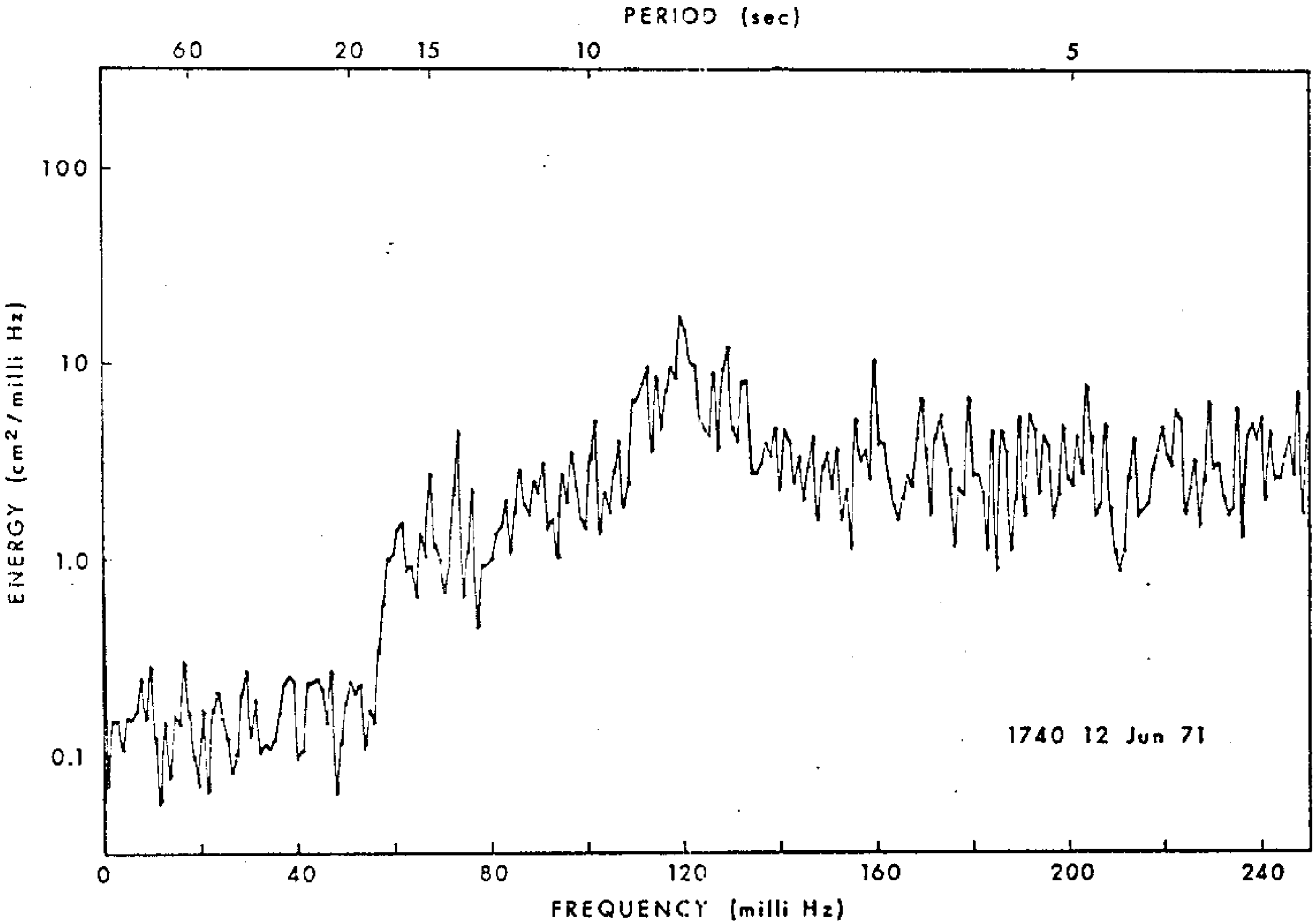

Figure 52. Wave energy spectrum.

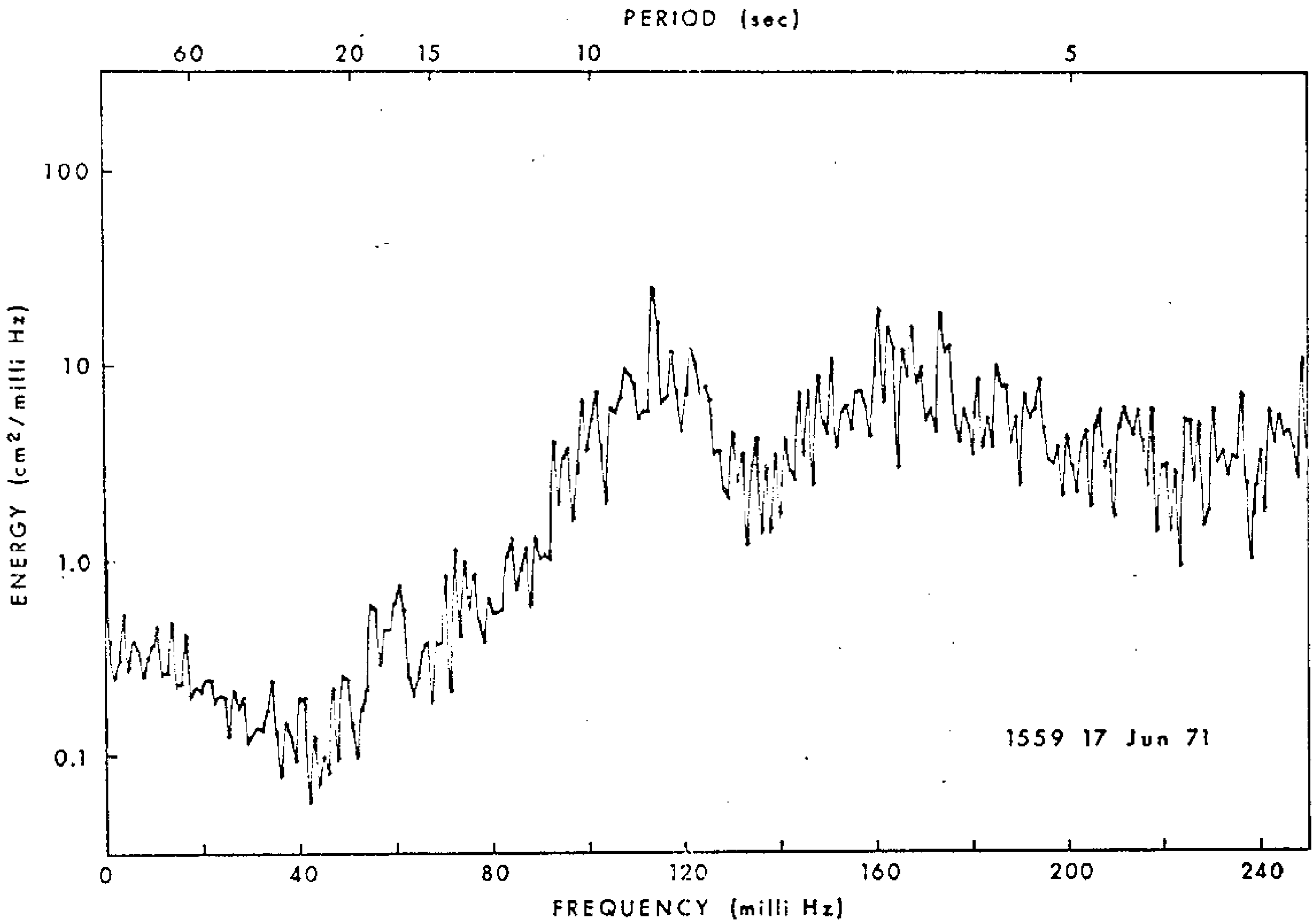

Figure 53. Wave energy spectrum.

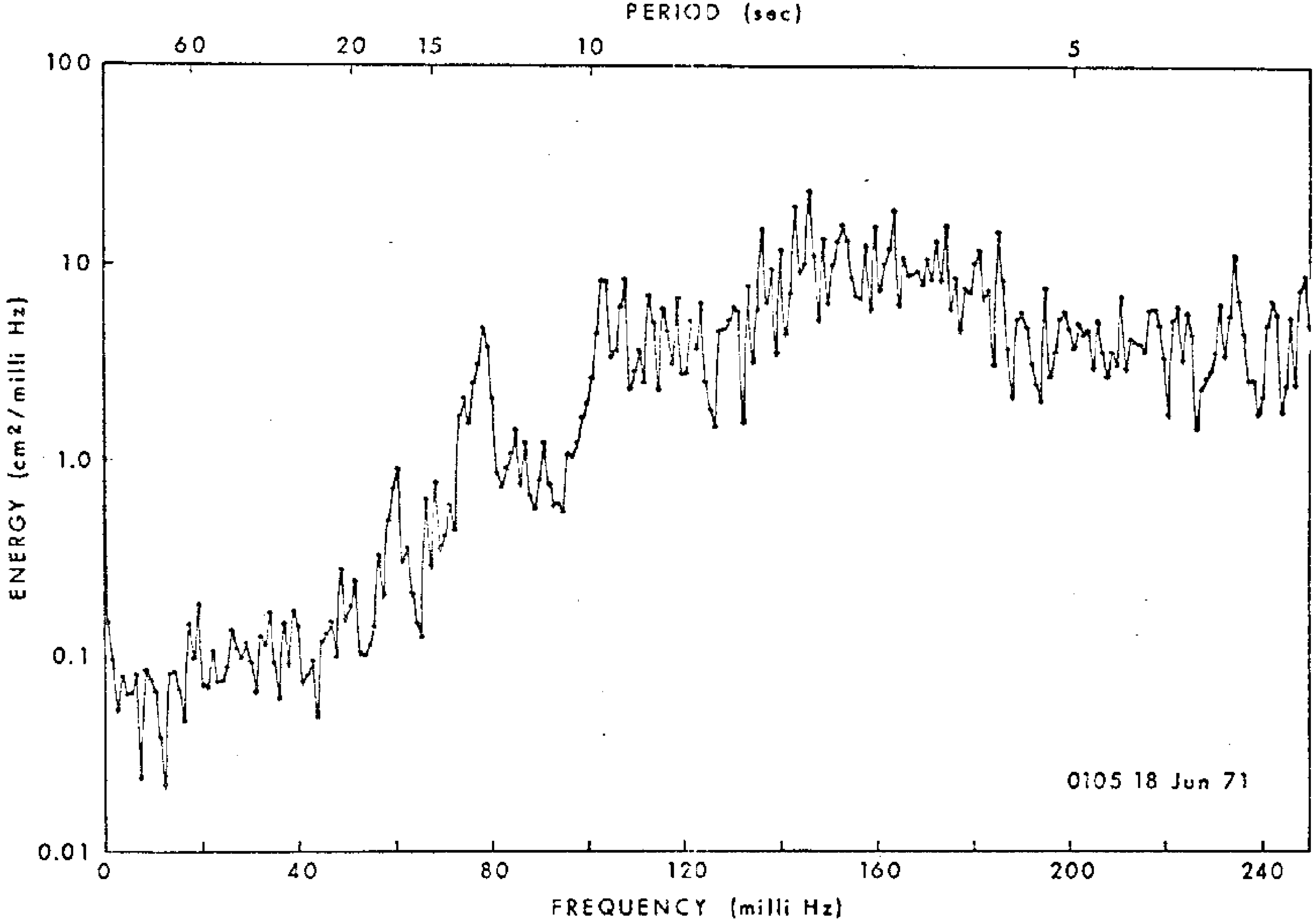

Figure 54. Wave energy spectrum.

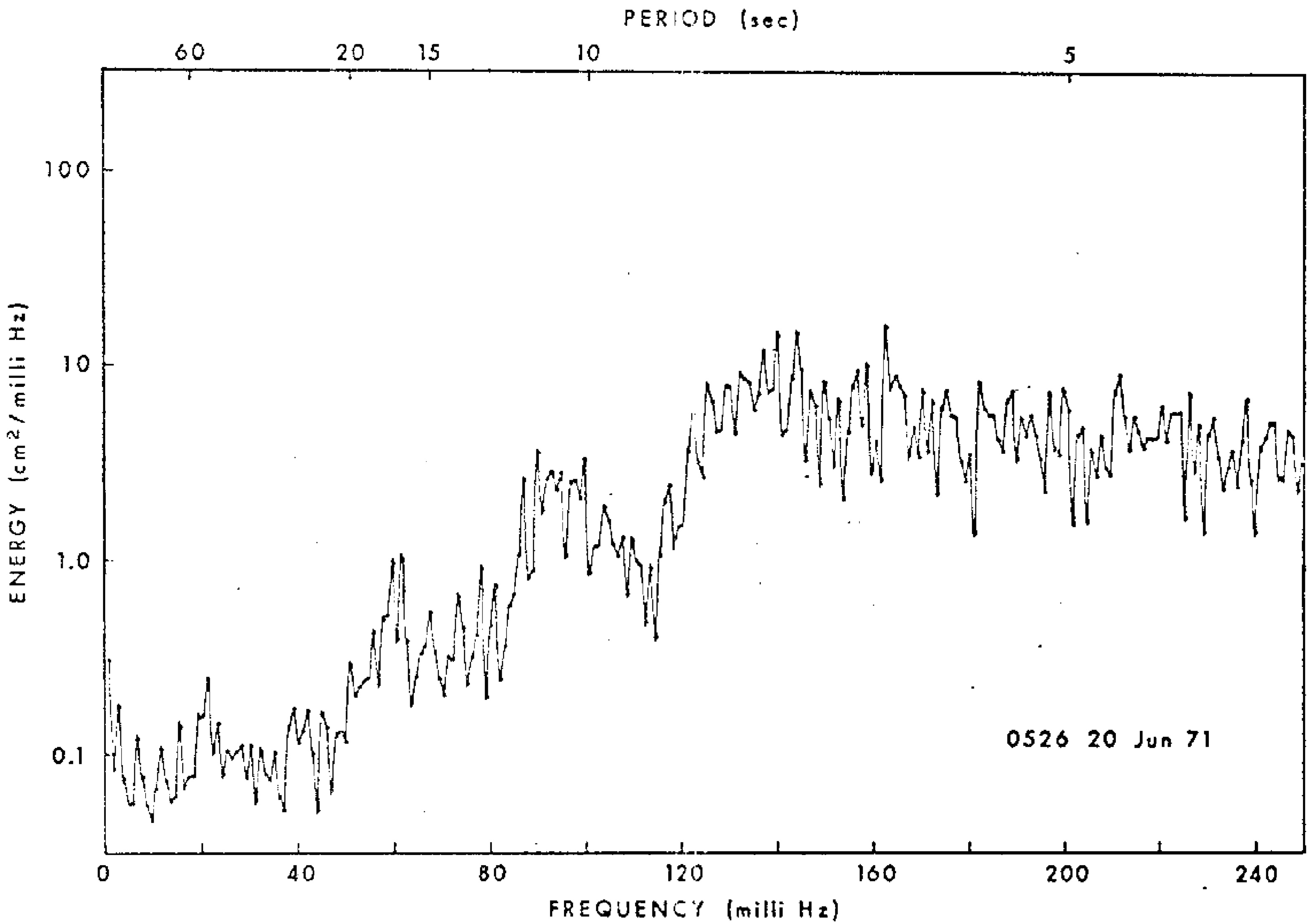

Figure 55. Wave energy spectrum.

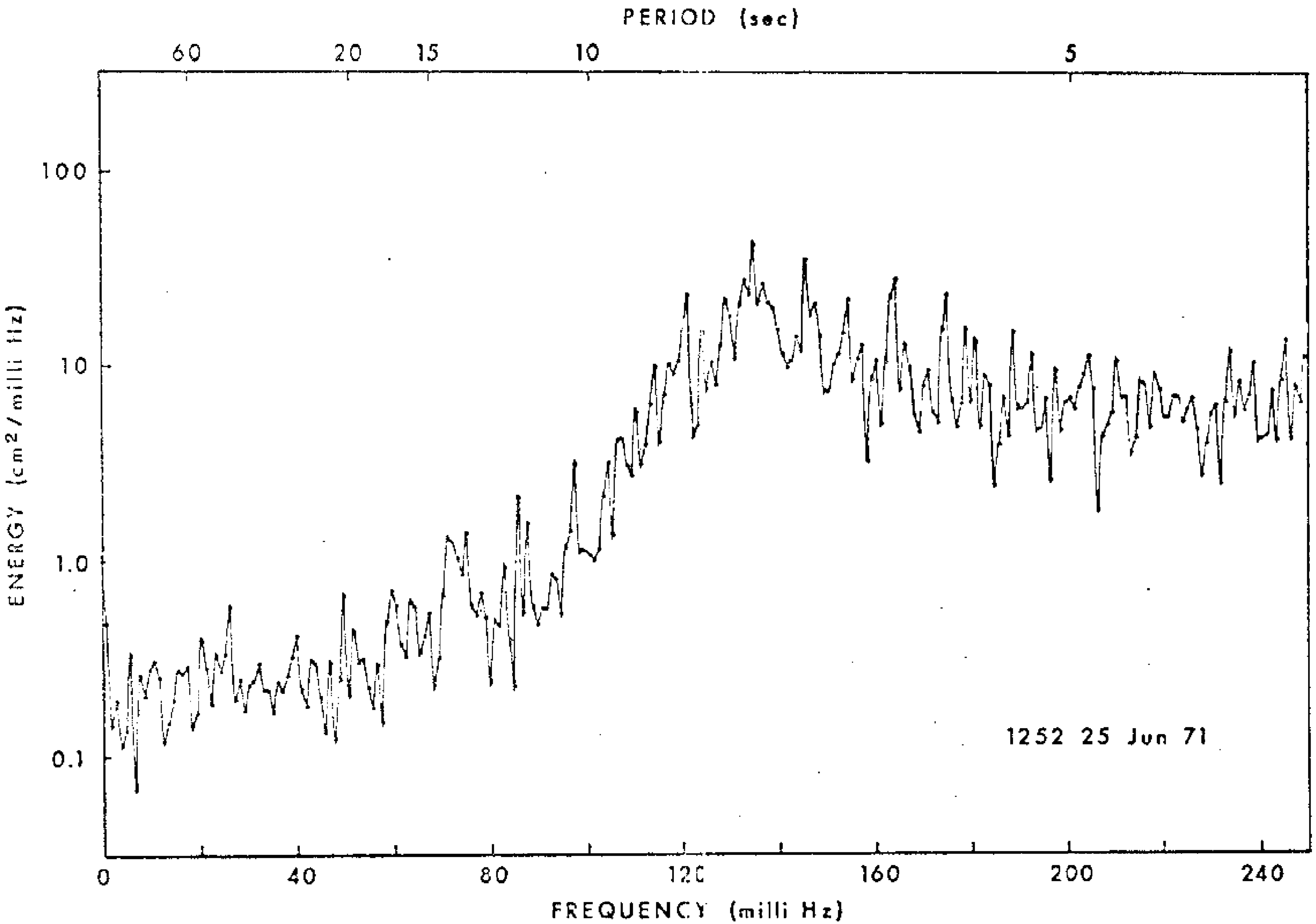

Figure 56. Wave energy spectrum.

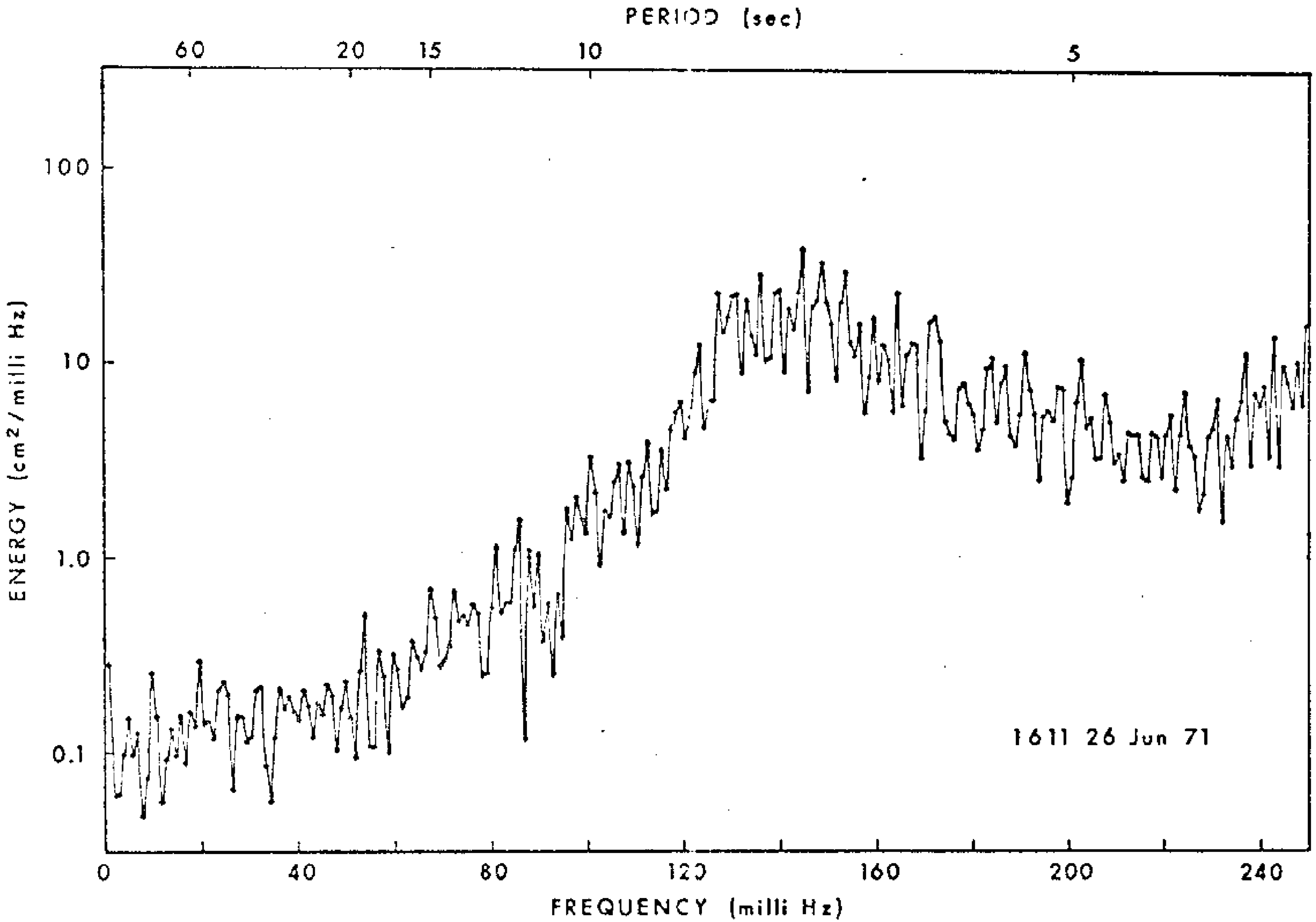

Figure 57. Wave energy spectrum.

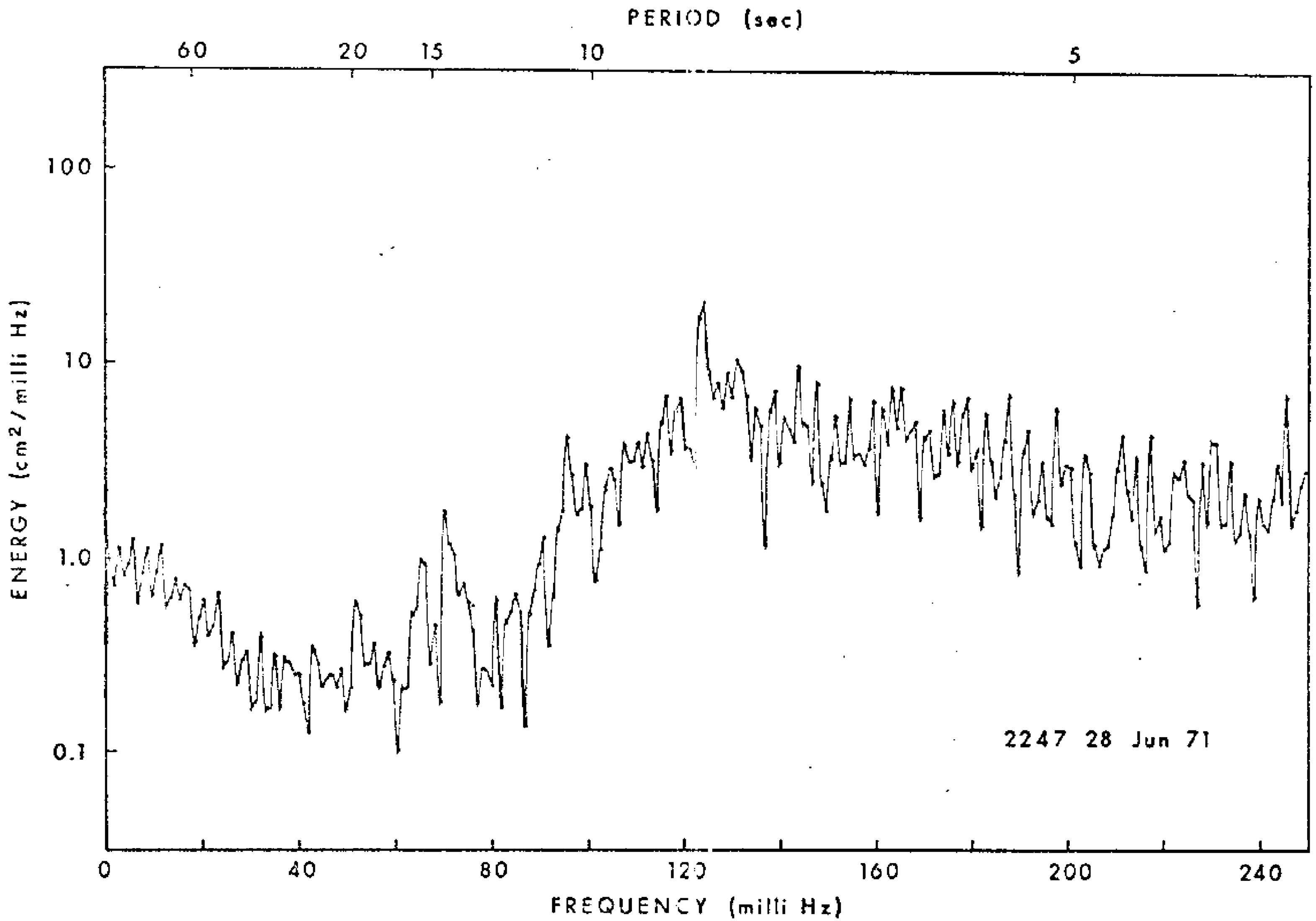

Figure 58. Wave energy spectrum.

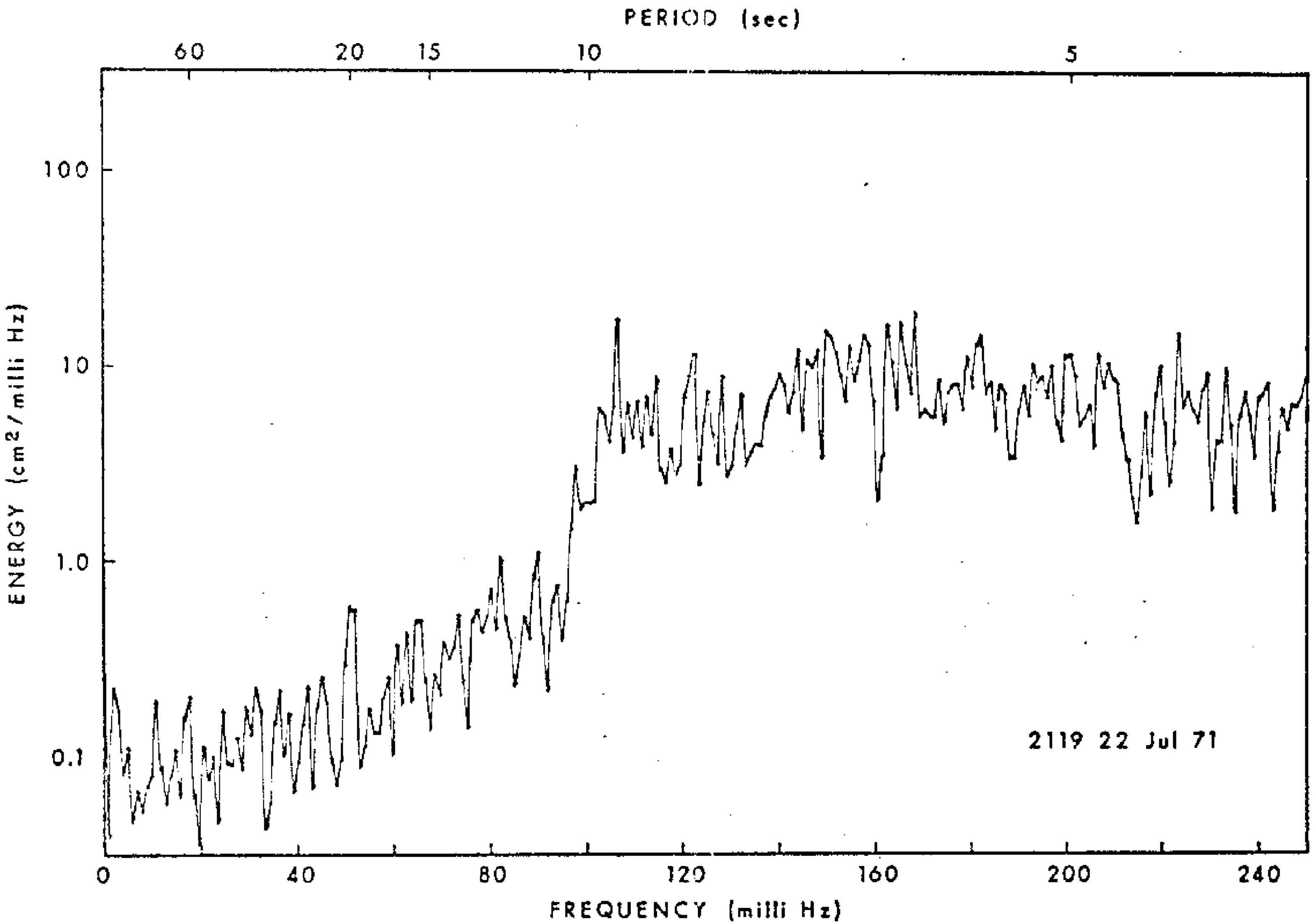

Figure 59. Wave energy spectrum.

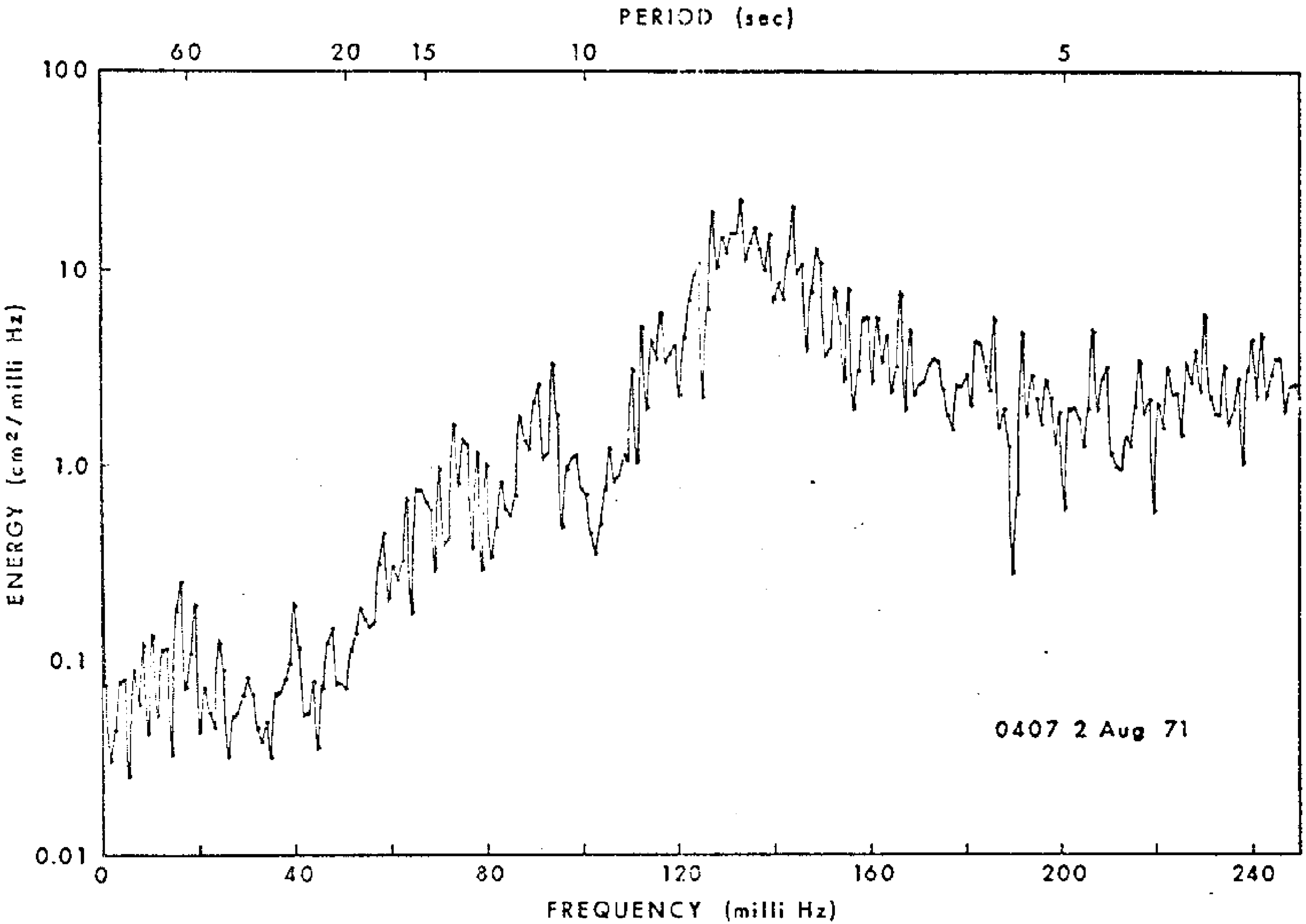

Figure 60. Wave energy spectrum.

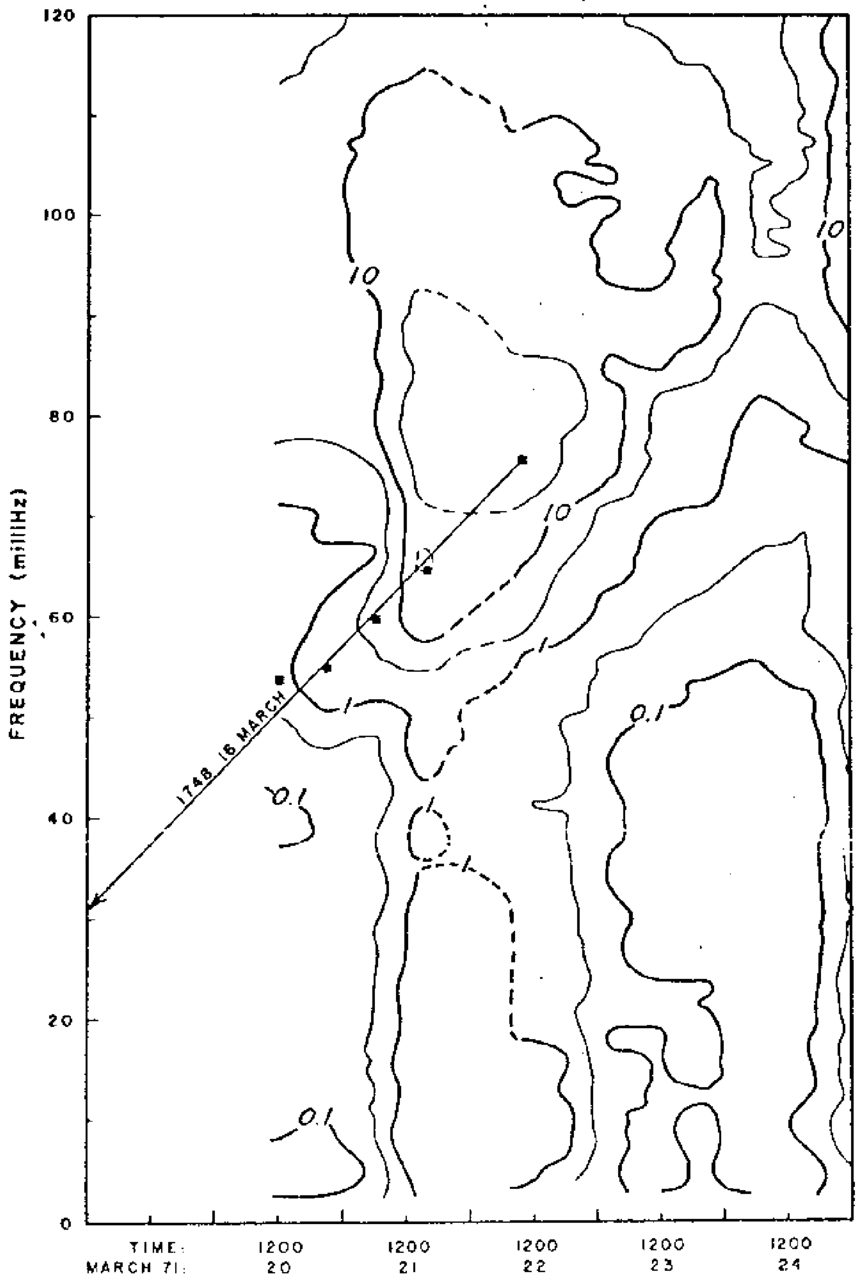

Figure 61. Contours of equal energy density on a frequency-time plot. The contours are at equal intervals of the log of energy. Heavy contours represent 0.1, 1.0, and 10 cm^2/milliHz. Dashed lines indicate a missing spectrum for 0112 21 March. The ridge (marked by the arrow) in the energy contours represents the dispersive arrivals from a source originating at 1748 16 March. Dark circles, along the arrow, mark the energy peaks.

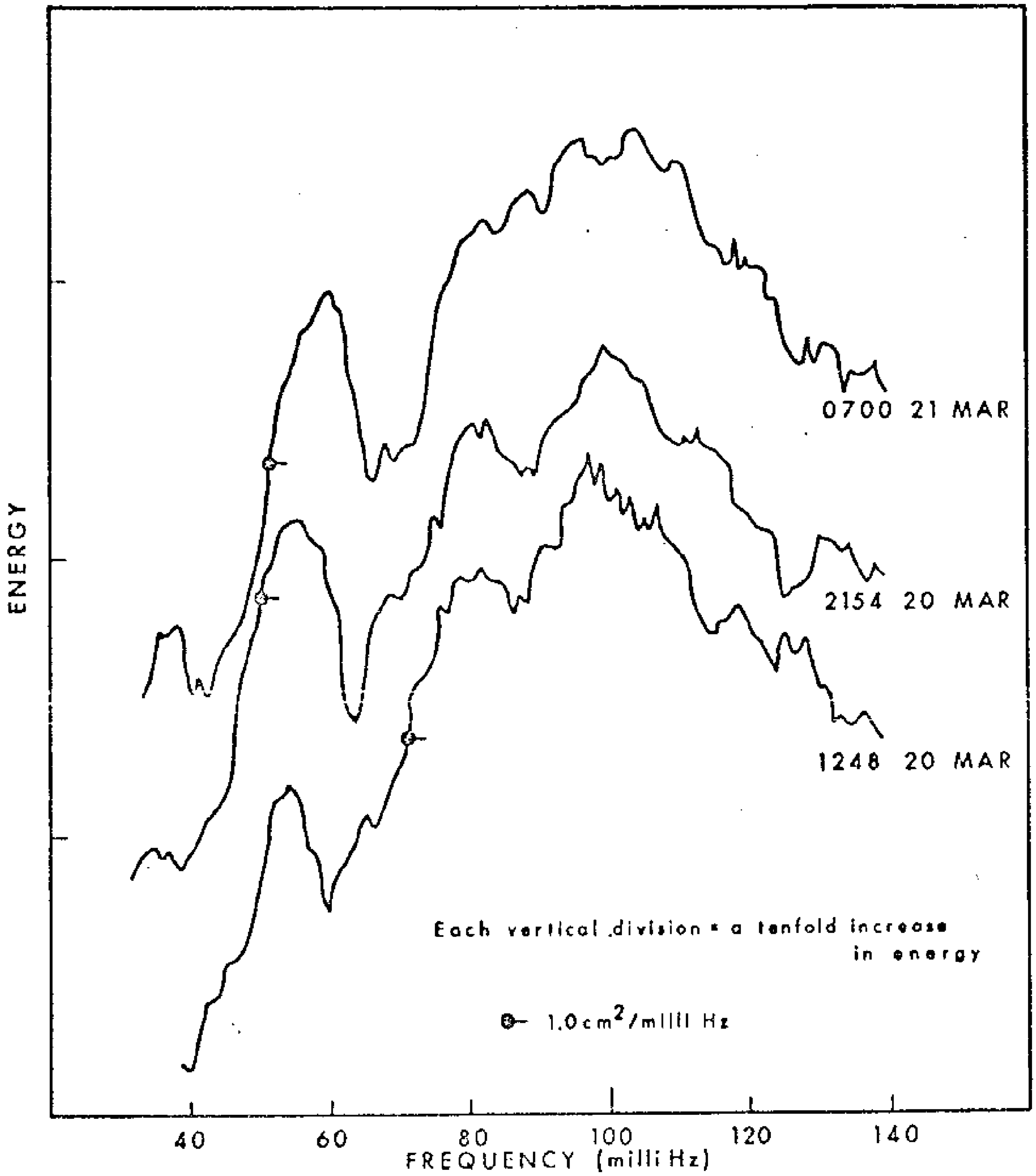

Figure 62. Sequence of wave-energy spectra showing the shift in frequency with time of the energy peaks.

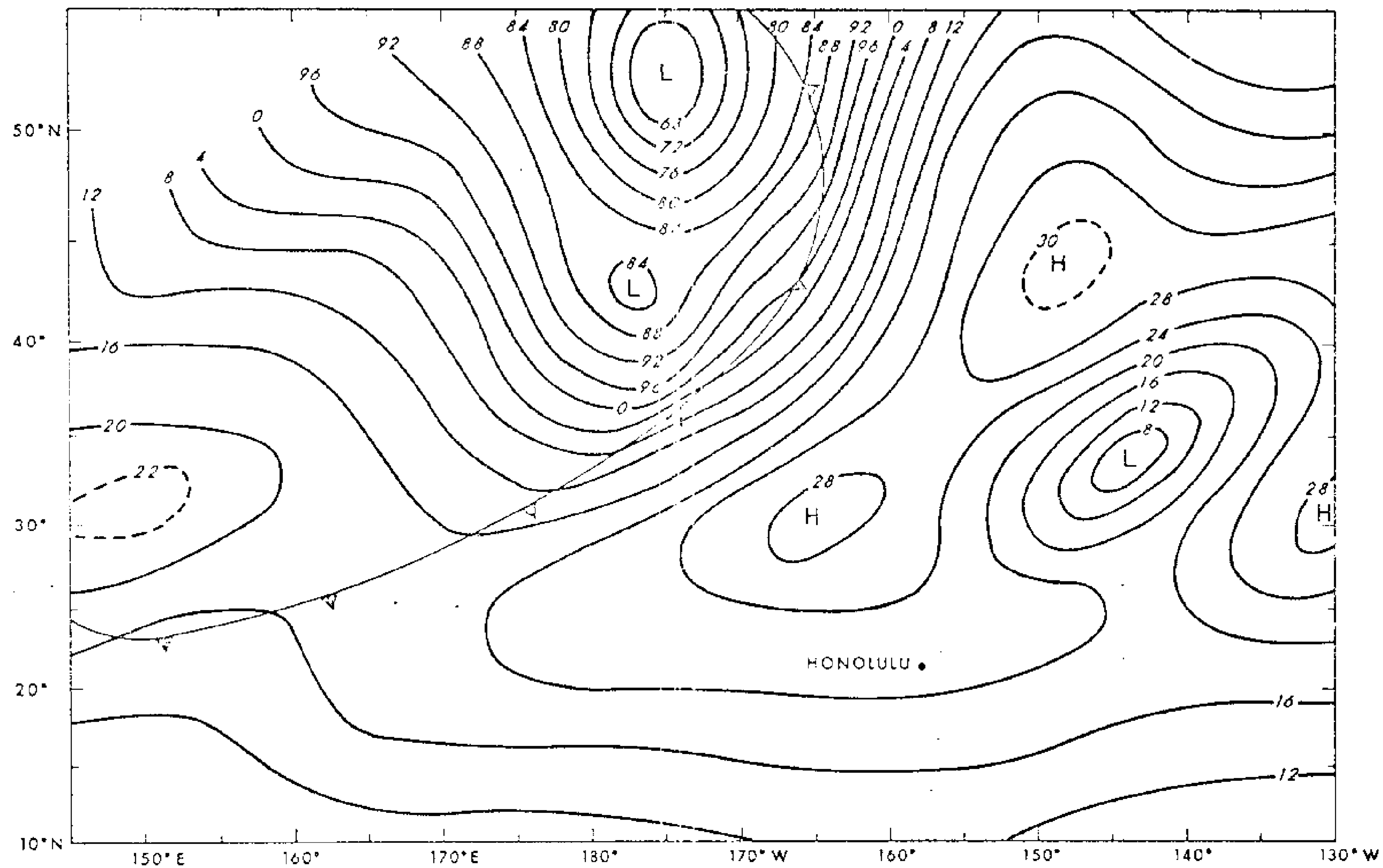

Figure 63. From National Weather Service surface analysis for 0200 16 March 1971.

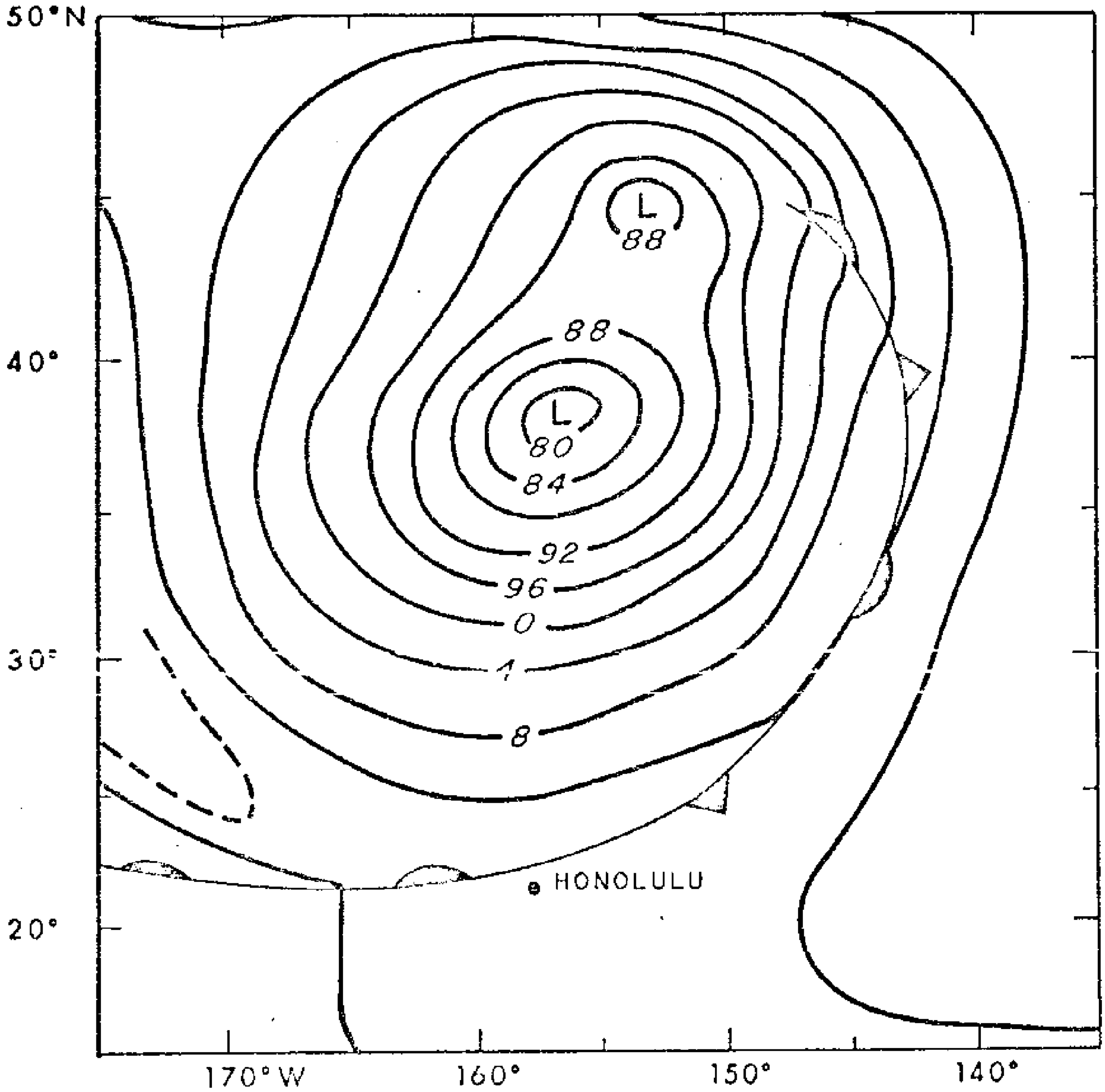

Figure 64. From National Weather Service surface analysis for 0200 21 March 1971.

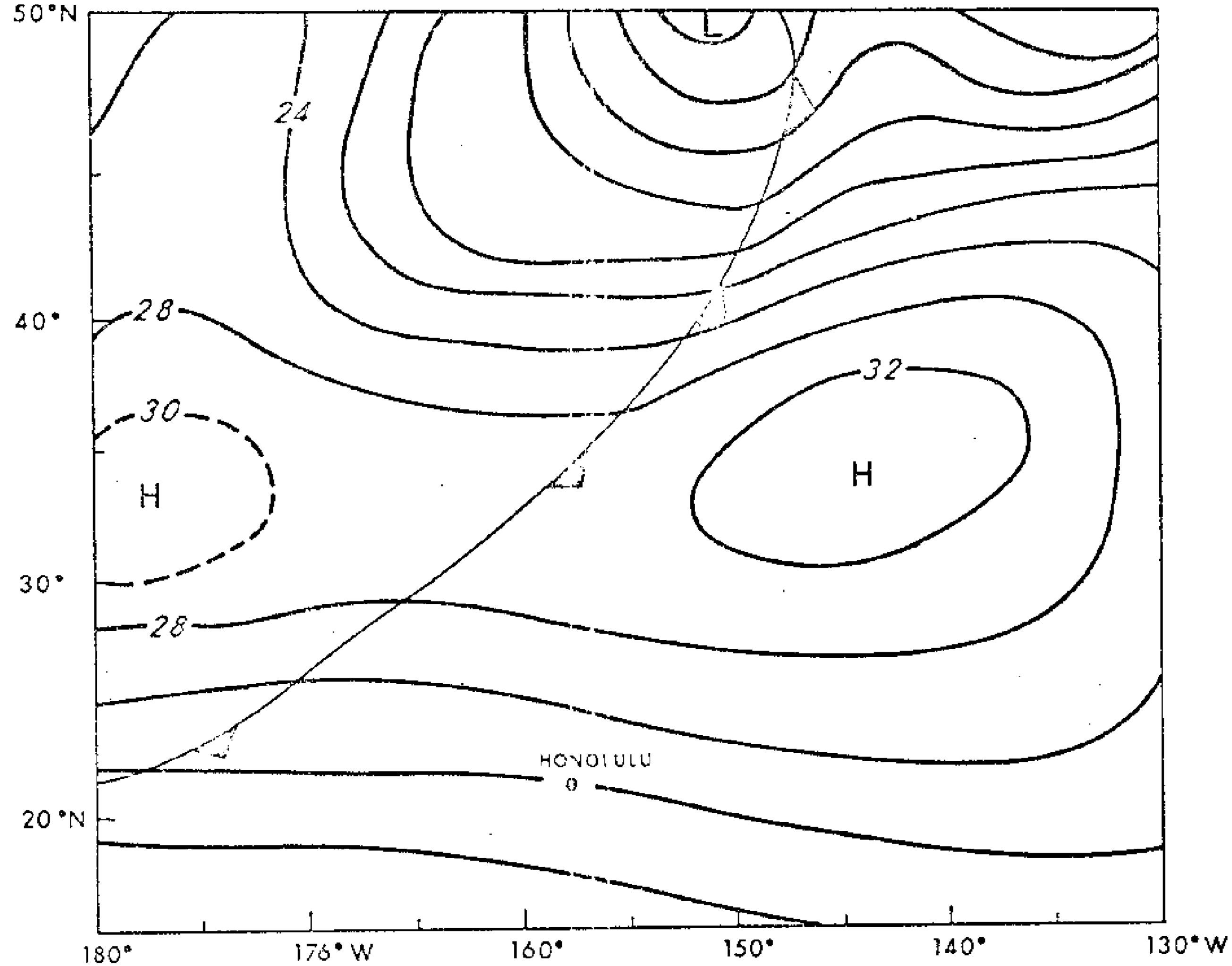

Figure 65. From National Weather Service surface analysis for 0200 23 February 1971.

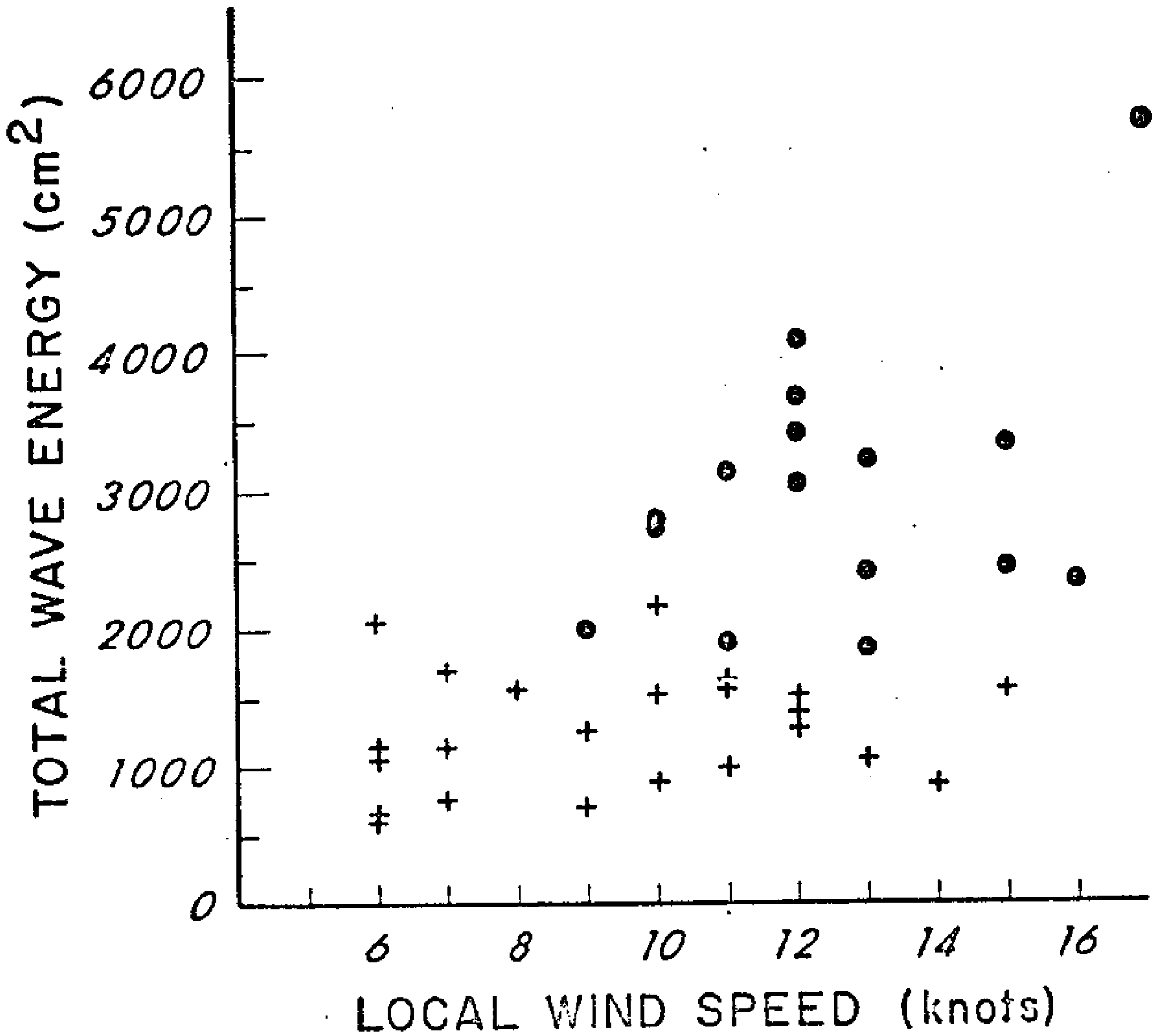

Figure 66. Wind speed and total wave energy. Wind speed data are from Kaneohe Marine Corps Air Station surface wind summaries. Dark circles indicate the total wave energies for tradewinds when smallcraft warnings were in effect. Crosses indicate the total wave energies for tradewinds when smallcraft warnings were not in effect.

BIBLIOGRAPHY

Blackman, R. B., and J. W. Tukey, 1958, The Measurement of Power Spectra, New York Dover Publications, pp. 21-23.

Dinger, J. E., 1962, Spectra of Ocean Waves and Microseisms as Related to Storms at Sea, U. S. Naval Research Laboratory Report No. 5804, 42 pp.

Ho, Francis P., and Lynn A. Sherretz, 1969, A Preliminary Study of Ocean Waves in the Hawaiian Area, Hawaii Institute of Geophysics Report No. HIG-69-16, 36 pp., 4 figs.

Kinsman, Blair, 1965, Wind Waves, New Jersey, Prentice-Hall, pp. 338, 433-453.

Moberly, Ralph, Jr., and Theodore Chamberlain, 1964, Hawaiian Beach Systems, Hawaii Institute of Geophysics Report No. HIG-64-2, pp. 15-19.

Munk, W. H., G. R. Miller, F. E. Snodgrass, and N. F. Barber, 1963, Directional Recording of Swell from Distant Storms, Philosophical Transactions of the Royal Society of London A, v. 255, no. 1062, pp. 505-584.

Roy, Kenneth, 1970, Change in Bathymetric Configuration, Kaneohe Bay, Oahu, 1882-1969, Hawaii Institute of Geophysics Report No. HIG-70-15, 26 pp., 22 fig., 18 tables.

Snodgrass, F. E., G. W. Groves, K. F. Hasselmann, G. R. Miller, W. H. Munk, and W. H. Powers, 1966, Propagation of Ocean Swell Across the Pacific, Philosophical Transactions of the Royal Society of London A, v. 259, no. 1103, pp. 431-497.